AD-A032 011 TECHNION RESEARCH AND DEVELOPMENT FOUNDATION LTD HAI--ETC F/G 11/1
MECHANICAL BEHAVIOR OF MULTIMATERIAL COMPOSITE SYSTEMS. INTERLA--ETC(U)
APR 76 O ISHAI, D PERETZ, S GALI DAJA37-75-C-1890

UNCLASSIFIED NL

1 OF 2
AD
A032011

SIFIED

1 OF 2

AD A032011

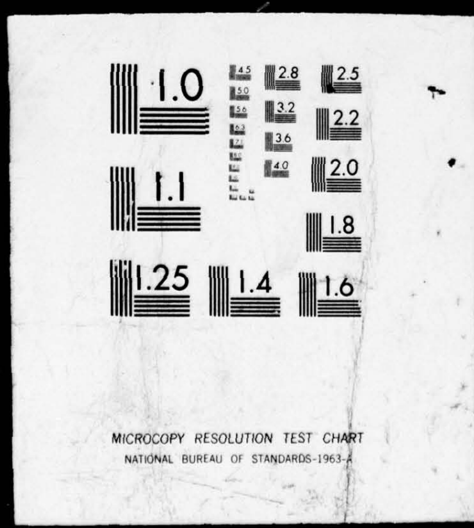

ADA032011

(13)

MECHANICAL BEHAVIOR OF MULTIMATERIAL COMPOSITE SYSTEMS

INTERLAMINAR BEHAVIOR

Final Technical Report

(Second Research Year)

by

Ori Ishai, Dan Peretz and Shlomit Gali

April 1976

EUROPEAN RESEARCH OFFICE
United States Army
London W. 1, England

Contract Number DAJA 37-75-C-1890

Technion Research and Development Foundation Ltd.
Technion — Israel Institute of Technology, Haifa, Israel

UNCLASSIFIED
SECURITY CLASSIFICATION OF THIS PAGE (When Data Entered)

REPORT DOCUMENTATION PAGE

READ INSTRUCTIONS BEFORE COMPLETING FORM

1. REPORT NUMBER

2. GOVT ACCESSION NO.

3. RECIPIENT'S CATALOG NUMBER 9

4. TITLE (and Subtitle) 6
MECHANICAL BEHAVIOR OF MULTIMATERIAL COMPOSITE SYSTEMS. Interlaminar Behavior.

5. TYPE OF REPORT & PERIOD COVERED
FINAL TECHNICAL REPORT.
Oct 75 - Mar 76.

6. PERFORMING ORG. REPORT NUMBER

7. AUTHOR(s)
PROFESSOR O. ISHAI, D. PERETZ, S. GALI

8. CONTRACT OR GRANT NUMBER(s) 15
DAJA37-75-C-1890

9. PERFORMING ORGANIZATION NAME AND ADDRESS
TECHNION RESEARCH & DEVELOPMENT FOUNDATION
HAIFA, ISRAEL.

10. PROGRAM ELEMENT, PROJECT, TASK AREA & WORK UNIT NUMBERS
6.11.02A-1T161102B35E-
-00-516

11. CONTROLLING OFFICE NAME AND ADDRESS
U.S. ARMY RESEARCH & STANDARDIZATION GROUP (EUR)
BOX 65, FPO NEW YORK 09510

12. REPORT DATE 11
April 1976

13. NUMBER OF PAGES 12
102
103p.

14. MONITORING AGENCY NAME & ADDRESS (if different from Controlling Office) 10
Ori /Ishai, Dan /Peretz
Shlomit /Gali

15. SECURITY CLASS. (of this report)
UNCLASSIFIED

15a. DECLASSIFICATION/DOWNGRADING SCHEDULE

16. DISTRIBUTION STATEMENT (of this Report)
APPROVED FOR PUBLIC RELEASE
DISTRIBUTION UNLIMITED

16 1T161102B35E / 17 00

17. DISTRIBUTION STATEMENT (of the abstract entered in Block 20, if different from Report)

18. SUPPLEMENTARY NOTES

19. KEY WORDS (Continue on reverse side if necessary and identify by block number)
COMPOSITE SYSTEMS, INTERLAYER STRENGTH, HYBRID COMPOSITES

20. ABSTRACT (Continue on reverse side if necessary and identify by block number)
SEE NEXT PAGE.

DD FORM 1 JAN 73 1473 EDITION OF 1 NOV 65 IS OBSOLETE

UNCLASSIFIED
SECURITY CLASSIFICATION OF THIS PAGE (When Data Entered)

388338

1B

20. Stress analysis of interlaminar adhesive layer (IAL) within a multimaterial doubler model which was evaluated in the previous years work is further investigated. Two dimensional IAL stress distribution were derived by means of the finite element method, with emphasis on the behavior close to the edges. Thermoelastic behavior of symmetrical and nonsymmetrical models was investigated analytically and experimentally. A direct method for measuring IAL stress and strain distribution was developed and compared successfully with the analytical predictions. These studies provide a wider basis for current and future research into the non-linearity and ultimate behavior of the IAL.

MECHANICAL BEHAVIOR OF MULTIMATERIAL COMPOSITE SYSTEMS

Interlaminar Behavior

O. Ishai*, D. Peretz** and S. Gali***

ABSTRACT

Stress analysis of interlaminar adhesive layer (IAL) within a multimaterial doubler model which was evaluated in the previous report, is further investigated. Two dimensional IAL stress distributions were derived by means of the finite element method, with emphasis on the behavior close to the edges. ThermoeIastic behavior of symmetrical and nonsymmetrical models was investigated analytically and experimentally. A direct method for measuring IAL stress and strain distribution was developed and compared successfully with the analytical predictions. These studies provide a wider basis for current and future research into the non-linearity and ultimate behavior of the IAL.

*) Associate Professor, Faculty of Mechanical Engineering, Technion - Israel Institute of Technology, Haifa, Israel

**) Lecturer, Faculty of Mechanical Engineering, Technion - Israel Institute of Technology, Haifa, Israel

***) Instructor, D.Sc. Candidate, Faculty of Mechanical Engineering, Technion - Israel Institute of Technology, Haifa, Israel

MECHANICAL BEHAVIOR OF MULTIMATERIAL COMPOSITE SYSTEMS

Interlaminar Behavior

TABLE OF CONTENTS

LIST OF FIGURES

LIST OF TABLES

LIST OF APPENDICES

1. INTRODUCTION

Most of the work conducted during the second research year concentrated on extending and refining the results found during the first year.

Based on up-dating of the literature survey on mechanics of bonded joints, our data and analytical solutions were compared to the results of others, which then raised certain questions necessitating additional study. The main objectives were to clarify some dubious points and to check the controversial information on this subject.

Accordingly, the work was conducted as follows:

- The finite element method (FEM) was used to solve the problem of stress distribution through the adhesive layer thickness and closer to its edges.

- The thermoelastic behavior of symmetrical and non-symmetrical doubler configurations was studied with the use of approximate models, and analytical results were verified experimentally.

- A direct method for measuring stress distribution along the interlaminar adhesive layer (IAL) was developed and the analytical results of the first year were confirmed at a region very close to the IAL edges.

- Improved techniques for the evaluation of strength characteristics and deformational behavior of bonded adhesives were developed to provide a data base for nonlinear and ultimate stress analysis.

- The effect of adhesive layer thickness on the above characteristics was studied.

At present, most of the efforts focus on two major topics: an analytical study of the effect of the nonlinear (inelastic) IAL stress-strain relation on stress distribution, and an investigation of failure mechanism and strength characteristics of doublers composed of aluminum and different composite adherends. It is planned to continue these subjects during the next research year.

The current program and future goals are illustrated schematically in Figs. 36 and 37.

2. LITERATURE SURVEY

An up-to-date bibliography on the subjects of bonded joints and interlaminar behavior is provided in chronological order at the end of this report in Appendix 1 which classifies this literature according to several categories.

Most of the literature reviewed here deals with joints composed of rigid adherends and flexible polymeric adhesives. The adherends were metal-to-metal (aluminum and titanium), composite-to-composite, and, less frequently, metal-to-composite.

The mechanical, analytical representation consisted of main thin beams or plates on elastic substrate in bending. The common structural models were single and double lap joints and, mainly in the case of composite material bonding, scarfed and stepped joints.

Linear elastic behavior of both adherends and adhesives and a state of plane strain in the adhesive and of plane stress in the adherends were assumed in most cases. The common, approximate assumptions were uniform stress distributions through the adhesive thickness, negligible transverse shear deformations, and axial normal interlaminar stresses. Consequently, two main variables were assumed to have a predominant role in adhesive layer behavior, namely, axial shear and lateral normal interlaminar stresses.

Boundary conditions were zero forces and moments at the adherend ends and zero shear stress at the adhesive free edges in the case of square geometry. In several closed form solutions, the last condition was not satisfied because the analytical model did not have enough degrees of freedom.

Earlier works neglected the presence of lateral normal stresses and dealt only with axial shear along the IAL. Volkersen (1938), in his first study of the problem [2], obtained a simple expression for the shear distribution of a single lap joint (SLJ) composed of uniform adherends of different materials and thicknesses. According to Volkersen, maximum shear stress is attained at the adhesive free edge; the IAL stress level is mainly dependent on a parameter consisting of the rigidities and thicknesses of adherends and adhesive layers.

DeBruyen (1944) [3] demonstrated the improvement achieved in stress distribution by varying the thickness of adherends down to zero at the edge. Basing his analytical prediction on Volkersen's solution, he found the dependence of joint strength on the IAL thickness/length ratio to be the governing relationship for an assessment of the performance of bonded joints.

Damarkless (1955) [8] extended Volkersen's solution to cover the effects of shear deformation in the adherend. An earlier publication by Inglis (1923) [1] indicated the existence of pronounced transverse stresses and stress concentration at the joint edges. This problem was studied much later by Adams and Peppiatt (1973) [40], who revealed the presence of high transverse shear stresses on the IAL which were due to the Poisson effect of the adherend.

The breakthrough in this field was achieved by the classical contribution of Goland and Reissner (1944) [4], who provided a closed form analytical solution for single lap joints with expressions of shear and lateral normal stress distributions through the IAL. They presented a model of thin adherend plates of equal thickness and rigidity under cylindrical bending. Here again, though, the boundary conditions of zero shear stress at the IAL edges was unsatisfied. An approximate solution based on their work was given by Plantema (1949) [5]; it included the effect of external moment on IAL shear stresses, but neglected this effect on the respective normal stresses.

Sherrer (1957) [10] extended the work of [4] to cover adherends of different materials by assuming a plane stress for the adherends and a plane strain for the adhesive.

Cornell (1953) [7] presented a model of beams representing the adherends not affected by the adhesive layer, which was represented by a series of tensile and torsional springs.

Iyengar and Alwar (1961) [13] attempted to solve the model of [4] by fulfilling boundary conditions for the free IAL edges. Kunzi and Stevens (1963) [15] corrected the solution of [4] and extended it to cover adherends of different characteristics.

Volkersen (1965) [18], in a later work, suggested a solution which included both shear and normal stresses and satisfied the IAL free edge conditions.

The above-mentioned solutions following [4] were based on many approximate assumptions and over-simplified models. This was due to the complexity of an exact model. It was later found that a few assumptions led to an incorrect solution at the critical region near the edges. Numerical solutions were suggested in order to obtain a more exact solution, and the major effort was devoted to applying the finite element method (FEM) to solve the problem. At first, this method was applied for checking experimental tests to determine joint strength and, especially, the effect of edge geometry. Later, the whole IAL stress distribution was derived by the FEM.

In recent years, several works were published which used FEM to solve the problems of SLJ and DLJ models. Among the first was the report by Kutscha *et al.* (1969) [25], which is based on available FEM programs. The solution derived is for states of plane stress and plane strain. The model used was the same as those of [2] and [4], and the results provided a measure for the accuracy of the closed form analytical solution.

Wooley and Carver (1971) [33] developed a general solution for SLJ, based on FEM, which agreed well with [4] but did not account for the free edge boundary conditions.

Dickson *et al.* (1972) [36] derived analytical solution for joints with orthotropic adherends; they also developed a computer program based on FEM which enables one to deal with different joint geometries and non-linear IAL stress-strain behavior.

A similar attempt to deal with non-linear behavior was carried out by Grimes *et al.* (1972) [39], who suggested a numerical solution to the problem of joints composed of orthotropic FRP adherends.

Contributions by Barker and Hatt (1973) [47], and Adams and Peppiatt (1974) [51], dealt with the problem of singularity at the IAL edges by means of the finite element method. At the same time, works by Hart-Smith (1973) [42-46] and Renton and Vinson (1974) [41,58] suggested analytical solutions to the problem of structural bonded joint including anisotropic composite adherends.

An attempt to tackle the problem of stress distribution through the IAL thickness was undertaken by Pirvics (1974) [5] using finite difference methods. His solution may violate the common assumption of uniform shear and tension through the IAL that was postulated by many authors.

In recent years, much more attention has been given to the present subject; the scope was expanded, and efforts were more orinted towards the applied aspects of analysis and the design of structural bonding.

To sum up, the numerous contributions on the subject during the past decade may be classified into the following topics:

I. Mechanics of joints composed of orthotropic composite adherends [reference numbers: 20, 23, 25, 29, 36, 37, 39, 41, 42, 43, 55, 56, 58, 59, 63].

II. Fracture mechanics approach and testing methods [reference numbers: 49, 53, 60, 64].

III. Environmental effects on bonded joint performance (including thermoelastic behavior), [reference numbers: 21, 35, 49, 50, 54, 64].

IV. Dynamic behavior (fatigue) of structural joints [reference numbers: 21, 32, 36, 41, 54, 55, 56, 63].

V. Effect of non-elastic adhesive characteristics on bonded joint performance [reference numbers: 29, 37, 38, 39, 42, 46, 63].

VI. Effect of varying geometry and adhesive composition at the IAL boundaries on structural performance of the joint, (this may provide guidelines for optimization of structural bonding) [reference numbers: 17, 3 , 40, 47, 51, 61].

VII. Analysis of joints (stepped and scarfed) with complex configurations to fit design requirements [reference numbers: 34, 45, 46, 47, 55, 59, 61].

VIII. Design considerations and evaluation of design allowables for structural bonded joints [reference numbers: 19, 23, 24, 29, 31, 37, 46, 54, 58].

The last topic, VIII, is based on the work by Hughes and Rutherford (1968) [24], who developed a testing methodology for direct measurement of stress-strain behavior, modulus and strength of the adhesive layer *in situ*. In the course of their investigation, they evaluated the mechanical characteristics in shear and tension of different structural adhesives of varying thicknesses.

Numerous articles are available on the chemical and physical aspects of the problem, as well as on the more technological aspects involved in the fabrication and inspection of adhesive joints. These contributions are beyond the scope of the present survey, which is limited to the subject of the mechanical behavior of structural bonded systems.

3. TWO DIMENSIONAL INTERLAMINAR STRESS DISTRIBUTION IN THE ADHESIVE LAYER OF A SYMMETRICAL DOUBLER MODEL.

3.1 Introduction

In order to derive a closed form analytical solution for stress distribution of the IAL, the previous report [65] postulated certain simplified assumptions, which were shared by other authors [4, 7,15,18,41]: uniform shear and normal stress distribution through the thickness direction (z).

The neglect of axial normal stress (σ_x) in the adhesive is also common to many publications on bonded lap joints. These simplified assumptions and the fact that the analytical model does not have sufficient degree of freedom lead to several inconsistencies in equilibrium relationships and violate the boundary condition of zero shear stress at the free IAL square edges.

Because of the mathematical complexity required of a more rigorous solution, and the fact that a realistic bond-line is very thin relative to adherend thickness, only a few studies have been made on IAL lateral stress distribution. Pirvics [52 obtained a solution by finite difference minimization of the internal energy distribution for typical simple lap and butt joint models. His solution, though suffering from inconsistencies, clearly indicates the pronounced non-uniformity in the distribution of both shear and normal stresses through the adhesive thickness.

The present study is intended to deal with the problem by means of the finite element method. The main purposes were to check analytical solutions and to provide basic data for an investigation of strength and failure, for which the local principal stress components, rather than their average values, are required.

3.2 Model Representation

The model for the finite element solution of the SMD is based on orthogonal and triangular elements with a uniform strain field. The elements satisfy the compatability conditions at each of the material points, as well as equilibrium conditions in each element. The mechanical behavior is limited to the elastic-linear range and to the two-dimensional case. A state of plane strain was assumed for the IAL (x-z plane) because of its high width to thickness ratio and its low adhesive-to-adherend stiffness ratio. Although this assumption is less accurate when relating to the adherend layers, it is justified for the present study, which focuses on the IAL. The results of preliminary comparative studies between plane stress and plane strain conditions for the adherends exhibited only small differences.

IAL behavior is best represented by the SMD structural model shown in Fig. 1. This model was also selected for the FEM program because of the following advantages:

- Double symmetry in geometry, materials, boundary, and loading conditions, which allows treatment of one quarter of the model only (in contrast with the SLJ model).

- Wide separation between external loading region and the critical IAL zones where maximum stresses and strains are located. This allows the isolation of the IAL boundary zone which is of main interest for both experimental and analytical study.

- Continuity of stress and strain fields over all the IAL region, which reduces the number of boundary conditions (in contrast to the case of the SLJ model).

The model for the present specific case is composed of aluminum adherends and epoxy adhesive, the characteristics of which are given in Table 1 (test model A21).

The FEM program consisted of three steps. In the first step, uniform stress distributions through IAL thickness was assumed and the IAL was divided into rectangular elements having the IAL lateral dimensions (Fig. 2a).

In the second step, the IAL thickness was divided into two longitudinal strips (Fig. 2b). In the final step, which aimed at deriving the stress distribution through the IAL thickness, it was divided into 4 longitudinal strips as shown in Fig. 2c.

3.3 FEM vs. Analytical Solution

The FEM was first examined by comparing its results (based on the model of Fig. 2A) to the analytical closed-form solution of ref. [65]. Good agreement was found between numerical and analytical results both for the normal stress distribution (Fig. 3) and for the shear stress distribution, except at the region close to the IAL edges (Fig. 4).*) A preliminary study of the effect of a finer network in the axial direction showed only slight differences in results.

The second step revealed different stress patterns close to the edges. Shear stress distribution was found to reverse its slope at the boundary zone ($\chi > 0.98$) and to drop to zero towards the IAL edges (Fig. 3). Normal stress, on the other hand, increased steeply towards the edge of the IAL layer close to the

---

*) In all stress distributions (Figs. 3-17) the stresses are normalized with respect to average applied stress acting at the central adherend $p_c = F/2h$. Accordingly: $\bar{\tau}_{xzi} = \tau_{xzi}/p_c$; $\bar{\sigma}_{xi} = \sigma_{xi}/p_c$ $\bar{\sigma}_{xzi} = \sigma_{xzi}/p_c$.

central adherend but reversed their slope and dropped to zero towards the free edges of the IAL layers close the external adherends (Fig. 4).

3.4 Two-Dimensional Stress Distribution

The third step of the FEM solution, in which the IAL was divided into 4 sub-layers, yielded a two-dimensional stress distribution for both adhesive and adherend.*)

3.4.1 Stress Distribution in Adherends

The predominant stress component obtained at the adherends is the axial normal one - σ_{xi} (Figs. 5-6), which was higher by an order of magnitude than the other adherend stresses, σ_{zi} and τ_{xzi} (Figs. 7-10); σ_{xi} was almost uniform through the adherend thickness.

In the case of metallic adherends, in which other stresses besides σ_{xi} are negligible, the assumption of uniform stress distribution through the adherend thickness was justified. However, with adherends composed of multilayer, composite laminates, in which interlaminar stiffness and strength characteristics are significantly lower than axial ones, adherend lateral stresses τ_{xzi} and σ_{zi} have a major role and cannot be neglected. These stresses exhibited pronounced variations through the thickness. In this case, a finer mesh for the FEM solution is essential, especially if strength characteristics are required.

The axial distribution of axial normal stresses through the external layer of adherend 2 exhibited the pattern which was found both analytically and experimentally in ref. [65] (Fig. 30), namely a change from tension to compression close to the adherend edge (Fig. 5).

3.4.2 Stress Distributions Through Adhesive

In the IAL, all stress components are of the same order of magnitude and exhibited a pronounced variation through the thickness (along the z axis); (Figs. 11-13, 14-16). The axial distribution of shear stress (τ_{xzo}) showed a trend similar to that in Step 2, i.e., slope reversal at the 'boundary zone' (from each edge up to a distance of 1% of the IAL length), and a drop towards zero at the free IAL edges. This finding is consistent with boundary conditions but contradicts the closed-form analytical solution (Figs. 12,15).

Axial distribution of lateral normal stresses (σ_{zo}) along the 'boundary zone' showed a pronounced divergence from their

---

*) The results obtained in the present report were related to a model of isotropic adherends. The FEM program, which is given in Appendix 2, is, however, adequate for orthotropic adherend cases as well.

average reference distribution, whereas the normal stress through the external IAL layer rose steeply towards the edge far beyond its slope and dropped towards zero at the free edge (Figs. 13,16).

Axial distribution of axial normal stresses (σ_{xo}) was uniform throughout the "middle zone" (98% of the IAL length) but dropped steeply at the "boundary zone" towards zero at the free edges (Fig.s 11, 14).

It may be concluded that axial interlaminar stress distributions (σ_{zo}, τ_{xzo}) derived by FEM are in close agreement with the closed-form solutions along the "middle zone". The major divergence between the numerical and closed-form solutions resulted from the assumption of uniform lateral stress distributions. As shown in Figs. 15,16, such an assumption did not hold up at the "boundary zone" in cases of shear and normal lateral stresses. The neglect of axial normal stresses through the IAL is also unjustified as these stresses attained a level having the same order of magnitude as other stress components (Fig. 14).

Lateral normal stress distribution at the boundary zone shows the maximum deviation from uniformity (Figs. 13,16), being almost zero close to the external adherend and increasing steeply and linearily to its maximum level towards the central adherend. Similarly, both IAL shear and axial normal stresses attained their maximum value close to the intersection of the free IAL edge and the upper surface of the central adherend (point m of Fig. 1).

3.5 Discussion

Given the values of the three stress components at the IAL boundary zone, their principal value can be derived. Fig. 17 shows the axial and lateral distributions of the principal stresses emphasizing the major trends found for the stress components. The expected finding of the location of maximum stress being close to point m is also demonstrated.

In the case of brittle IAL characteristics, the data given by the principal stress distribution may provide the basic clue for failure mechanism, the delamination process, and strength evaluation for the overall bonded structure as represented by the SMD model. The finite element method seems to provide an accurate solution which conforms well to basic mechanical and boundary conditions. The interrelation among the different functions found for the different stresses can be examined by satisfying the classical equilibrium conditions.

According to the first equilibrium equation

$$\frac{d\sigma_x}{dx} = - \frac{d\tau_{xz}}{dz} \qquad (1)$$

which means that τ_{xz} is uniformly distributed along the z axis in the region where σ_x is uniformly distributed along x. This interrelation prevails at the "middle zone" of the IAL, as is shown when Fig. 15 is compared with Fig. 14.

According to the second equilibrium equation,

$$\frac{d\sigma_z}{dz} = - \frac{d\tau_{xz}}{dx} \tag{2}$$

which means that where the τ_{xz} distribution along x reverses its slope, the σ_z function along z will also reverse but in the opposite direction. This change occurs simultaneously for the two functions at about χ=0.99 within the "boundary zone", as demonstrated by a comparison of Fig. 15 with Fig. 16.

At the middle zone, the $\tau_{xz}(x)$ functions coincided (Fig. 15), thus σ_z functions are supposed to be linear functions of z, as is clearly shown in Fig. 16.

The above findings referred to an idealized case of thick adhesive relative to its adherends. It is expected that similar distribution patterns will be found, though to a lesser degree, for the more practical cases of thinner and stiffer adhesives. The most important finding of the locations of the maximum principal stresses is also expected to be generally valid.

A more detailed solution for interlaminar adherend stresses is essential for the strength analysis of orthotropic composite bonded systems.

In order to obtain more realistic solutions which provide quantitative data for design allowables, the effects of nonlinearity in an adhesive stress-strain relationship and the effect of edge geometry have to be studied.

Some of the above topics are currently being treated by the finite element method and will be presented in the future.

3.6 Conclusions

The following conclusions emanate from the solutions obtained by applying the finite element method to the symmetrical doubler model, composed of aluminum adherends bonded by thick adhesive layers (IAL). Most of the conclusions concern the stress distributions through the IAL, which is the main subject of the present investigation.

1. The distribution of shear and lateral normal stress through the IAL thickness was approximately uniform within the "middle zone" ($-0.98<\chi<0.98$).

2. Axial normal stress distribution [$\sigma_x(x)$] was uniform within the "middle zone" but varied linearly through the IAL thickness.

3. For all interlaminar stress functions, drastic variations occurred at the "boundary zone".

4. The distribution of IAL axial shear stress attained its maxima within the "boundary zone", reversed its slope and dropped towards zero at the free edge. A similar trend was found for σ_z distributions close to the external adherends.

5. The normal lateral stress function $\sigma_z(z)$ exhibited an approximately linear distribution, which reversed its slope abruptly within the "boundary zone".

6. Maximum values of all stresses and their principal counterparts were attained at the "boundary zone", close to the central adherend interface.

7. The different patterns which characterized stress functions along the z and x axes were consistent with basic differential equilibrium equations and boundary conditions of the IAL.

8. The average interlaminar stress levels were significantly lower than their actual individual extreme levels; thus, they could not be used to predict the doubler strength.

9. Because of the narrow dimensions of the boundary zone, its stress behavior will not be reflected in the overly deformational behavior of the bonded structure, nor could this behavior be directly detected experimentally. It is, however, predominantly influential on the ultimate behavior of the IAL and has to be considered when failure mechanism and strength characteristics are discussed.

4. DIRECT DETERMINATION OF AVERAGE INTERLAMINAR STRESS DISTRIBUTIONS IN A POLYMERIC ADHESIVE LAYER.

4.1 Introduction

The real stress distribution through IAL is still undecided because of the controversy over the different solutions of the problem. Unfortunately, there is no satisfactory experimental means of direct characterization of these stresses. Matting [16] and Kreiger [49] measured directly only the shear displacement of SLJ and compared it with solutions of [2] and [4]. Most attempts at such characterization employed indirect measurement of strains at the external adherend surfaces by means of strain gages [65,42], or photoelastic [65,36,9], or Moiré [70] methods. In all cases, the patterns were obscured by the interference of other factors such as stress concentrations, edge effects of the photo-stress coating, etc. Moreover, the interlaminar stress distribution cannot be conclusively established from data on adherend strains. This problem is crucial, considering that the location of the joint, where extreme stresses develop and enhance delamination, is very close to the edges of the adhesive layer. The object of the present investigation is, therefore, twofold:

a. To develop a method for direct determination of the interlaminar strain and stress distribution which will provide a check on the validity of existing analytical solutions;

b. to devise a tool for the direct measurement of the critical stresses which control the ultimate performance of the joint or laminate under different loads and environmental conditions.

4.2 Analytical Background

A simplified expression of IAL shear stress distribution for the SMD model (Fig. 1) is given in eq. (3):

$$\tau^* = \frac{h_2\phi}{c}\,\frac{\sinh\phi\chi}{\cosh\phi} \qquad (\chi = \frac{x}{c}) \tag{3}$$

where $\tau^* = \frac{\tau}{p_0}$ is the normalized shear stress;

$$\phi^2 = \frac{c^2 G_0}{h_0 h_1 E_1}\,(1 + \mu) \tag{4}$$

$$\mu = \frac{E_1 h_1}{E_2 h_2} \tag{5}$$

and

$$p_0 = \frac{F}{2h_2(1+\mu)} \quad (6)$$

is the reference axial normal stress (acting at the external adherend layer -(EAL) midpoint under the action of F). The derivation of eq. (3) and the more exact solution for shear stress distribution is given in ref. [65].

The similarity of the simplified to the more exact solution for a case of multimaterial doubler model is shown in Fig. 9 of ref. [65].

The derivation of the expression for interlaminar lateral normal stresses, $\sigma_z^{(0)}$, is more complex than that for shear stress analysis. It involves the solution of differential equations of the 6th order, as is fully described in ref. [65]. Typical distribution curves of σ^* for different boundary conditions are shown in Fig. 10 of this reference. ($\sigma^*=\sigma_z^{(0)}/p_0$ is the normalized expression for IAL lateral stresses.)

4.3 Experimental Procedure

Shear strain γ and shear stress τ are obtainable from the shear displacement Δu, i.e., the differential displacement of the adherend surfaces (Fig. 19):

$$\gamma_0 = \frac{\Delta u}{h_0} \qquad \tau_0 = \frac{\Delta u}{h_0} G_0 \quad (7)$$

Similarly, by measuring the net lateral displacement, normal lateral stresses are obtainable from eq. (8):

$$\sigma_0 = \frac{w_0}{h_0} E_0 \quad (8)$$

Instron electromechanical extensometers were modified and used for measuring Δu and w_0, respectively.

Measuring Devices. The shear-displacement extensometer shown in Fig. 20 is a modification of the Instron Extensometer Type G51-11. It consisted of two parts, each attached to a point at the mid-thickness of the adherends, all of which were originally located on the same line (along the z-axis), but which were shifted relative to each other under axial loading, thereby creating the shear displacement. The normal displacement distribution was obtained in the same manner, utilizing the normal-displacement extensometer shown in Fig. 21, which is a modification of Instron Extensometer G57-11 (originally used for measuring

the Poisson ratio).

The displacements were measured within an accuracy of 0.2μm. The distributions were obtained by applying the extensometers at different points along the model axis.

Preparation of Test Model. The measuring systems were checked on test models consisting of two aluminum adherends and an epoxy IAL having the characteristics given in Table 1.

The surfaces of the adherends were sand blasted, cleaned with MEK and coated with a thin layer of resin, as described in detail in ref. [65]. Immediately following the coating, the adherend strips were inserted into a special fixture which ensured the exact spacing for the IAL phase. The external adherends were longer than the adhesive bond-line in order to enable measurement of displacements at IAL edges (see Fig. 1).

The epoxy-versamid mix (2:1) was prepared under vacuum and poured into the gap; its temperature was kept at 40°C to reduce viscosity and ensure good wetting. The model was unmolded after 24 hours and exposed for 8 hours at 40°C to post-cure the resin.

Loading Procedure. The model was loaded uniaxially on an Instron Tester at the rate of about 10^{-3} (min^{-1}), up to failure. Shear displacement values were recorded continuously. The specimen was unloaded at different loading levels as a check on the reversibility of the response.

4.4 Test Results and Discussion

The relationship between the shear displacement and the reference axial stress, as shown in Fig. 22, is characterized by linear behavior up to approximately 80% of the loading range. Beyond this level, nonlinearity prevailed to the delamination stage.

The shear stresses at the various points along the IAL were calculated from the measured shear-displacement data with the aid of eq. (7). The experimental interlaminar shear stress distribution, shown in Fig. 22, was compared with the approximate analytical solution of eq. (3). Considering the approximations involved, agreement between the experimental data and the analytical prediction is good, especially with regard to the shape of the distribution curve close to the boundary.

The tendency of the shear stresses to increase to their maximum value at the IAL edge was in agreement with the analytical solutions of ref. [4] for bonded joints and of ref. [65] for doubler models. It conflicted, however, with the boundary condition of zero shear stress at the free IAL edge and with solutions based on the finite-element method (Fig. 15).

In order to obtain the exact value of lateral displacement resulting from interlaminar normal stress $\sigma_z^{(0)}$, the contribution of Poisson's effect to the overall displacement must be determined. The Poisson displacement data hardly vary along the model axis and may be calculated or measured separately.

The relationship between lateral normal displacement and the reference axial stress is shown in Fig. 22, where similar trends to those of the shear-displacement data are apparent, i.e., linearity within 80% of the loading range.

The lateral normal stresses at the various points along the IAL were calculated from the net lateral displacement data with the aid of eq. (8).

The experimental interlaminar normal stress distribution (Fig. 24) was compared to the analytical solution given in eq. (33) of ref. [65]. The agreement between the experimental data and the analytical prediction was good, especially with regard to the shape of the distribution curves close to the IAL edges.

4.5 Conclusions

A method of direct measurement of shear and normal displacements and a simple way of determining strain and stress distributions along an interlaminar adhesive layer were examined successfully on a symmetrical doubler model.

The experimental interlaminar stress data were in agreement with available analytical solutions for this model. The advantages of the direct method compared with others are as follows:

a. It is based on direct, local measurement of the deformations of the adhesive layer (as against indirect measurements of adherend strains).

b. It is a simple method utilizing the standard accessories of an Instron extensometer with only slight modifications.

c. The accuracy in measuring displacements to within 0.2μ permits detection of stress variations of about 0.2 kg/mm^2, which is less than 5% of the ultimate shear and stress delamination level.

d. The continuous recording of interlaminar adhesive strains against axial load permits monitoring of IAL behavior from the linear elastic range to the nonlinear inelastic range up to initiation of the failure process.

This study may reveal the actual mechanism of adhesive and cohesive failure modes which are eventually responsible for the delamination of laminates, joints, and other bonded systems that are subjected to mechanical and thermal loading.

5. THERMOELASTIC BEHAVIOR OF MULTIMATERIAL DOUBLER MODELS

The analytical expressions in Ref [65], (eqs. 63, 68, 43), covered the effect of thermal changes on mechanical behavior with respect to elastic and thermoelastic parameters.

The solution was based on the assumption that the coefficient of thermal expansion, and of other material parameters, were not affected by thermal changes. The solution also neglected transverse behavior and its interrelation with axial behavior. Within these limitations, which apply for an isothermal regime, there is a wide range of materials, geometries, and thermoelastic parameters for which the solution is valid.

The thermoelastic behavior of symmetrical and nonsymmetrical doubler models (SMD and NMD, respectively) were studied with a view to checking the validity of analytical formulations of the stress distribution by means of strain- and deflection-measurements along the model's external facings.

5.1 Thermoelastic Behavior of a Symmetrical Doubler Model (SMD)

5.1.1 Analytical Background.

The normalized approximate expression for the external strain distribution of the EAL is given by eq. 9 (eq. (73) of ref. 65):

$$\varepsilon^* = 1 - \frac{\cosh\phi\chi}{\cosh\phi} = \frac{E_2}{p_0}\,\varepsilon_2 \qquad (9)$$

where

$$p_0 = \frac{E_1 h_1 (\alpha_1 - \alpha_2) T}{h_2 (1+\mu)} \qquad (10)$$

For non-loaded specimens, eqs. (9) and (10) yield the strain distribution along the EAL external facing:

$$\varepsilon_2 = \frac{\mu}{1+\mu}(\alpha_1 - \alpha_2) T \left[1 - \frac{\cosh\phi\chi}{\cosh\phi}\right] \qquad (11)$$

where $\mu = \frac{E_1 h_1}{E_2 h_2}$; α_1, α_2, E_1, E_2, are the thermal coefficients and the elastic moduli in the x-direction, respectively.

Eqs 9-11 are based on the assumption of negligible transverse stresses, i.e.:

$$\sigma_{zy} << \sigma_{zx}$$

In the thermoelastic case, such conditions require near-uniformity of the thermal expansion coefficient in the transverse direction, i.e., $\alpha_{1y} \simeq \alpha_{2y}$.

5.1.2 Experimental Procedure.

Model A02, which had served previously for experimental verification of eq. (9) in the the case of mechanical axial loading, was also used in the thermal tests. Its basic characteristics are given in Table 2.

The axial thermal coefficients α_{x_1} and α_2 were measured by strain gage, whereas α_{y_1} is given by the manufacturer for the GRP 1002 prepregs used.[1] It can be seen from Table 2 that the near-uniformity requirement was satisfied. The test was carried out as follows:

Fourteen gages were glued to the aluminum external EAL surfaces of the test model, as shown in Fig. 25. The specimen was exposed to changes in temperature within a thermal chamber that ranged from 30°C to 60°C. (Higher temperatures were expected to affect the elastic parameters of the polymers.) Strains were recorded simultaneously at the different gage points. The temperature was raised and lowered several times to check reproducibility and reversibility. The results are shown in Figs. 26 and 27, and indicated the following conclusions:

a. The near-linearity of the thermal increase of the elastic strain justified use of the normalized form of eq. (9) for the thermoelastic case (Fig. 26).

b. The measured strain distribution along the external EAL surface was in fair agreement with eq. (9). The near-uniformity of the strain distribution through the major midsection was evident in Fig. 27.

The experimental results provided, however, only an indirect and partial confirmation of the interlaminar shear and normal stress distributions; it did not indicate the actual interlaminar characteristics close to the edge, which is one of the main objectives of the present investigation.

5.2 Thermoelastic Behavior of a Nonsymmetrical Doubler (NMD)

The following experimental and analytical work deals with a nonsymmetrical model composed of two strips, each of a different material, bonded together by a thin layer of polymeric material and subjected to thermal changes (see Fig. 28). These changes and the different coefficients of expansion, bring about thermal stresses causing the strips to deflect. The deflection can be measured and compared with analytical solutions.

5.2.1 Analysis.

Equilibrium conditions of the NMD model give (see Fig. 28):

$$N_1 = N_2 = N \tag{12}$$

$$M_1 + M_2 = N[\frac{h_1}{2} + h_0 + \frac{h_2}{2}] = N[\bar{H}] \tag{13}$$

$$V_1 + V_2 + \tau h_0 = 0 \tag{14}$$

This leads to

$$\frac{dN}{dx} = \tau \tag{15}$$

$$\frac{dV}{dx} = \sigma \tag{16}$$

$$V + \frac{dM}{dx} - \tau \frac{h}{2} = 0 \tag{17}$$

The six equations, together with the compativility conditions yield:

$$\frac{\varepsilon_1 - \varepsilon_2}{h_0} = \frac{1}{G}\frac{d\tau}{dx} \tag{18}$$

$$\frac{1}{\rho + h} = \frac{1}{\rho^2} \tag{19}$$

ρ being the beam curvature.

Introducing elastic stress-strain relations and linear thermal coefficients of expansion results in

$$\varepsilon_1 = \frac{N_1}{E_1 h_1} + \frac{6M_1}{E_1 h_1^2} + \alpha_1 T \qquad (20)$$

T being the thermal change

$$\varepsilon_2 = \frac{N_2}{E_2 h_2} - \frac{6M_2}{E_2 h_2^2} + \alpha_2 T \qquad (21)$$

This leads to the following governing differential equation

$$[D^2 - C_{21}]M_2 = C_{31} \qquad (22)$$

where

$$C_{ij} = \frac{C_i}{C_j} \qquad (23)$$

$$C_1 = \frac{2h_0}{c^2 HG}(1+\mu) \qquad (24)$$

$$C_2 = \frac{6}{E_2 h_2^2} + \frac{6\mu}{E_1 h_1^2} + \frac{2(1+\mu)}{HE_1 h_1} - \frac{2(1+\mu)}{HE_2 h_2} \qquad (25)$$

$$C_3 = (\alpha_2 - \alpha_1)\, T \qquad (26)$$

where $2c = \ell$ - is the NMD length and

$$\mu = \frac{E_1}{E_2}\frac{h_1}{h_2} \qquad (27)$$

Solving these governing equations with the boundary condition $M_1 = M_2 = 0$ at $\chi = x/c = \pm 1$ yields:

$$M_2 = \frac{C_3}{C_2}\left[1 - \frac{\cosh\sqrt{C_{21}}\chi}{\cosh\sqrt{C_{21}}}\right] \qquad (28)$$

and

$$M_1 = M_2\,\mu = M_2 \frac{E_1}{E_2} \qquad (29)$$

Eqs. 15-17 lead to the following expressions:

$$\tau = \frac{C_3}{\sqrt{C_1 C_2}} \frac{2(1+\mu)}{cH} \frac{\sinh\sqrt{C_{21}}\chi}{\cosh\sqrt{C_{21}}} \tag{30}$$

$$\sigma = \frac{C_3}{C_1} \frac{(\mu-1)}{2c^2} \frac{\cosh\sqrt{C_{21}}\chi}{\cosh\sqrt{C_{21}}} \tag{31}$$

which are the interlaminar tensile and shear stress distributions through the adhesive layer.

5.2.2 Discussions.

Once the stress distributions of τ and σ_z are known, significant conclusions may be drawn as to the effect of the material and geometrical parameters on the IAL shear and normal stresses while subjected to temperature changes.

For the special case of $h_1 = h_2$, one obtains

$$C_1 = \frac{2h_0}{c^2 HG} (1+\mu) \tag{32}$$

$$C_2 = \frac{4[12\mu + 1-\mu^2]}{E_1 H^2} = \frac{4\bar{\mu}}{E_1 H^2} \tag{33}$$

$$C_3 = \Delta\alpha T \tag{34}$$

Assuming $\frac{h_0/G}{H} = R_0$ to be the rigidity parameter of the IAL leads to the following equations:

$$\bar{\tau} = \frac{\tau}{T} = \Delta\alpha \sqrt{\frac{(1+\mu)E}{2\bar{\mu}}} \sqrt{\frac{1}{R}} \frac{\sinh\sqrt{C_{21}}\chi}{\cosh\sqrt{C_{21}}} \tag{35}$$

$$\bar{\sigma} = \frac{\sigma}{T} = \Delta\alpha \left(\frac{(\mu-1)}{4(1+\mu)}\right) \frac{1}{R} \frac{\cosh\sqrt{C_{21}}\chi}{\cosh\sqrt{C_{21}}} \tag{36}$$

Both $\bar{\tau}$ and $\bar{\sigma}$ are affected by three main parameters:

a. $\Delta\alpha$, which is the measure of thermal incompatibility;

b. a moduli incompatibility;

c. the rigidity parameter of the adhesive layer.

In Figs. 29 and 30, both $\bar{\tau}$ and $\bar{\sigma}$ were drawn as functions of three different adhesive rigidities for strips composed of aluminum 2024/T-3 and unidirectional (GRP) prepreg 1002 (a 3M product). (See Table 3.)

5.2.3 Experimental Procedure.

The main objective of the experimental phase was to examine the validity of the analytical solution postulated in the previous chapter. For this purpose, the relation between the moments in the different strips and the central deflection w of a simply supported beam was calculated and found to be:

$$w = \frac{1}{EI}\left[\frac{C_3}{C_2}\left(\frac{C_1 c^2 (1-\cosh\sqrt{C_2}\,{}_1\chi)}{C_2\cosh\sqrt{C_2}\,{}_1}\right) + \frac{\chi^2}{2}\right] \qquad (37)$$

Special grips were designed to enable the measuring of the deflection. The testing device, together with the test specimen, was spaced in an oven, and the temperature was changed by 10 degree intervals. The deflections were measured by a catatometer at several points along the beam (see Fig. 31). The mid-point deflection was drawn as a function of temperature. In Fig. 32, the experimental results are compared with the analytical ones; as shown, there was a good agreement between the two.

5.2.4 Conclusions.

a. The nonsymmetrical multi-material doubler system proved to be a good tool for the analysis of stress distribution through an adhesive layer.

b. The stresses within the IAL were reflected in a measureable deflection of the doubler. This fact may serve as a simple yet effective indirect method for deriving experimentally the distribution and critical values of interlaminar shear and normal stresses caused by thermal changes.

c. As seen from Figs. 29 and 30, adhesive rigidity parameters had a major influence on both stress peak and its gradient. Thick layers of flexible adhesive will result in low stresses at the edges. On the other hand, thin layers of rigid adhesive will cause a very high stress concentration at the doubler edges. These stresses are critical as they cause premature failure.

6. SHEAR STRESS-STRAIN CHARACTERISTICS OF THE ADHESIVE LAYER *IN SITU*

6.1 Introduction

The main problem in characterizing an adhesive as a structural material is whether its behavior in a confined state differs from that of its bulk material reference. To resolve this problem, which is essential for an evaluation of design allowables of bonded joints, it is necessary to carry out elaborate and precise measurements and to develop a special testing device.

A crucial problem in such testing stems from the fact that the thickness of an adhesive has a major effect on its mechanical performance because of the adherend-adhesive boundary constraints and the small measurable displacements obtained in the case of commonly used adhesives, which are relatively very thin. These restrictions limited the available data [23,37,46,54] which originated in the work of Hughes and Rutherford [24]. The available information, which is mainly concerned with adhesive behavior under torsion and uniaxial tension, indicates the following: beyond approximately 0.25 mm, adhesive strength and effective modulus decrease moderately with adhesive thickness and tends to level off at a value close to that of the bulk material. Below this thickness, a steep increase in adhesive strength, and to a lesser degree, of effective tensile modulus, is evident.

During the past research year, shear strength data of adhesives *in situ* were evaluated by a specially constructed torsion device [65]. During the present year, this device was improved and modified by the attachment of a torsional displacement accessory (Fig. 33) which enabled the recording of the shear moment-displacement relationship by means of an Instron extensometer and recorder. The testing procedure is also more efficient because of the separation between the adhesive-adherend unit (which is exchangeable) and the measuring system.

6.2 Testing Procedure

The main objective of this test series was the evaluation of the initial shear characteristics at the linear elastic range far below the ultimate level. Hence, aluminum surfaces were not treated but only cleaned by MEK. The adhesive was composed of Shell resin 828 and General Mills Versamid V-140, in a ratio of 2:1. The adhesive was cast between the adherends' controlled spacing, which varied from 0.1 to 2.0 mm. Curing was for 24 hours at room temperature followed by 48 hours at 50°C.

After curing, the shear specimens were installed in the torsional device which was mounted on the Instron tester. Cross-head speed was 0.5 mm/min. For calibration, shear displacement of specimens composed of tightened adherends of zero adhesive thickness, were recorded to be deducted from the over-all shear displacement of the bonded specimens.

6.3 Results and Discussion.

Shear strains and stresses were computed from the recorded torsional moment-displacement curves by assuming linear shear-strain distribution throughout the adhesive thickness and uniform shear strain distribution at the corss-sectional area. Typical shear stress-strain relationships for different adhesive thicknesses are shown in Fig. 34. Low ultimate values were obtained due to the deliberately weak interfacial bonding. However, a qualitative difference can be distinguished between the behavior of relatively thin and thick adhesives, namely: larger ultimate strains at lower stress levels which may indicate higher ductility and are typical of thin adhesives compared with their thick counterparts.

Initial effective shear modulus values, which were derived from the stress-strain curves with the same assumptions, are shown in Fig. 35 as a function of adhesive thickness.

In spite of the reasonable scatter of the moduli data, the general trend is clear, i.e., an almost linear increase of modulus with an increase in thickness. The higher values of shear modulus, within the range of 90-110 kg/mm^2 found for thick adhesive layers (above h =1.0mm), are compatible with shear data obtained for the bulk epoxy material.

The conflicting evidence of higher effective tensile modulus of thin adhesive layers reported earlier can be settled by two arguments:

a. This trend was found to prevail below 0.1 mm.

b. The case of tensile loading where the lateral restraint of metal adherends reduced longitudinal deformations, is basically different from the relatively free and pure shear situation which prevailed in the torsional shear test.

6.4 Future Program.

The intension is to continue the present investigation along the following lines:

a. Study of the effect of adhesive thickness on tensile modulus, both experimentally and analytically, which will take into account the lateral constraint of adherends and the different characterstics of the interfacial adhesive boundary layers.

b. Taking the same approach, an experimental and analytical study of the effect of adhesive layer thickness on strength in shear and uniaxial tension

c. A device for combined shear-axial loading of adhesive *in situ* had been designed and will be utilized for deriving adhesive strength characteristics under combined states of stress. Resultant data, it is hoped, will provide the basis for evaluating failure envelopes of adhesives which is essential for strength prediction of the SMD model specifically, and for different adhesive bonded joint models in general.

7. SUMMARY AND GENERAL CONCLUSIONS

The present report consists of several topics concerned with stress and strain analysis of the interlaminar adhesive layer within a doubler model. The following conclusions were drawn:

a. Two dimensional stress distribution through IAL derived by the finite element method revealed the following characteristics:

i) Almost uniform shear and lateral normal stress distribution prevailed throughout the IAL thickness along its "middle zone".

ii) Extreme non-uniform distributions exist at the "boundary zone".

iii) Shear stresses attained their peak at the "boundary zone" and dropped steeply towards zero at the IAL edges, which is consistent with boundary and equilibrium conditions.

iv) Axial normal stresses, which were negligible at the IAL "boundary zone", attained the same order of magnitude as other interlaminar stresses along the "middle zone" close to the central adherend.

v) The principal interlaminar stresses reached their extreme value close to the intersection of the IAL edge and the IAL central adherend interface.

b. Stress distributions along the IAL which were determined by a direct measurement of shear and normal relative displacements, show good agreement with both analytical closed form solution and with numerical solution derived by finite element method.

c. Thermoelastic investigation of IAL stresses within symmetrical and nonsymmetrical doubler models showed good agreement between experimental measurements and analytical closed form solutions.

d. The stress-strain relationship of the adhesive layer *in situ*, when measured by a special torsion device, indicated that the adhesive shear modulus increased moderately with the thickness of the adhesive and approached the respective modulus of the bulk epoxy at a thickness of about 1.0 mm.

8. RECOMMENDATIONS FOR FUTURE RESEARCH

It is recommended that the present research be continued along the following lines (see Figs. 36,37):

a. Parametric study of the effects of variations in IAL thickness and its edge geometry, as well as its material characteristics (by FEM).

b. Two dimensional stress analysis of SMD at the nonlinear range of IAL behavior (by FEM).

c. Study of the elastic and thermoelastic three dimensional behavior of SMD.

d. Investigation of strength and failure characteristics of IAL within SMD as related to respective behavior of adhesive *in situ*, under combined loading.

e. Investigation of the environmental effects (temperature and humidity) on IAL mechanical behavior, as reflected by SMD performance.

BIBLIOGRAPHY

ADHESIVE BONDED JOINTS

1. C.E. Inglis, Stress Distribution in a Rectangular Plate Having Two opposing Edges Sheared in Opposite Directions. Proc. Royal Soc. London, Series A., 103, pp. 598-610 (1923).

2. O. Volkersen, Luftfahrtforschung, 15, pp. 41-47 (1938).

3. N.A. DeBruyne, The Strength of Glued Joints, Aircraft Engineering, 16, pp. 115-118 (1944).

4. M. Goland and E. Reissner, The Stresses in Cemented Joints, J. of Applied Mechanics, 11(1), pp. A17-A27 (1944).

5. F.J. Plantema, The Shear Stress in a Glued Joint, National Lucht. Lab., Amsterdam, Report M 1181 (1949).

6. B.J. Aleck, J. of Applied Mechanics, 16, p. 118 (1949).

7. R.W. Cornell, Determination of Stress in Cemented Lap Joints, J. of Applied Mechanics, 20(3), pp. 355-364 (1953).

8. L.R. Demarkles, Investigation of the use of a rubber analog in the study of stress distribution in rivited and cemented joints, Tech. Notes, 3413 (1955).

9. C. Mylonas, Experiments on Composite Models with Applications to Cemented Joints, Proceedings of the Spring Meeting of the Society for Experimental Stress Analysis, 12(2), p. 129 (1955).

10. R.E. Sherrer, Stress in a Lap Joint with Elastic Adhesive, USDA Forest Products Lab. Report No. 1864 (1957).

11. A.S. McLaren and I. Madnnes, British J. of Applied Physics, 9, p.72 (1958).

12. A. Hartman and J.B. DeJange, Nondestructive Tests on Redux Bonded Single and Double Lap Joints with Various Glue Line Thicknesses, NAARI, Amsterdam (1960).

13. K.T.S. Iyengar and R.S. Alwar, Proc. Seventh Congress of Theoretical and Applied Mechanics, Bombay (1961).

14. D.D. Eley (Ed.), Adhesion, Oxford University Press, pp. 207-226 (1961).

15. E.W. Kuenzi and G.H. Stevens, Determinator of the Mechanical Properties of Adhesives for Use in the Design of Bonded Joints, US-FPL Report FPL-011 (1963).

16. A. Matting, Grenzflachen-reaktionen and spannungs-verteilung in metall-klebverbindungen", Kunstoffe,16, Jahrgang Nr 7, 387 (1963).

17. C.H. Lerchenthal, Design of Bonded Lag Joints for Optimum Stress Transfer, Part 1: The Symmetrical (or double) Lap Joint, Israel J. of Technology, 2(1) (1964).

18. O. Volkersen, Construction métalliane, No.4, pp. 3-13 (1965).

19. B.F. Prokhorov, Joints Used in Plastic and Composite Shipboard Super Structures, Deckhouses, Light Bulkheads and Enclosures, Sudostroyeniye, 9, pp. 44-51 (1965).

20. J.I. Gnopp, Measurement of Moments at Edges of Adhesive Lap Joints between Glass-Reinforced Plastic Laminates, Picatinny Arsenal T.M. 1932, (1965).

21. F. Szepe, Strength of Adhesive Bonded Lap Joints with Respect to Change of Temperature and Fatigue, Exper. Mech., 6, pp. 280-286 (1966).

22. A.J. Durelli and V.J. Parks, Experimental Stress Analysis of Loaded Boundaries in Two-Dimensional Second Boundary Value Problems, Report No. 11, Contract No. 2249(06)(1967).

23. G.A. Clark and K.I. Clayton, Structural Techniques for Joining Filamentary Composites, AIAA 5th Annual Meeting, Paper No. 68-1038 (1968).

24. E.J. Hughes, J.L. Rutherford, Study of Micromechanical Properties of Adhesive Bonded Joints, Aerospace Research Center, General Precision Systems, Technical Report 3744 (1968).

25. D. Kutscha et al., Feasibility of Joining Advanced Composite Flight Vehicle Structures, IIT Res. Inst. Technical Report AFML-TR-68-391 (1969).

26. L.J. Hart-Smith, The Strength of Adhesive Bonded Double Lap Joints, IRAD Report, No. MDC - J0367, November 1969.

27. V. Nieorgon, Bonded Joints, A Photoelastic Study, UTIAS Technical Note No. 138 (1970).

28. J.L. Lubkin and L.C. Lewis, Adhesive Shear Flow for an Axially Loaded, Finite Stringer Bonded to an Infinite Sheet, The Quarterly Journal of Mechanics and Applied Math., Vol. XXIII, Part 4, pp. 520-533 (1970).

29. A. Puppo and H. Evenson, Calculation and Design of Joints Made from Composite Materials, USA AV Labs Tech. Report 70-27, U.S. Army Material Laboratories (1970).

30. G.C. Grimes, Stress Distribution in Adhesive Bonded Lap Joints, SAE Transactions, 370-378 (1971)

31. V. Niranjan, Bonded Structures and the Optimum Design of a Joint, Technical Note No. 164, UTIAS (1971).

32. V. Niranjan, D.R. Hamel and C.A. Yang, Static and Fatigue Strength of FM-132-2 Adhesive in Double Strap Joints of Various Lengths of Overlap, UTIAS Technical Note No. 160 (1971).

33. G.R. Wooley and D.R. Carver, Stress Concentration Factors for Bonded Lap Joints, J. Aircr., 8, pp. 817-820 (1971).

34. F. Erdogan and M. Ratwani, Stress Distribution in Bonded Joints, J. Composite Materials, 5, pp. 378-393 (1971).

35. T. Hata, Mechanisms of Adhesive Failure, J. Adhesion, 4, pp. 161-170 (1971).

36. J.N. Dickson, T.M. Hsu and M.J. McKinney, Development of an Understanding of the Fatigue Phenomenal of Bonded and Bolted Joints in Advanced Filamentary Composite Materials, Vol. 1, Analysis Methods. Technical Report AFFDL-TR-72-64 (1972).

37. N. Correlli, Design of Bonded Joints in Composite Materials, NASA Res. Center, Proc. of the Symp. on Welding, Bonding and Fastening, 297-300 (1972).

38. T. Hayashi, Creep Analysis of a Bonded Lap Joint, Composite Materials and Structures, 1(2), pp. 58-63 (1972).

39. G.D. Grimes et al., The Development of Non-Linear Analysis Methods for Bonded Joints in Advanced Filamentary Composite Structures, Technical Report AFFDL-TR-72-97 (1972).

40. R.D. Adams and N.A. Peppiatt, Effect of Poisson's Ratio Strains in Adherends on Stress of an Idealized Lap Joint, J. of Strain Analysis, 8, pp. 134-139 (1973).

41. W.J. Renton and J.R. Vinson, The Analysis and Design of Composite Material Bonded Joints Under Static and Fatigue Loadings, AFOSR-1760-72, Scientific Report AFOSR-TR-73-1627 (1973).

42. L.J. Hart-Smith, Analysis and Design of Advanced Composite Bonded Joints, Final Report NASA CR-2218 (1973).

43. L.J. Hart-Smith, Adhesive-Bonded Double-Lap Joints, NASA Contract Report No. NASA-CR-112235 (1973).

44. L.J. Hart-Smith, Adhesive-Bonded Single-Lap Joints, NASA Contract Report No. NASA-CR-112236 (1973).

45. L.J. Hart-Smith, Adhesive Bonded Scarf and Stepped Lap Joints, NASA Contract Report No. NASA-CR-112237 (1973).

46. L.J. Hart-Smith, Non-Classical Adhesive Bonded Joints in Practical Aerospace Construction, NASA Contract Report No. NASA_CR-112238 (1973).

47. R.M. Barker and F. Hatt, Analysis of Bonded Joints in Vehicular Structures, AIAA Journal, 11(12), pp. 1650-1654 (1973).

48. T. Akasaka and M. Hirano, An Analytical Study on Shear Strength of Lap Joints, Composite Material and Structures, 2(4), pp. 1-4 (1973).

49. R.B. Krieger, Evaluating Structural Adhesives under Sustained Load in Hostile Environment, SAMPE Quart, 5, p.42 (1973).

50. J.E. Lohr, Factors Affecting the Survivability of Stressed Bonds in Adverse Environments, 18th National SAMPE Symposium, 18, pp. 418-426 (1973).

51. R.D. Adams and N.A. Peppiatt, Stress Analysis of Adhesive-Bonded Lap Joints, J. of Strain Analysis, 9(3) (1974).

52. J. Pirvics, Two Dimensional Displacement-Stress Distributions in Adhesive Bonded Composite Structures, J. Adhesion (6), pp. 207-228 (1974).

53. C.K. Lim, M.A. Acitelli and W.C. Haman, Failure Criterion of a Typical Polyamide Cured Epoxy Adhesive, J. Adhesion, 6, pp. 281-288 (1974).

54. E.E. House, Jr. and J.A. White, Adhesive Bonding Increases Fatigue Life of Wing Joint, AIAA Paper No. 74-382 (1974).

55. W.J. Renton and J.R. Vinson, On Fatigue Behavior of Bonded Joints in Composite Materials Structures, AIAA Paper No. 74-484 (1974).

56. W.J. Renton and J.R. Vinson, Fatigue Response of Anisotropic Adherend Bonded Joints, AMMRC MS 74-8, pp. 7-22 (1974).

57. W.N. Sharpe, Jr. and T.J. Muha, Jr., Comparison of Theoretical and Experimental Shear Stress in the Adhesive Layer of a Lap Joint Model, AMMRC MS 74-8, pp. 23044 (1974).

58. W.J. Renton and J.R. Vinson, The Analysis and Design of Anisotropic Bonded Joints, Report No. 2, AFOSR-TR-75-0125 (1974).

59. M.N. Reddy and P.K. Sinha, Stress in Adhesive Bonded Joints for Composites, Fiber Sci. & Tech., 8(1), pp. 33-47 (1975).

60. W.D. Bascom, Adhesive Fracture Behavior of Elastomer-Modified Epoxy Resin, Porc. of 30th Donf. SPI Reinforced Plastics/ Composites Institute, Section 22-D (1975).

61. S. Srinivas, Analysis of Bonded Joints, NASA TN D-7855, 50 pp. (1975).

62. L.M. Keer and K. Chantaramungkorn, Stress Analysis for a Double Lap Joint, J. Applied Mechanics, p.353, June (1975).

63. W.J. Renton and J.R. Vinson, Fatigue Behavior of Bonded Joints in Composite Material Structures, J. Aircraft, 12, pp.442-447 (1975).

64. A.W. Bethune, Durability of Bonded Aluminum Structure, SAMPE J., pp. 4-10 (1975).

65. O. Ishai, D. Peretz and N. Galili, Mechanical Behavior of Multimaterial Composite Systems, Final Technical Report, Contract No. DAJA-37-74-C-2531, January (1975).

INTERLAMINAR BEHAVIOR

66. R.A. Heller, Interlaminar Shear Stress in Sandwich Beams, Technical Report No. 33, Contract No. Nonr 266(78) (1967).

67. A.H. Puppo and H.A. Evensen, Interlaminar Shear in Laminated Composites Under Generalized Plane STress, J. Composite Materials, 4, 204-220 (1970).

68. R.B. Pipes and N.J. Pagano, Interlaminar Stresses in Composite Laminates Under Uniform Axial Extension, J. Composite Materials, Vol. 4, pp. 538-548 (1970).

69. N.J. Pagano and R.B. Pipes, The Influence of Stacking Sequence on Laminate Strength, J. Composite Materials, 5, pp. 50-57 (1971).

70. R.B. Pipes and I.M. Daniel, Moiré Analysis of the Interlaminar Shear Edge Effect in Laminated Composites, J. Composite Materials, 5, pp. 255-259 (1971).

71. A. Levy, H. Armen, Jr. and J. Whiteside, Elastic and Plastic Interlaminar Shear Deformation in Laminated Composites Under Generalized Plane Stress, Airforce Third Conf. on Matrix Methods in Structural Mechanics, W-P AFB, Ohio, pp. 19-21 (1971).

72. R.A. Heller and G.W. Swift, Solutions for the Multilayer Timoshenko Beam, Project THEMIS, Contract No. DAA-F07-70-C-0444 (1971).

73. R.B. Pipes, Interlaminar Stress in Composite Laminates, Technical Report AD-776-053, Air Force (1972).

74. J.M. Whitney, Stress Analysis of Thick Laminated Composite and Sandwich Plates, J. Composite Materials, 6, pp. 426-440 (1972).

75. J.M. Whitney and C.E. Browning, Free-Edge Delamination of Tensile Coupons, J. Composite Materials, 6, pp. 300-303 (1972).

76. J.M. Whitney, Free-Edge Effects in the Characterization of Composite Materials, ASTM STP 521, pp. 167-180 (1973).

77. G.B. McKenna, J.F. Mandell and F.J. McGurry, Interlaminar Strength and Toughness of Fiberglass Laminates, 29th Annual Technical Conf., Section 13-C, pp. 1-8 (1974).

78. C.W. Bert and P.H. Francis, Composite Material Mechanics: Structural Mechanics, AIAA J., 12(9), pp. 1173-1186 (1974).

GLOSSARY

C_{ij}	- Structural parameters of NMD
c	- length of IAL ($c = \ell/2$)
$E_0, E_1, E_2, (E_i)$	- Young's moduli of IAL, CAL and EAL, respectively
F	- axial applied force per unit width
G_0	- shear modulus of IAL
$\bar{H}$	- measure of NMD thickness
h_0, h_1, h_2	- thickness of IAL, CAL and EAL, respectively
K_i	- constants
ℓ	- IAL length ($\ell=2c$)
$M_2=M$	- moment function along the EAL
$N_1, N_2=N$	- normal force along the CAL and EAL, respectively
p_c	- effective applied axial normal stress
p_0	- reference axial stress acting on EAL under uniform axial strain
P	- axial applied force
R	- structural parameter of NMD
T	- temperature difference
u	- displacement in x-direction
$V_2=V$	- shear force along EAL
w	- displacement in z-direction
x,y,z	- axial, transverse and lateral coordinates, respectively

α_i - coefficient of thermal expansion

γ_0 - shear strain at IAL

δ - material and geometrical constant

$\varepsilon_0, \varepsilon_1, \varepsilon_2$ - axial normal strain at IAL, CAL and EAL, respectively

η - material and geometrical constant

λ - material and geometrical constant

μ - material and geometrical constant

ν, ν_0 - Poisson's ratio of adherend and adhesive layers respectively

ρ - curvature of beam

$\tau_{zx0} = \tau_0$ - axial shear stress (in x-direction) activing at IAL

τ_{zy0} - transverse shear stress (in y-direction) acting at IAL

$\sigma_{z0} = \sigma_0$ - lateral normal stress (in z-direction) acting at IAL

$\sigma_{x0}, \sigma_{x1}, \sigma_{x2}$ - longitudinal normal stresses acting at IAL, CAL and EAL respectively

σ_{y0} σ_{y1} σ_{y2} - transverse normal stresses acting at IAL, CAL and EAL respectively

ϕ - material and geometrical constant

χ - non-dimensional axial coordinate

SMD - symmetrical doubler model

NMD - nonsymmetrical doubler model

IAL - interlaminar adhesive layer

CAL - central adherend layer

EAL - external adherend layer

FRP - fiber reinforced plastics

SLJ - single lap joint

DLJ - double lap joint

FEM - finite element method

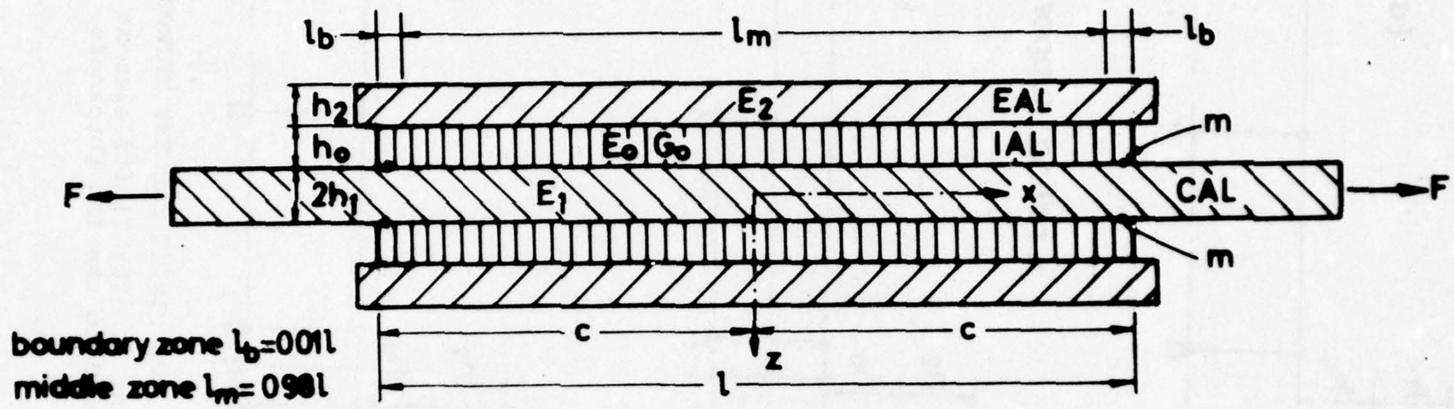

FIG. 1 SYMMETRICAL DOUBLER MODEL.

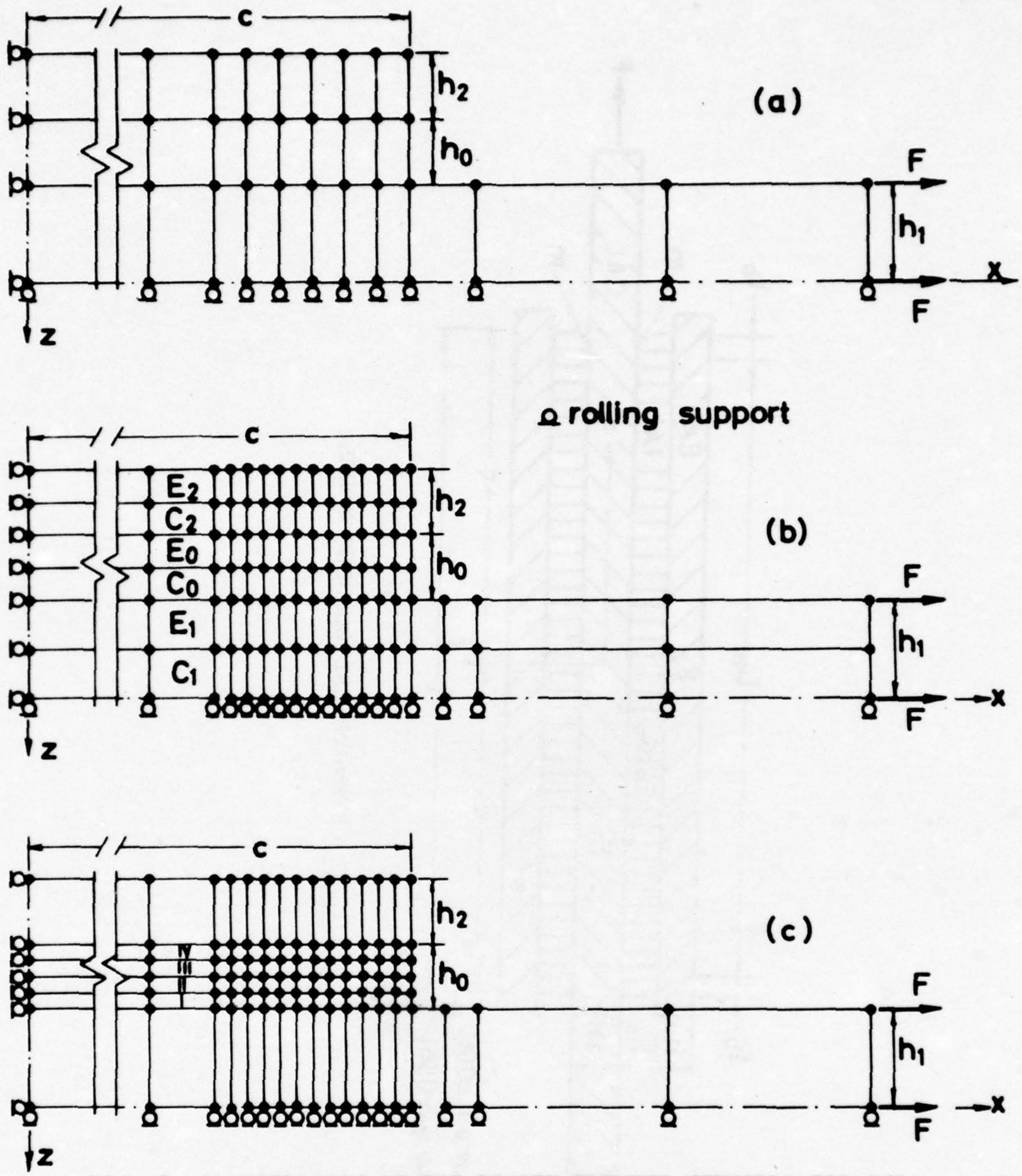

FIG. 2 ILLUSTRATION OF THE FINITE ELEMENT NETWORKS FOR SMD.
(a) finite element 1. (b) finite element 2.
(c) distribution along the IAL thickness.

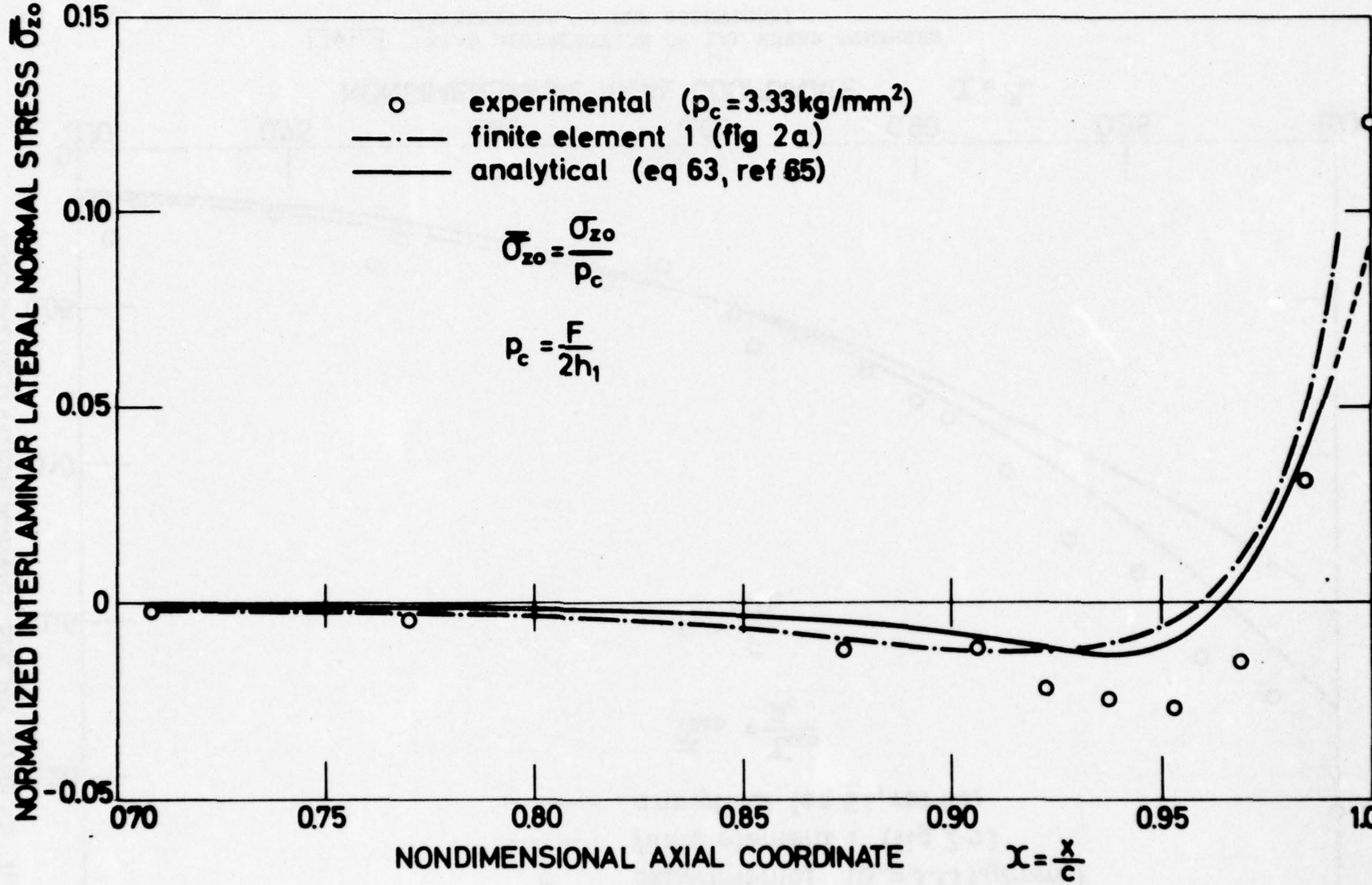

FIG. 3 AXIAL DISTRIBUTION OF IAL LATERAL NORMAL STRESSES (ANALYTICAL VS FEM SOLUTIONS).

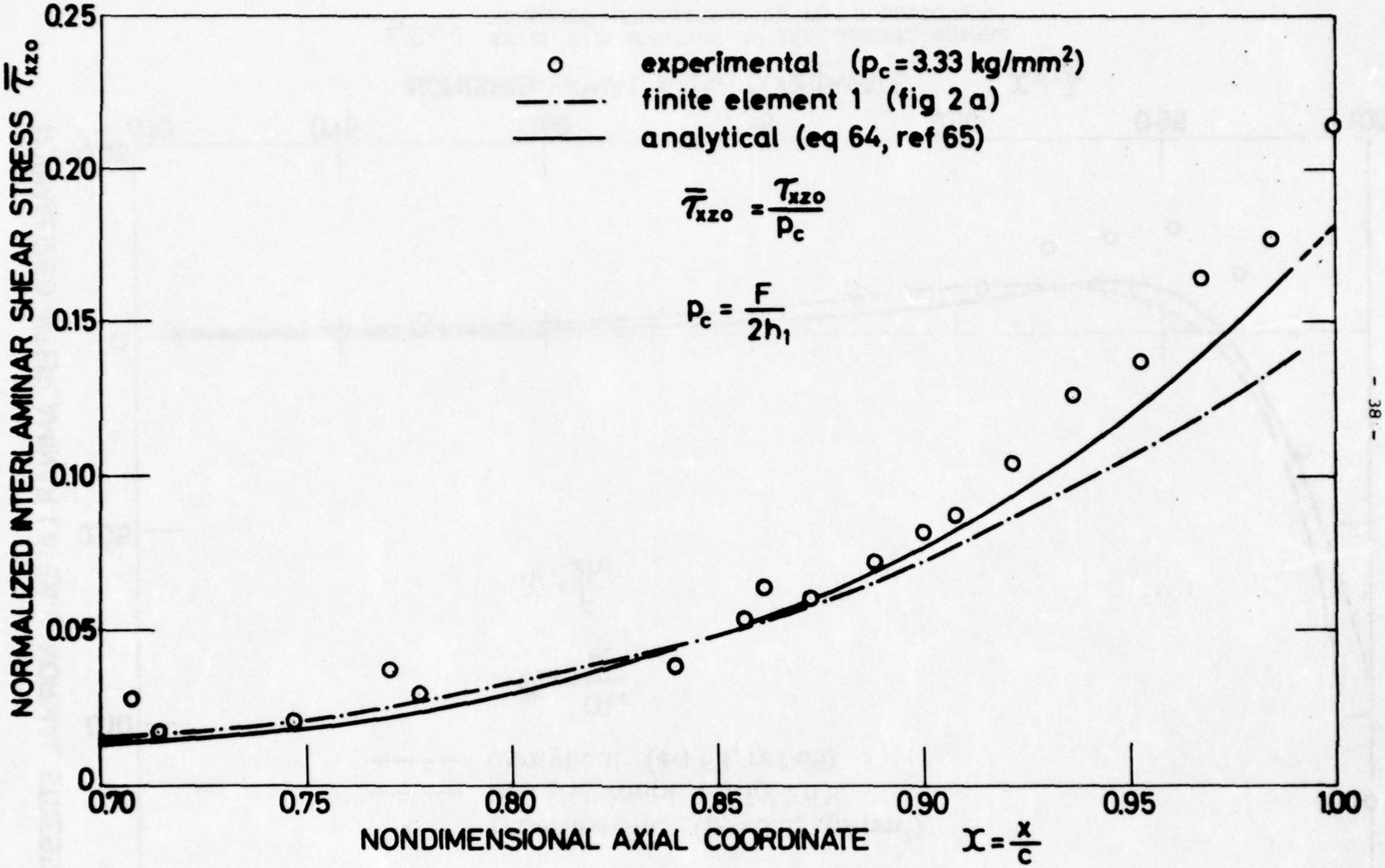

FIG. 4 AXIAL DISTRIBUTION OF IAL SHEAR STRESSES (ANALYTICAL VS FEM SOLUTIONS).

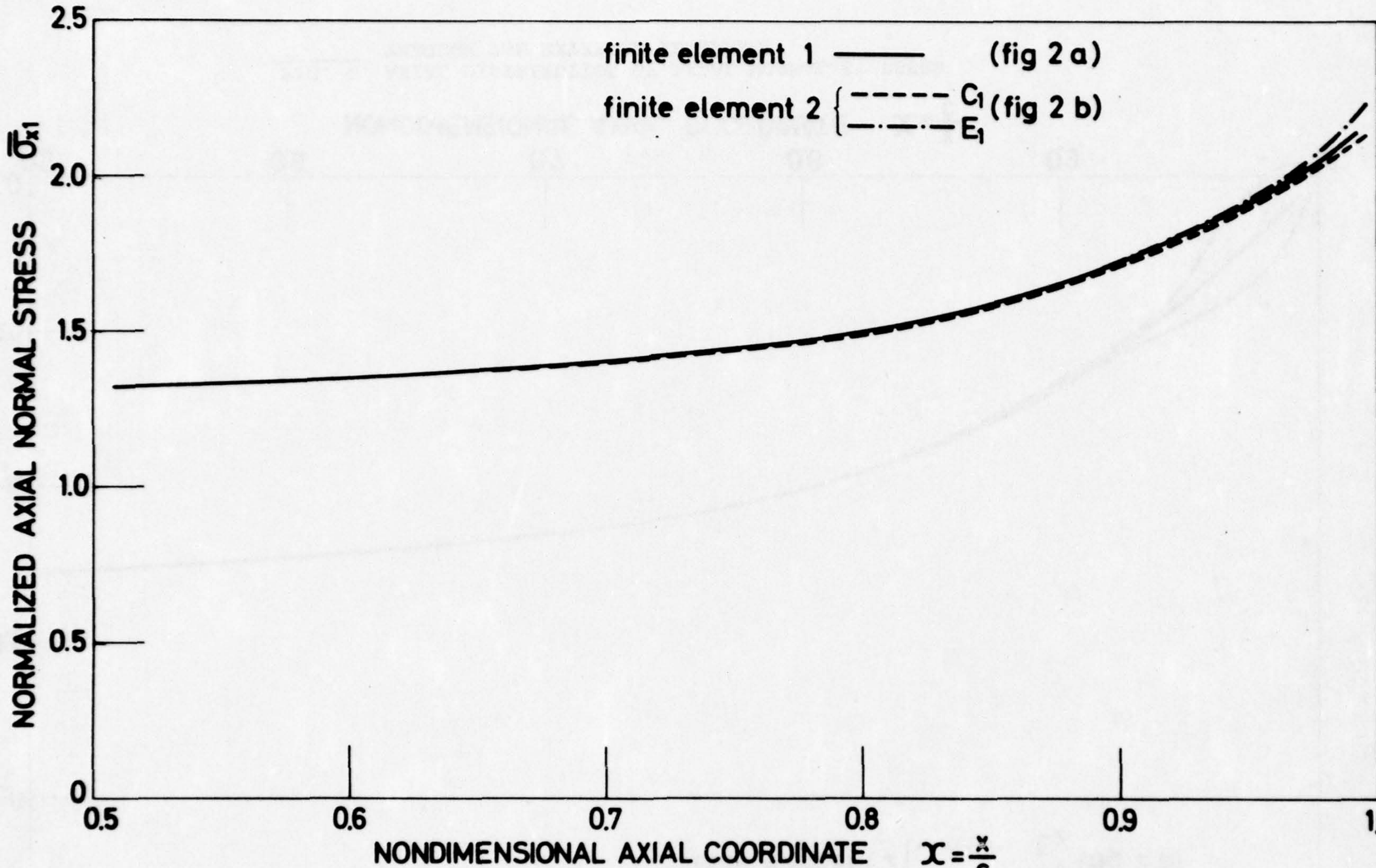

FIG. 5 AXIAL DISTRIBUTION OF AXIAL NORMAL STRESSES THROUGH THE CENTRAL ADHEREND.

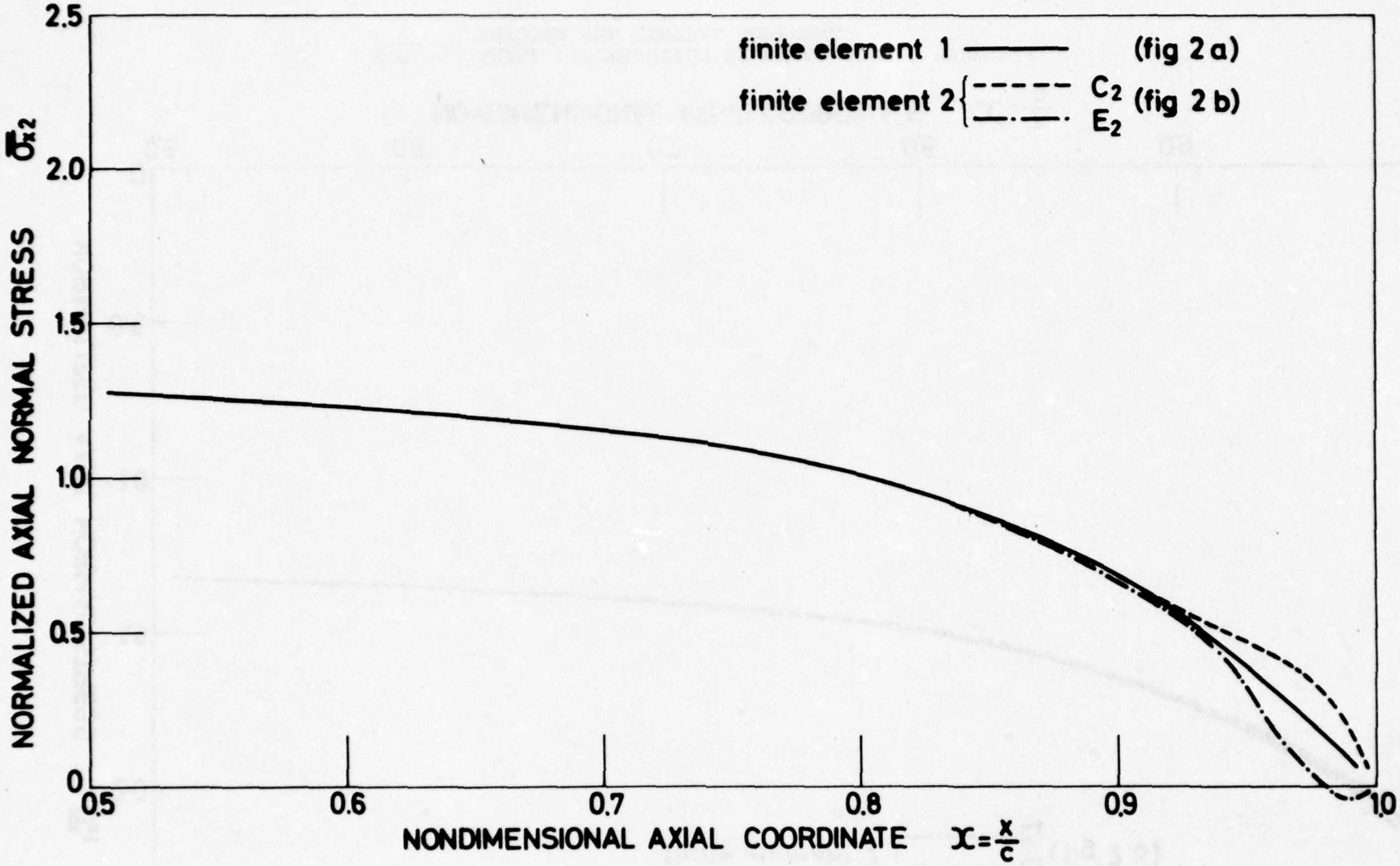

FIG. 6 AXIAL DISTRIBUTION OF AXIAL NORMAL STRESSES THROUGH THE EXTERNAL ADHERENDS.

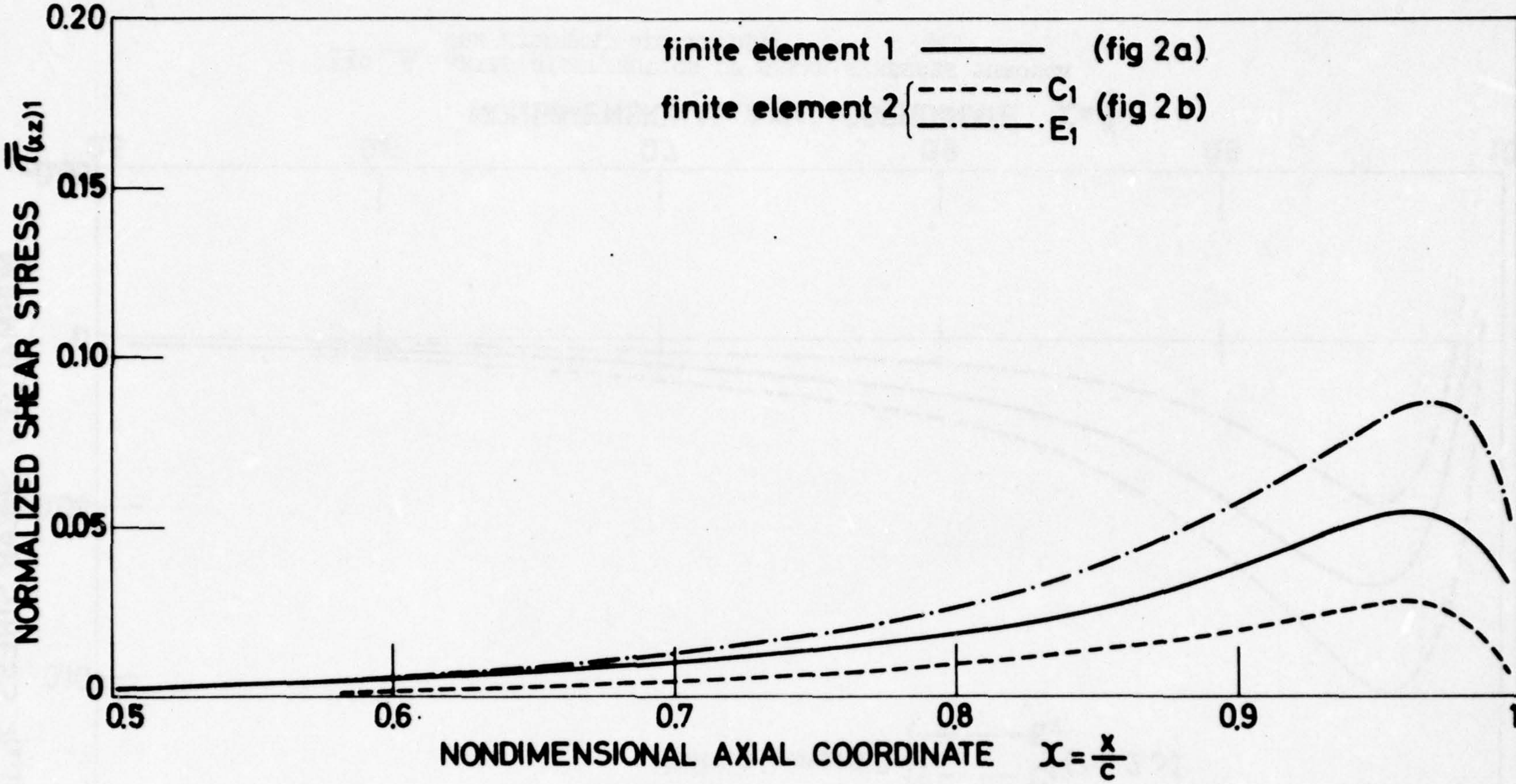

FIG. 7 AXIAL DISTRIBUTION OF SHEAR STRESSES THROUGH THE CENTRAL ADHEREND.

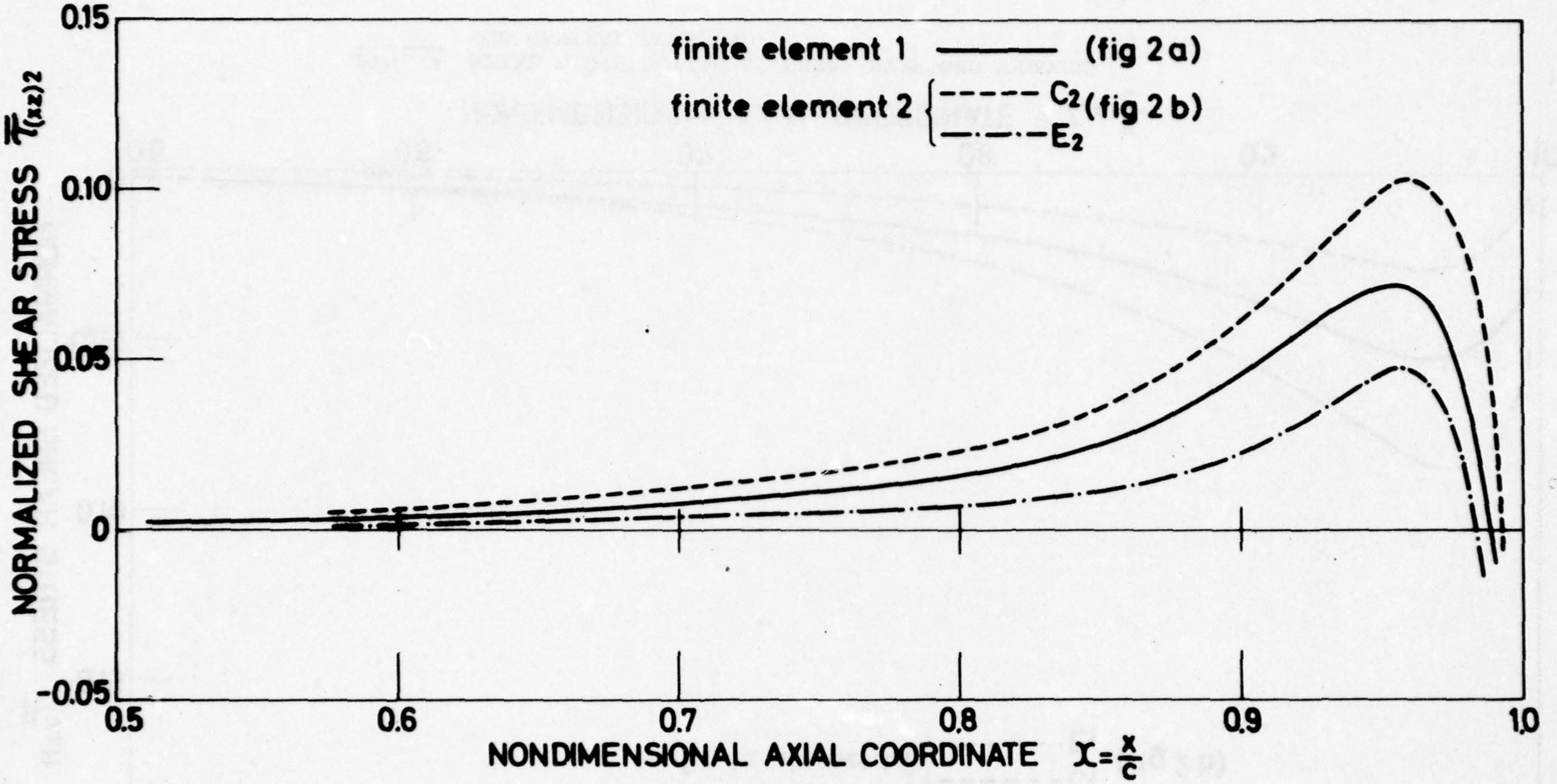

FIG. 8 AXIAL DISTRIBUTION OF SHEAR STRESSES THROUGH THE EXTERNAL ADHERENDS.

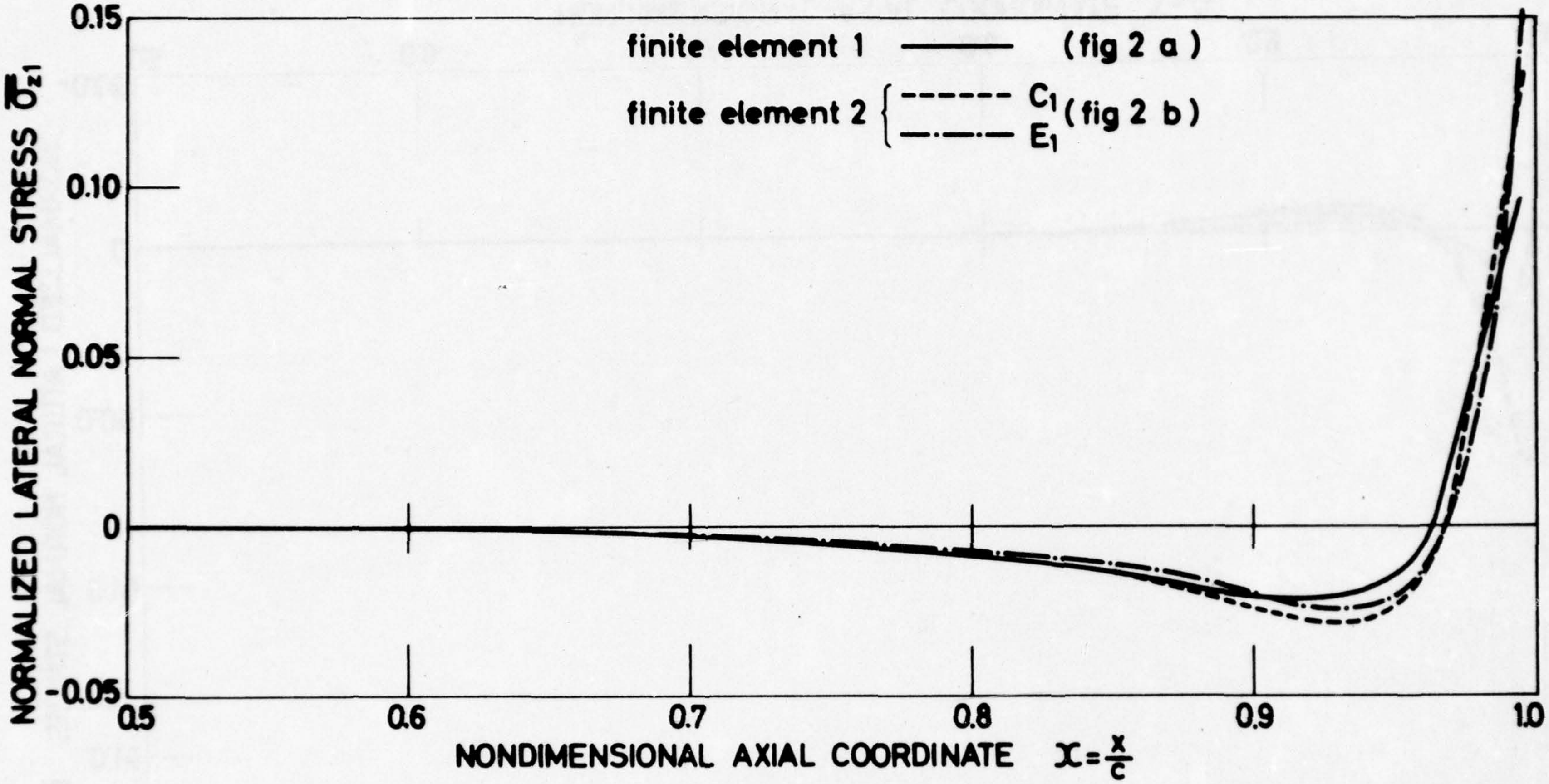

FIG. 9 AXIAL DISTRIBUTION OF LATERAL NORMAL STRESSES THROUGH THE CENTRAL ADHEREND.

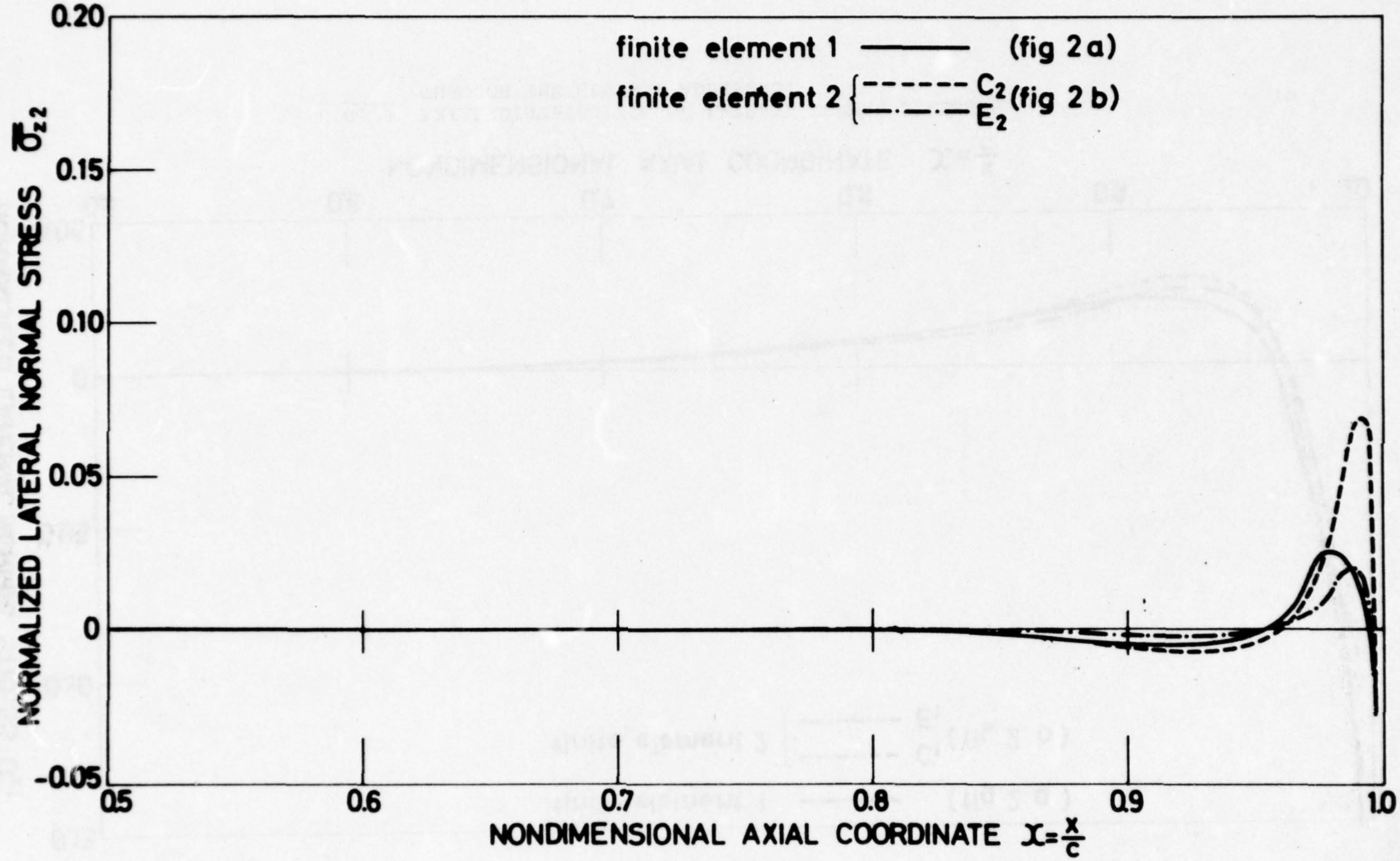

FIG. 10 AXIAL DISTRIBUTION OF LATERAL NORMAL STRESSES THROUGH THE EXTERNAL ADHERENDS.

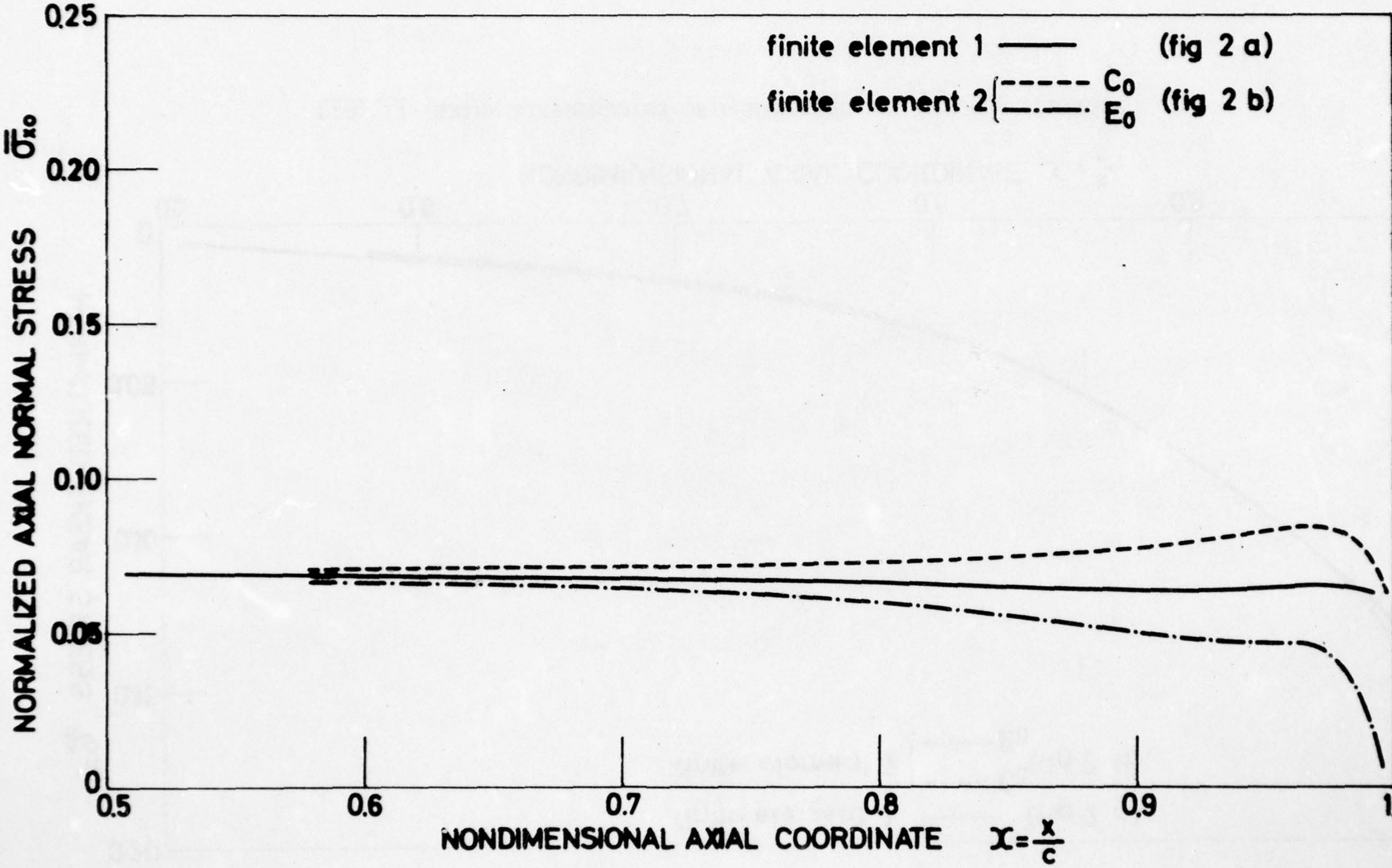

FIG. 11 AXIAL DISTRIBUTION OF AXIAL NORMAL STRESSES THROUGH THE IAL.

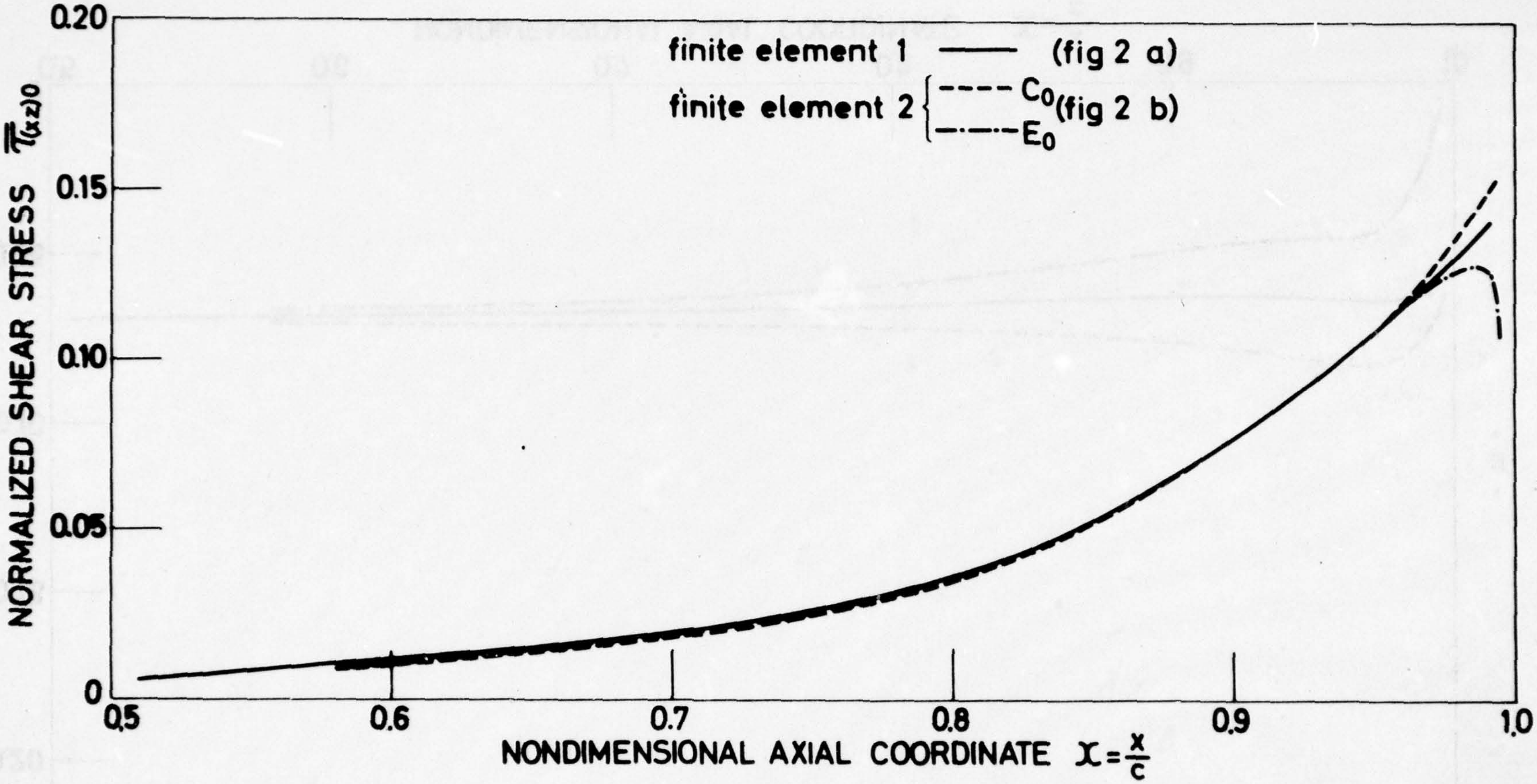

FIG. 12 AXIAL DISTRIBUTION OF SHEAR STRESSES THROUGH THE IAL.

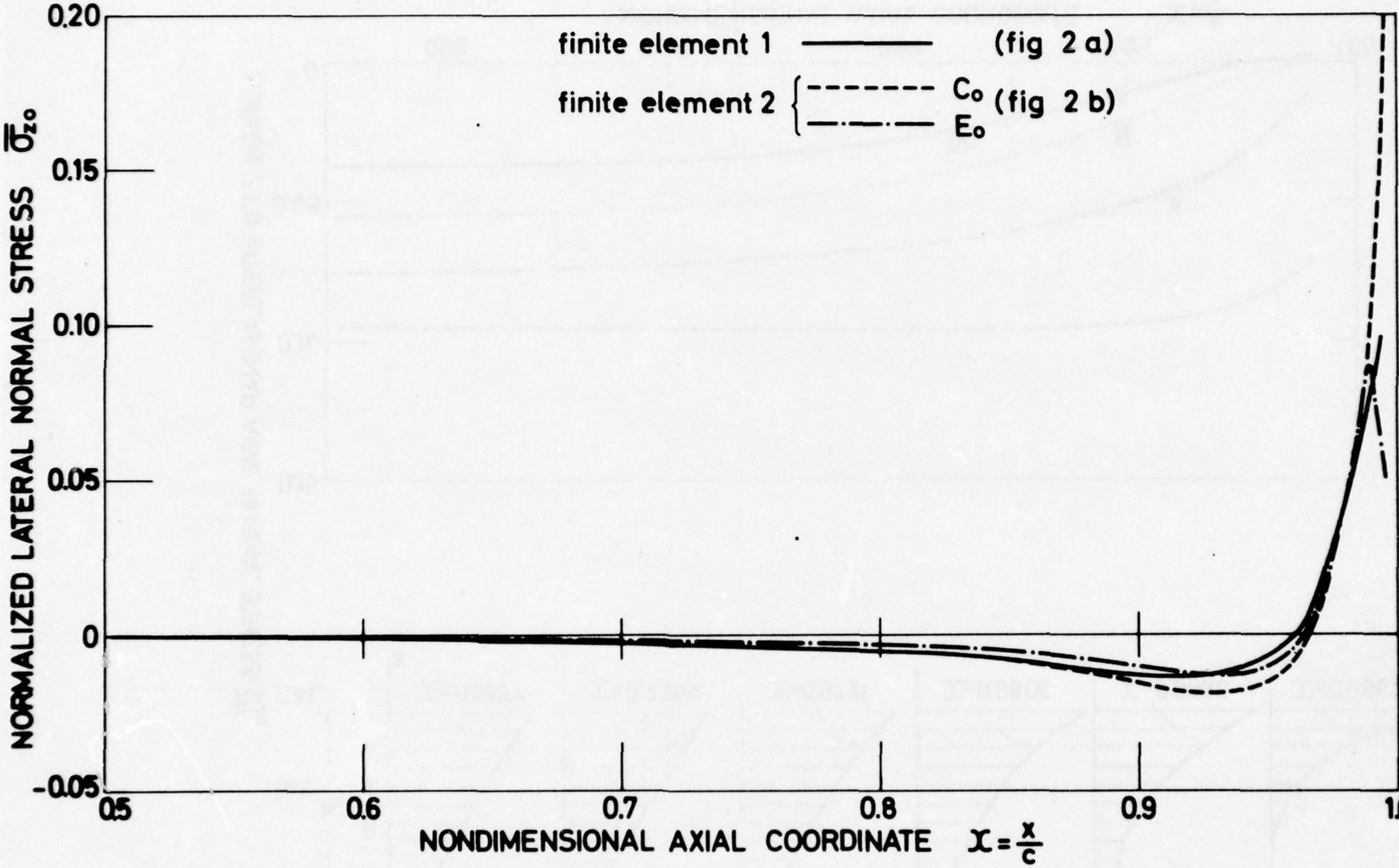

FIG. 13 AXIAL DISTRIBUTION OF LATERAL NORMAL STRESSES THROUGH THE IAL.

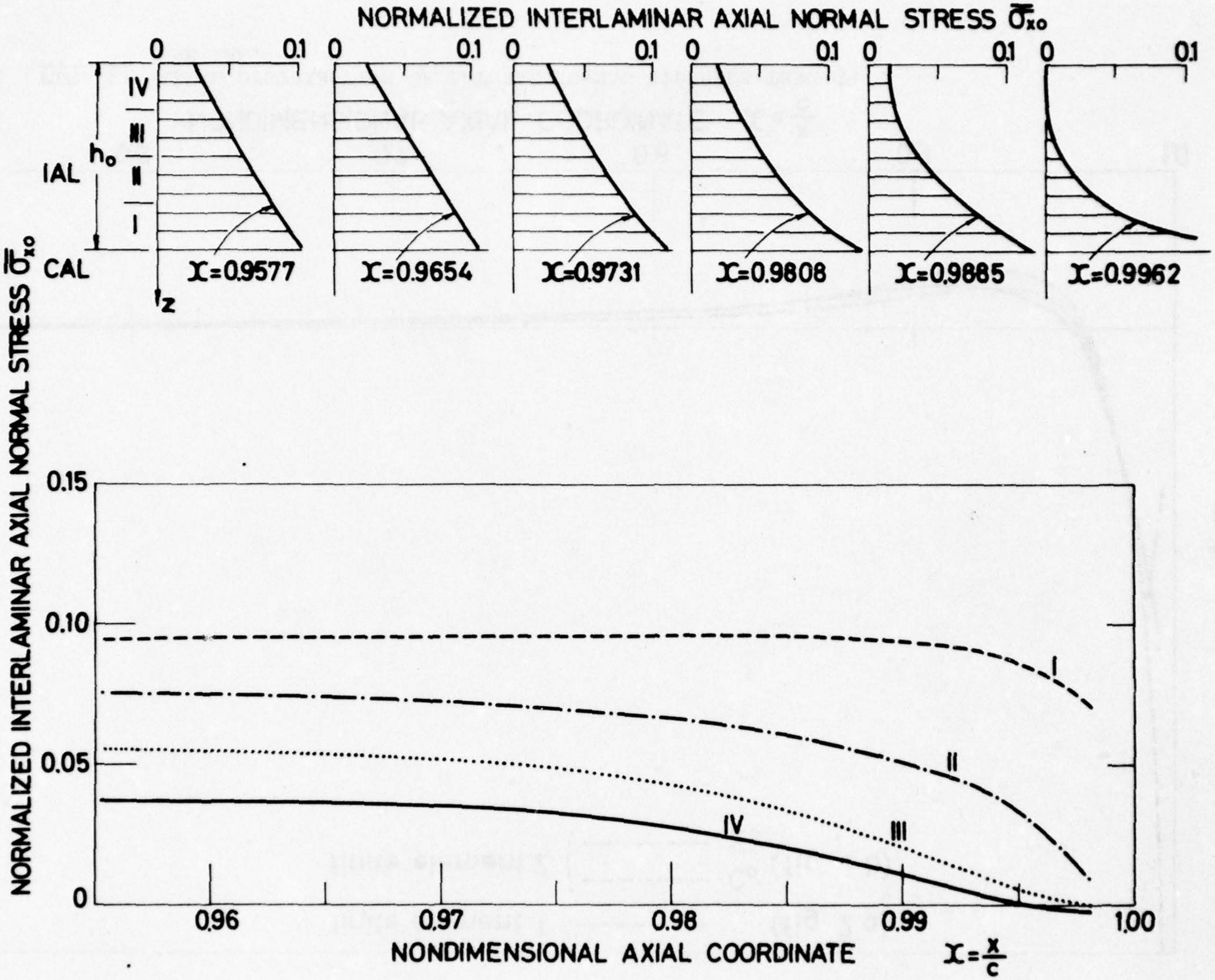

FIG. 14 DISTRIBUTION OF AXIAL NORMAL STRESSES CLOSE TO THE IAL EDGES.

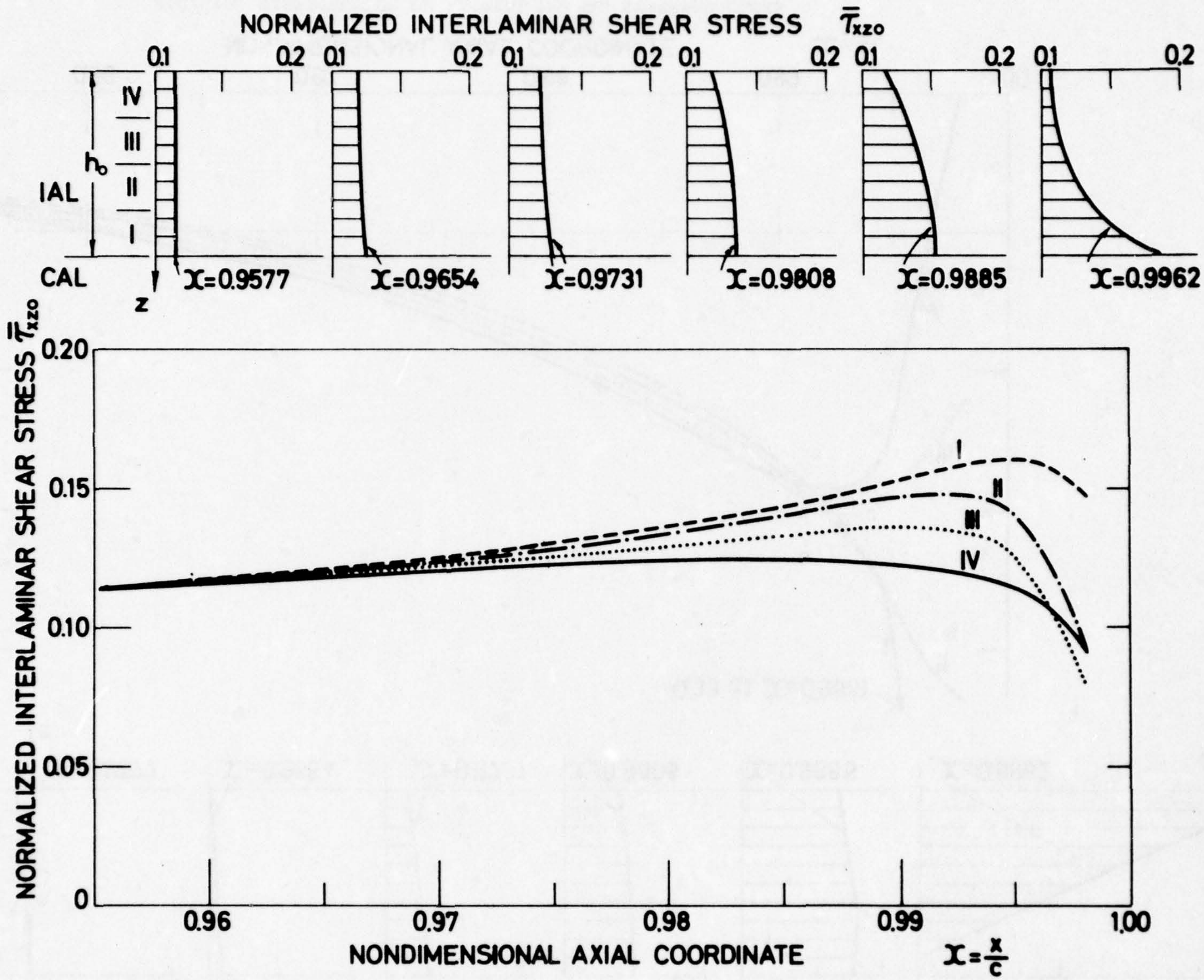

FIG. 15 DISTRIBUTION OF SHEAR STRESSES CLOSE TO THE IAL EDGES.

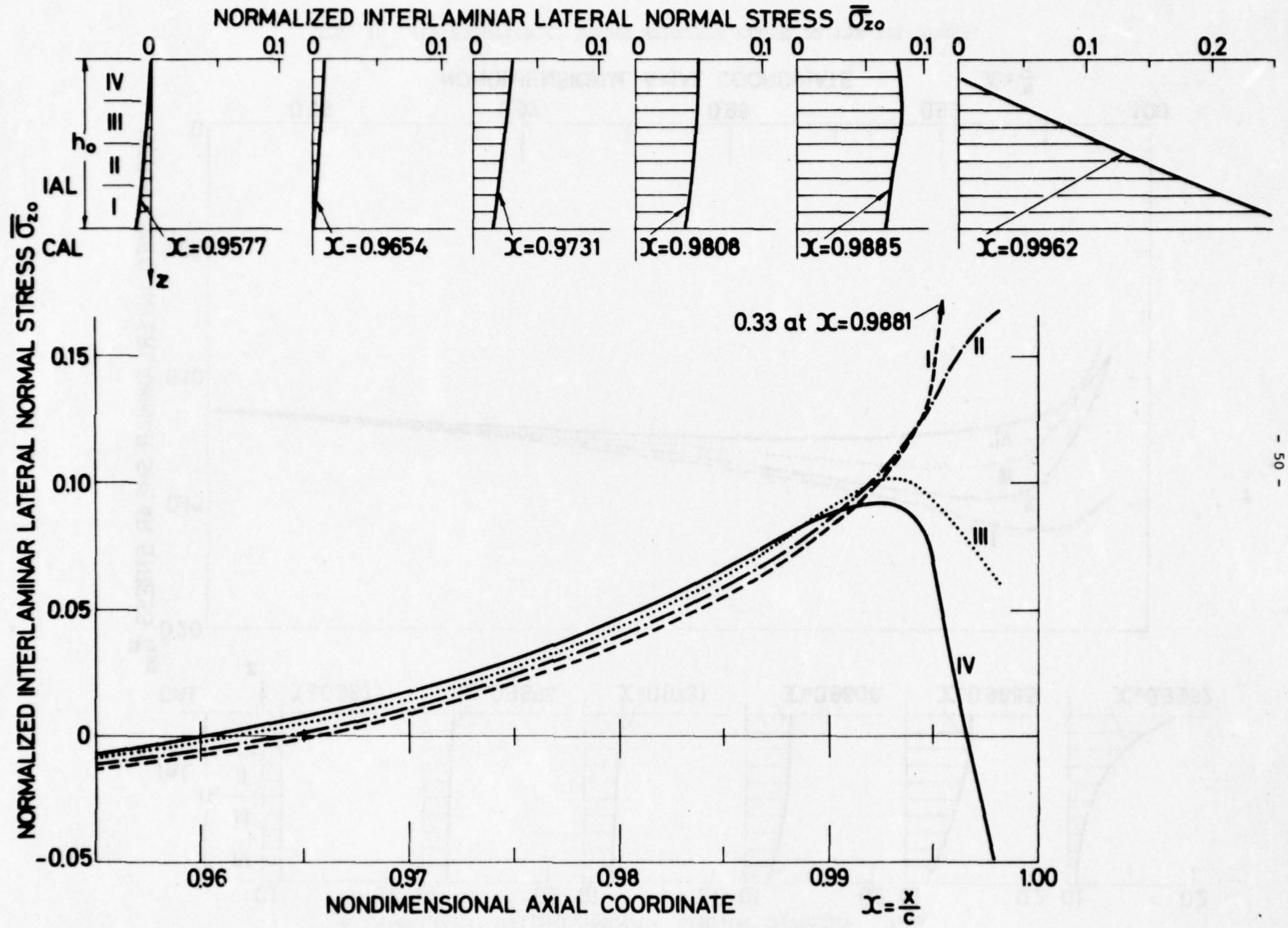

FIG. 16 DISTRIBUTION OF LATERAL NORMAL STRESSES CLOSE TO THE IAL EDGES.

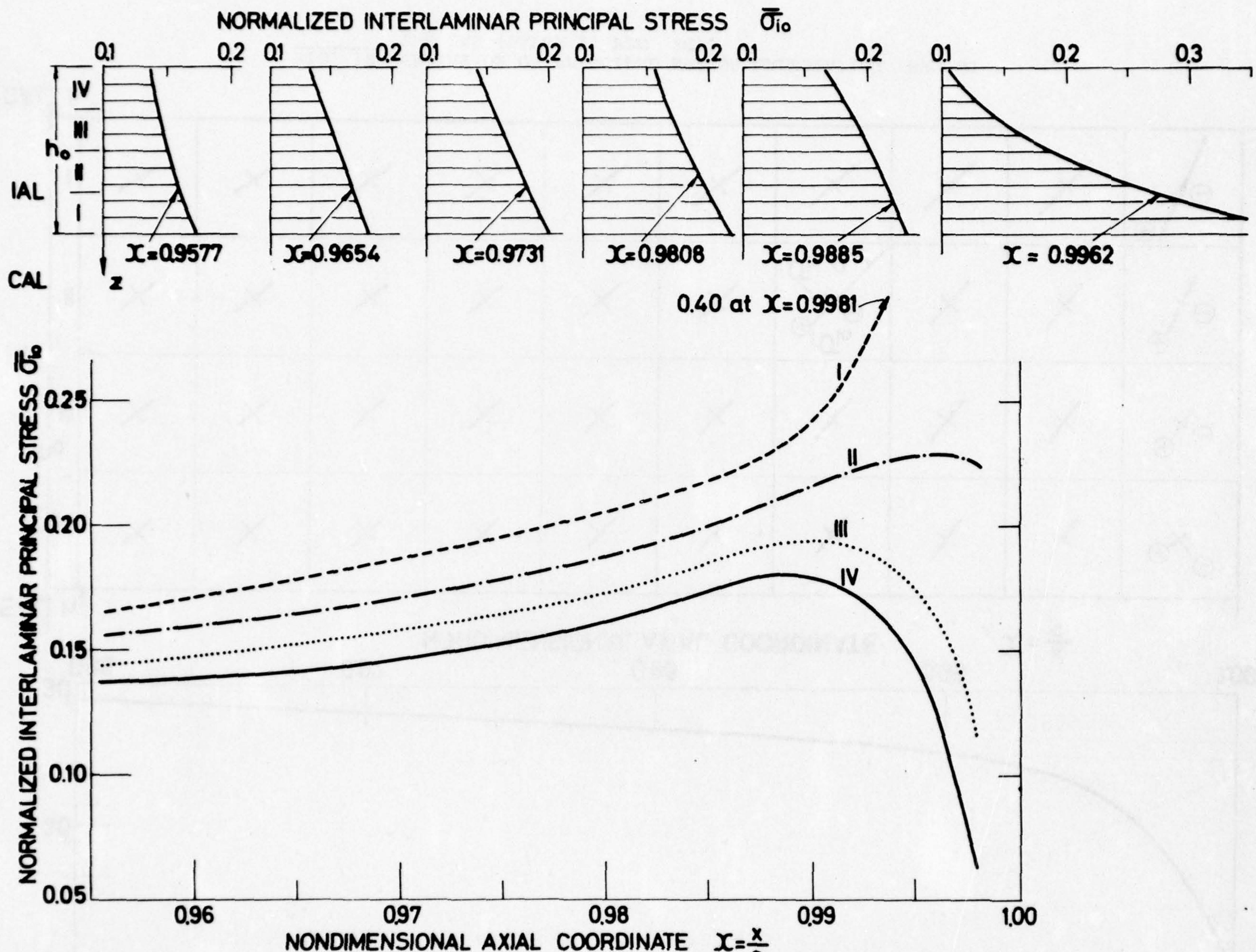

FIG. 17 DISTRIBUTION OF PRINCIPAL STRESSES CLOSE TO THE IAL EDGES.

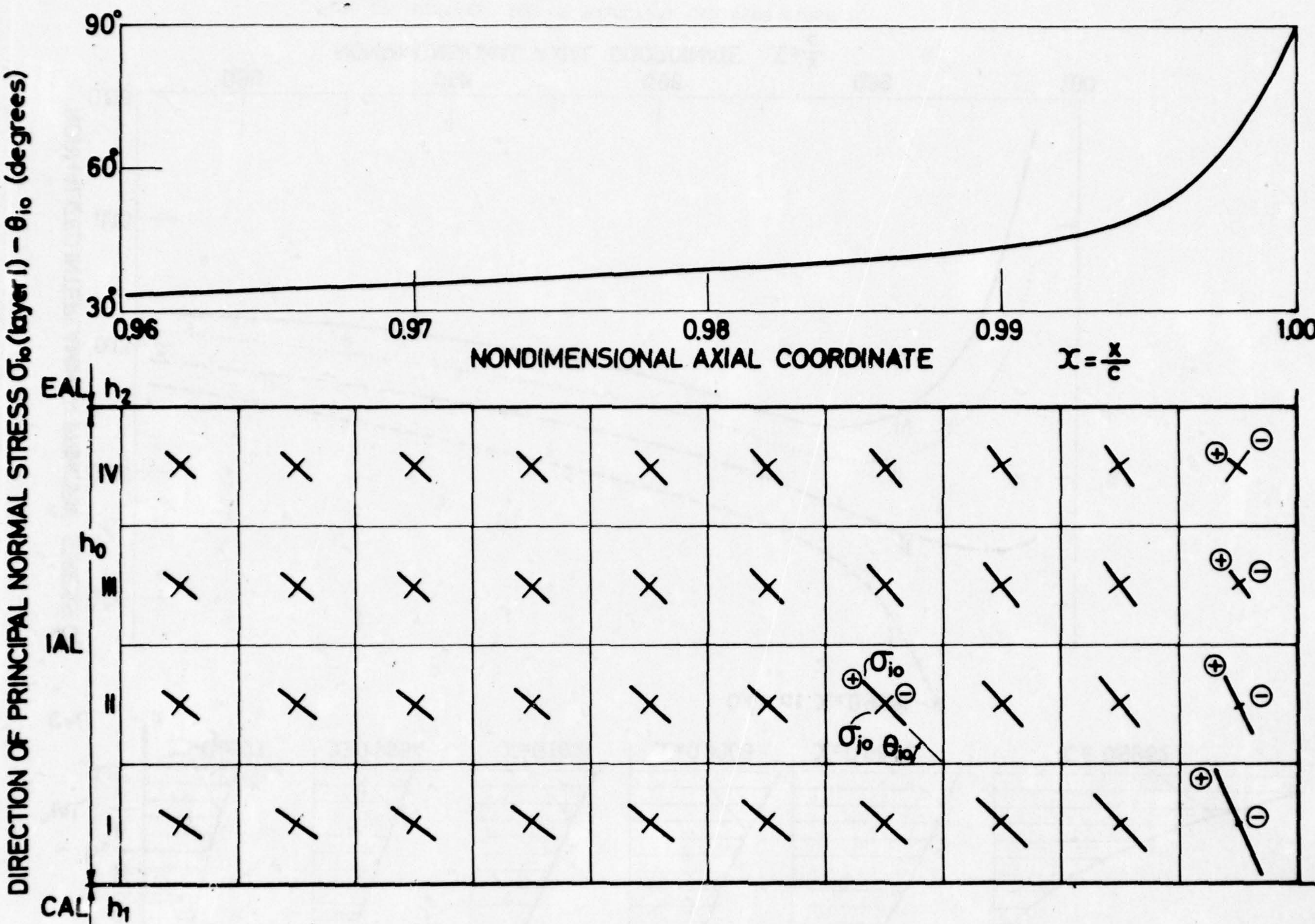

FIG. 18 VARIATION OF PRINCIPAL STRESS ORIENTATION THROUGH THE IAL (LAYER 1, FIG. 2C).

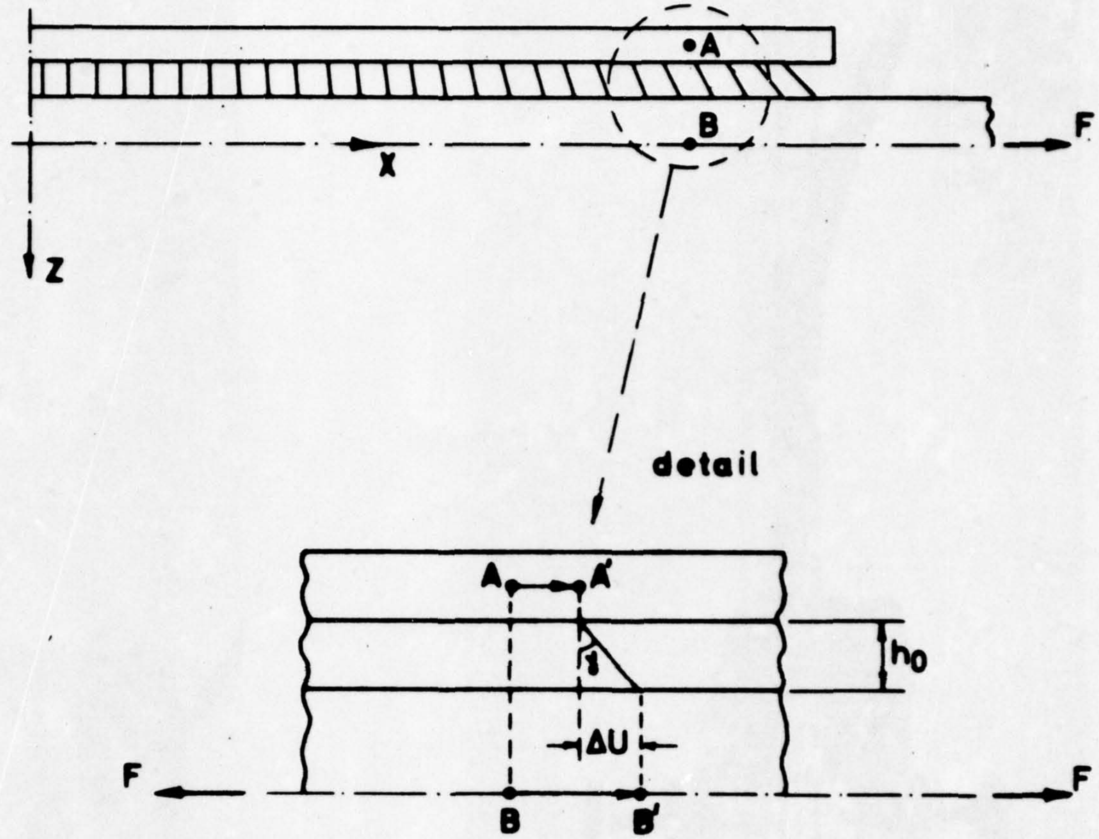

$$\gamma = \frac{BB' - AA'}{h_0} = \frac{\Delta U}{h_0}$$

FIG. 19 SCHEME OF SHEAR DISPLACEMENT PATTERN THROUGH THE IAL.

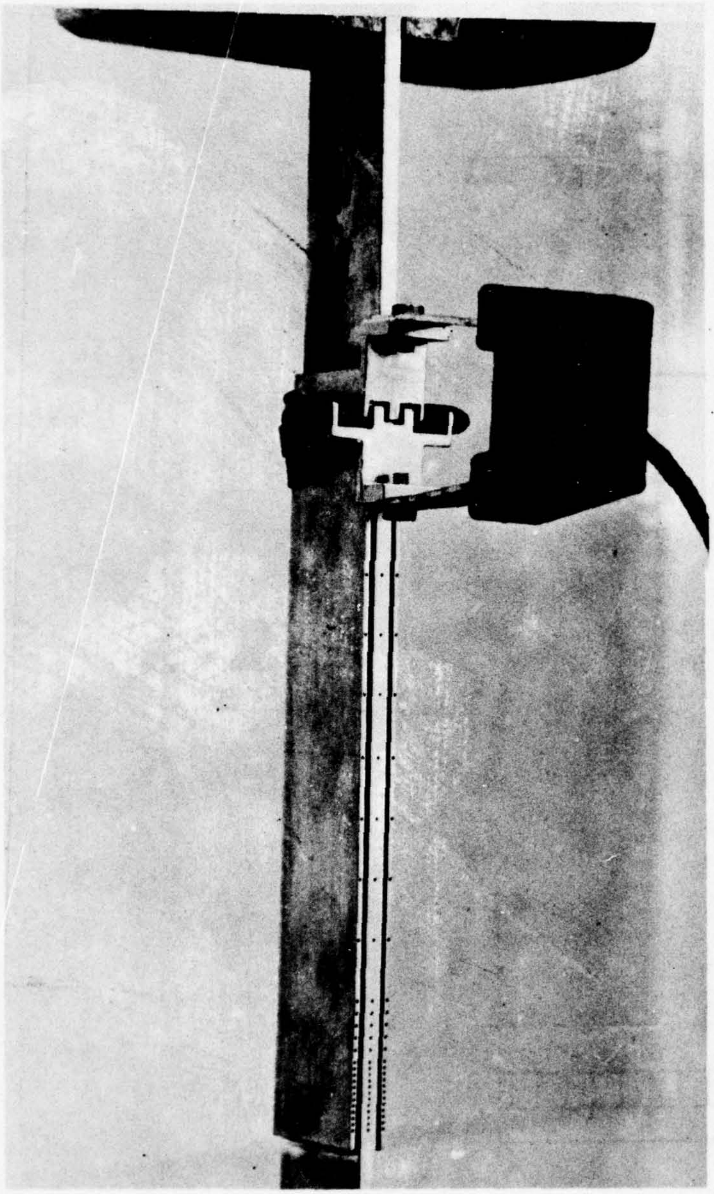

FIG. 20 ELECTROMECHANICAL EXTENSOMETER FOR MEASURING SHEAR DISPLACEMENT.

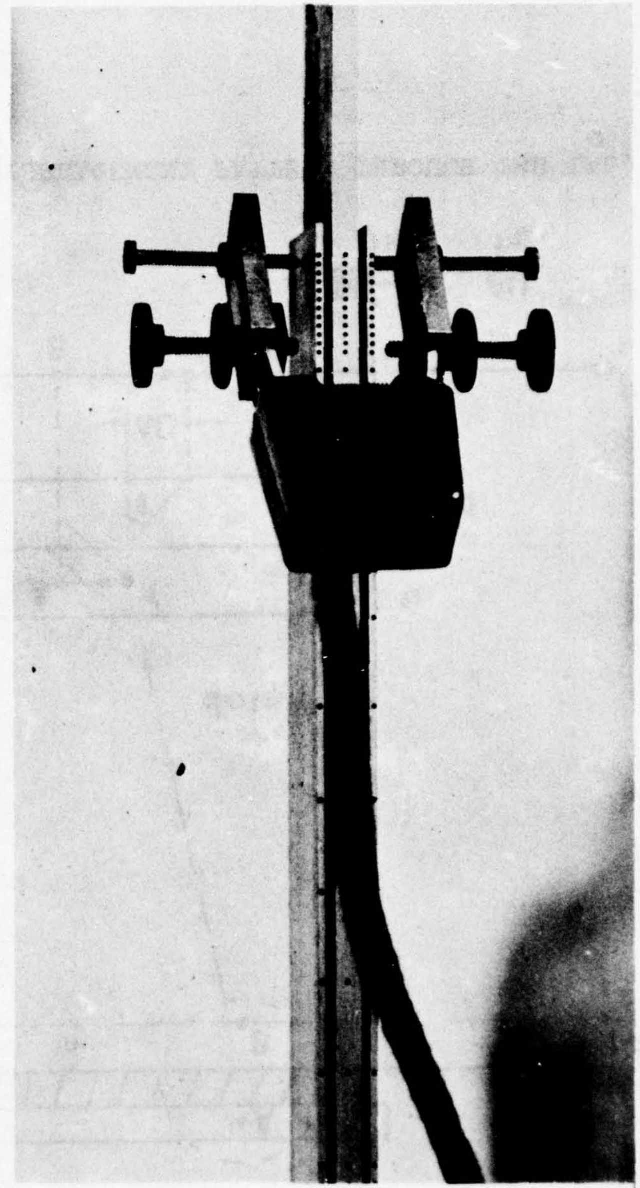

FIG. 21 ELECTROMECHANICAL EXTENSOMETER FOR MEASURING LATERAL NORMAL DISPLACEMENT.

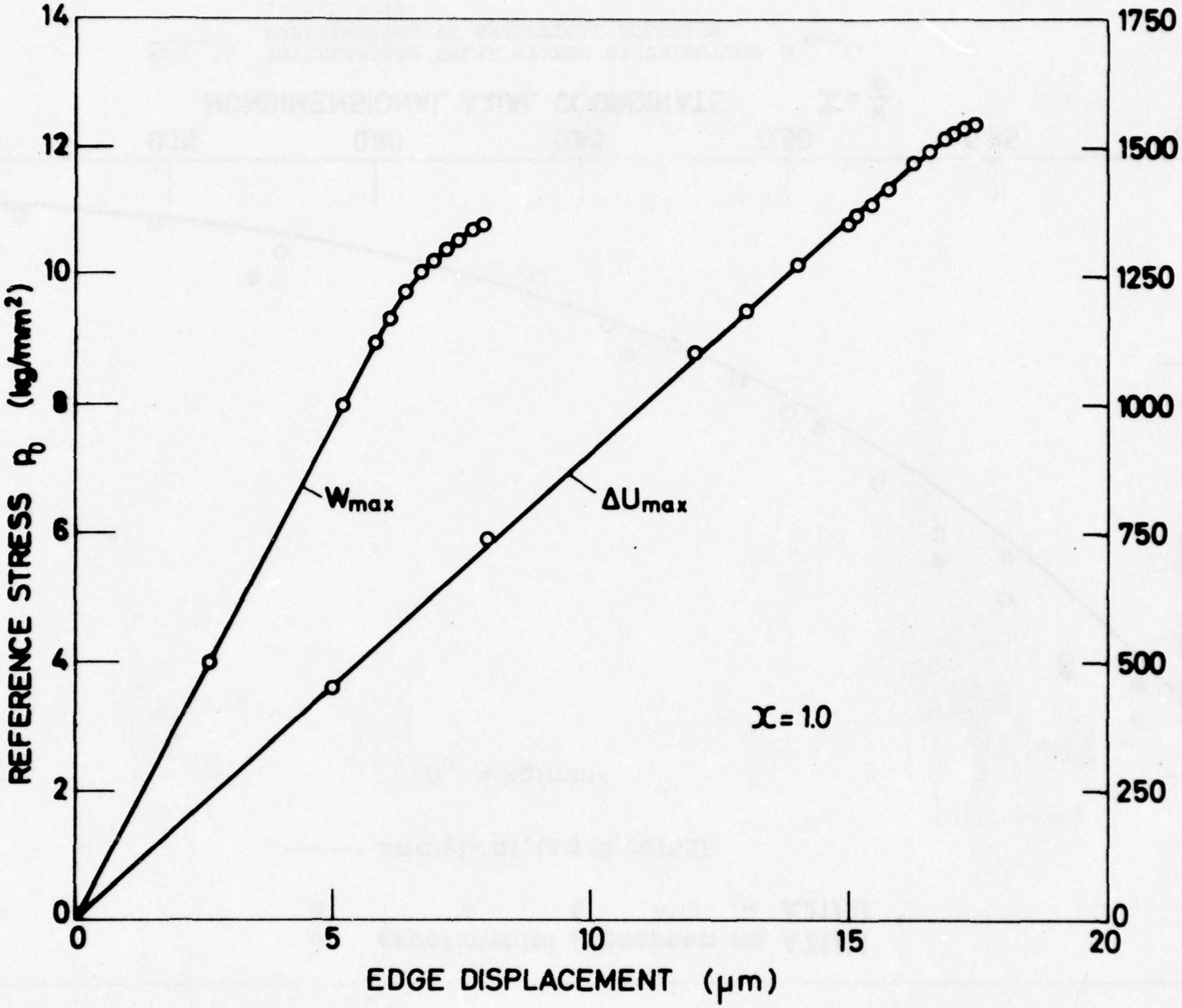

FIG. 22 APPLIED LOAD VS SHEAR AND LATERAL NORMAL DISPLACEMENT AT ADHESIVE LAYER EDGE.

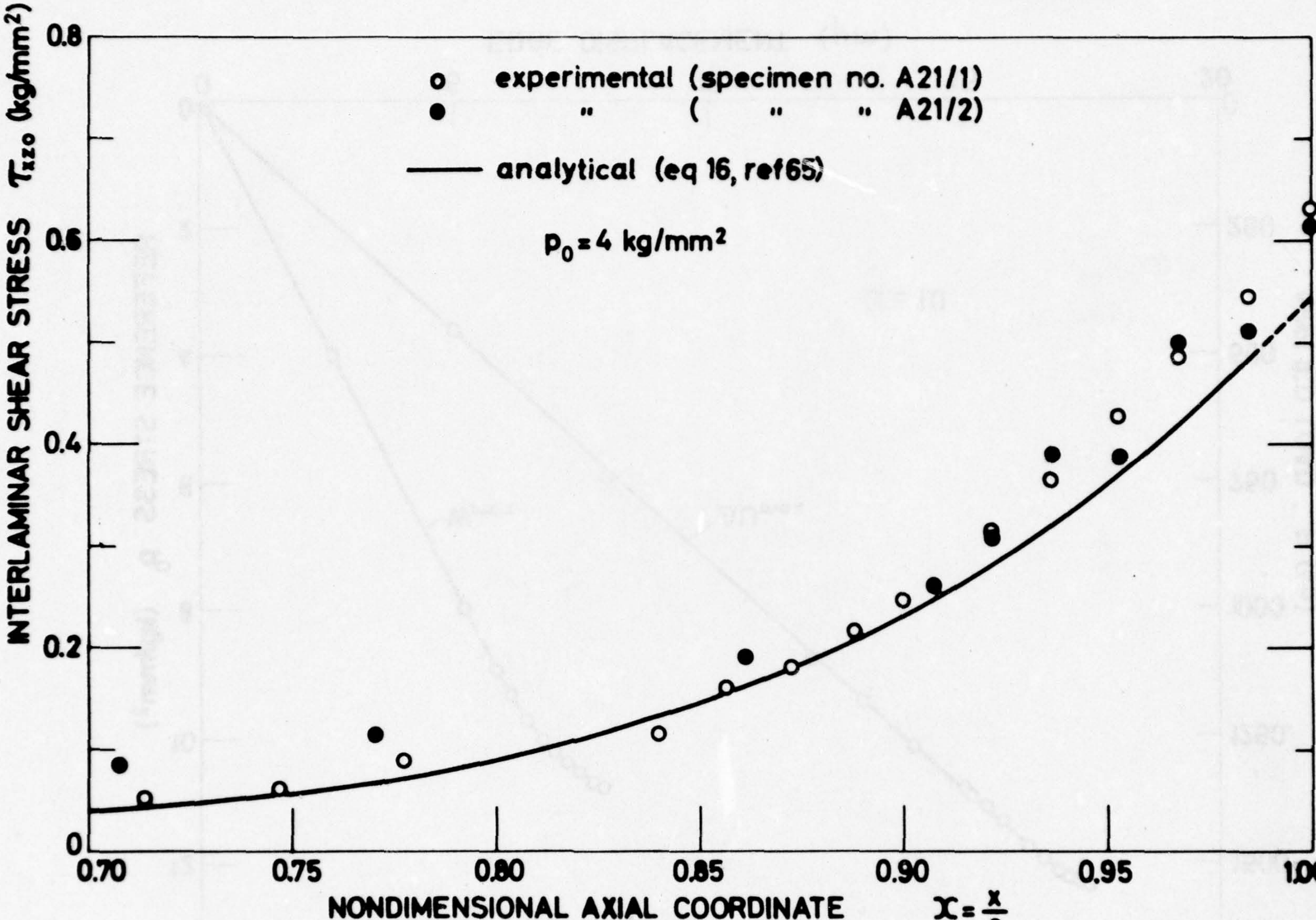

FIG. 23 INTERLAMINAR SHEAR STRESS DISTRIBUTION (τ_{xzo}). EXPERIMENTAL VS ANALYTICAL SOLUTION (MODEL A21).

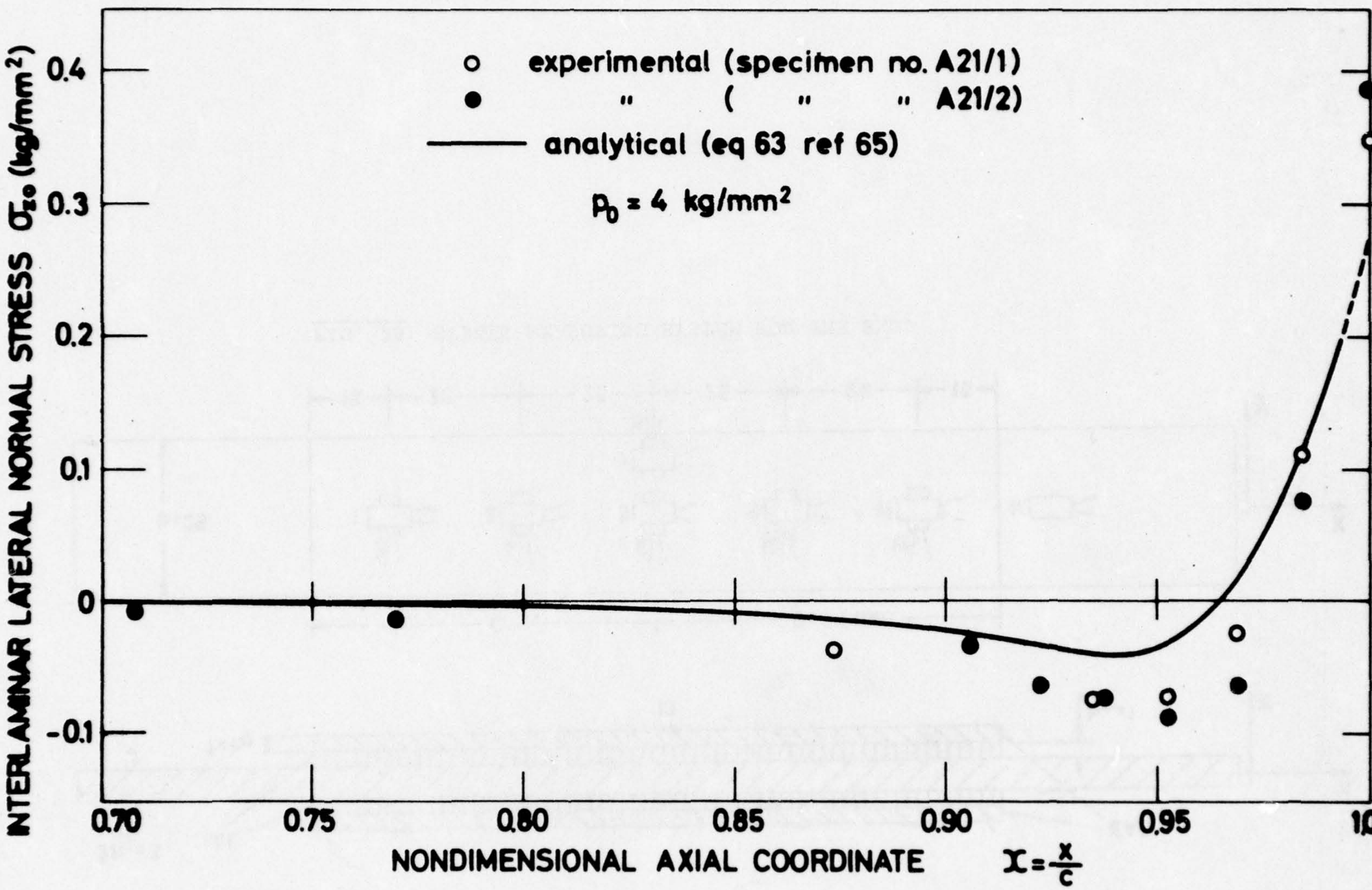

FIG. 24 INTERLAMINAR LATERAL NORMAL STRESS DISTRIBUTION (σ_{zo}). EXPERIMENTAL VS ANALYTICAL SOLUTION (MODEL A21).

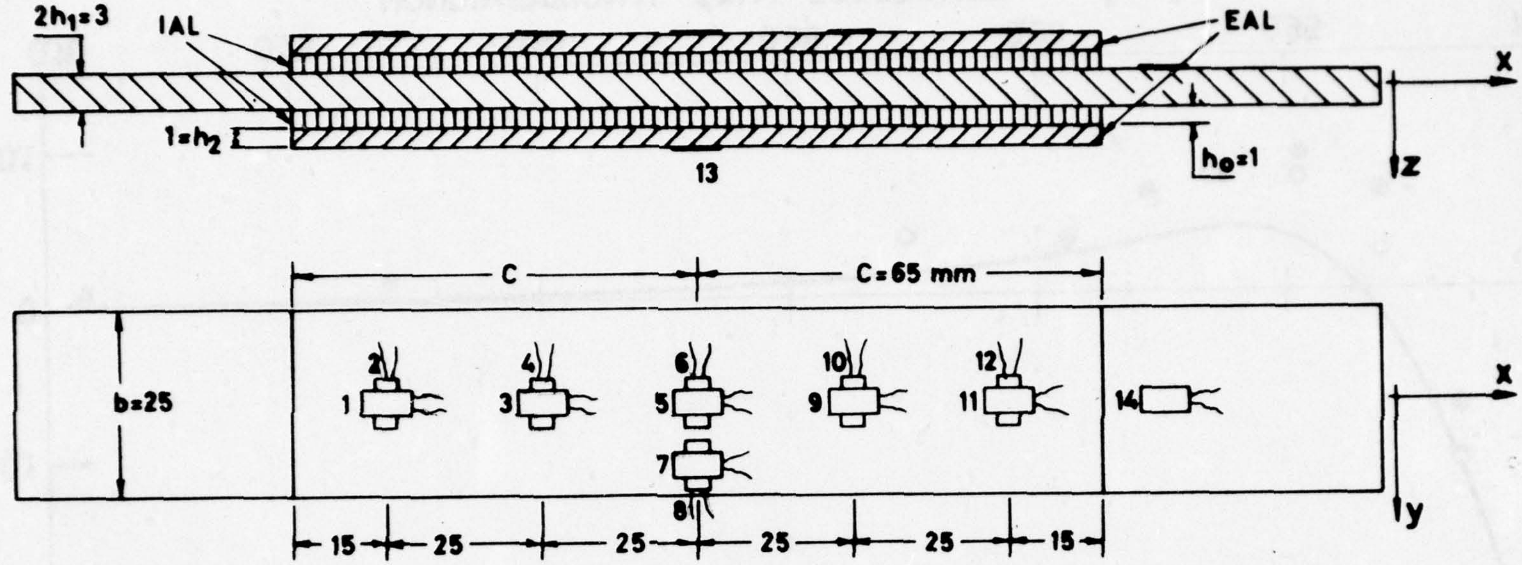

FIG. 25 STRAIN MEASURING SYSTEM FOR THE SMD.

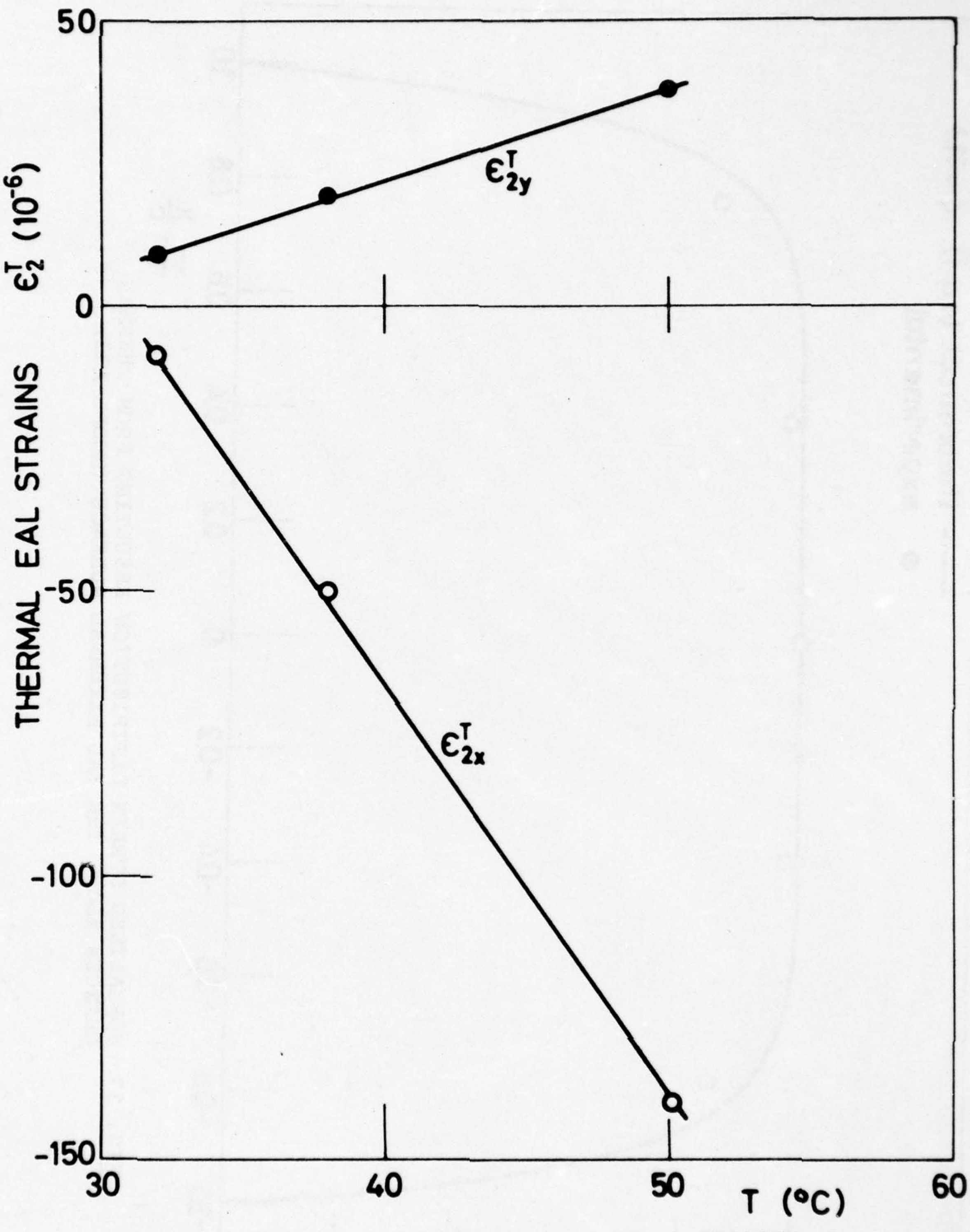

FIG. 26 EFFECT OF TEMPERATURE ON AXIAL STRAINS AT THE EAL SURFACE (MODEL A02).

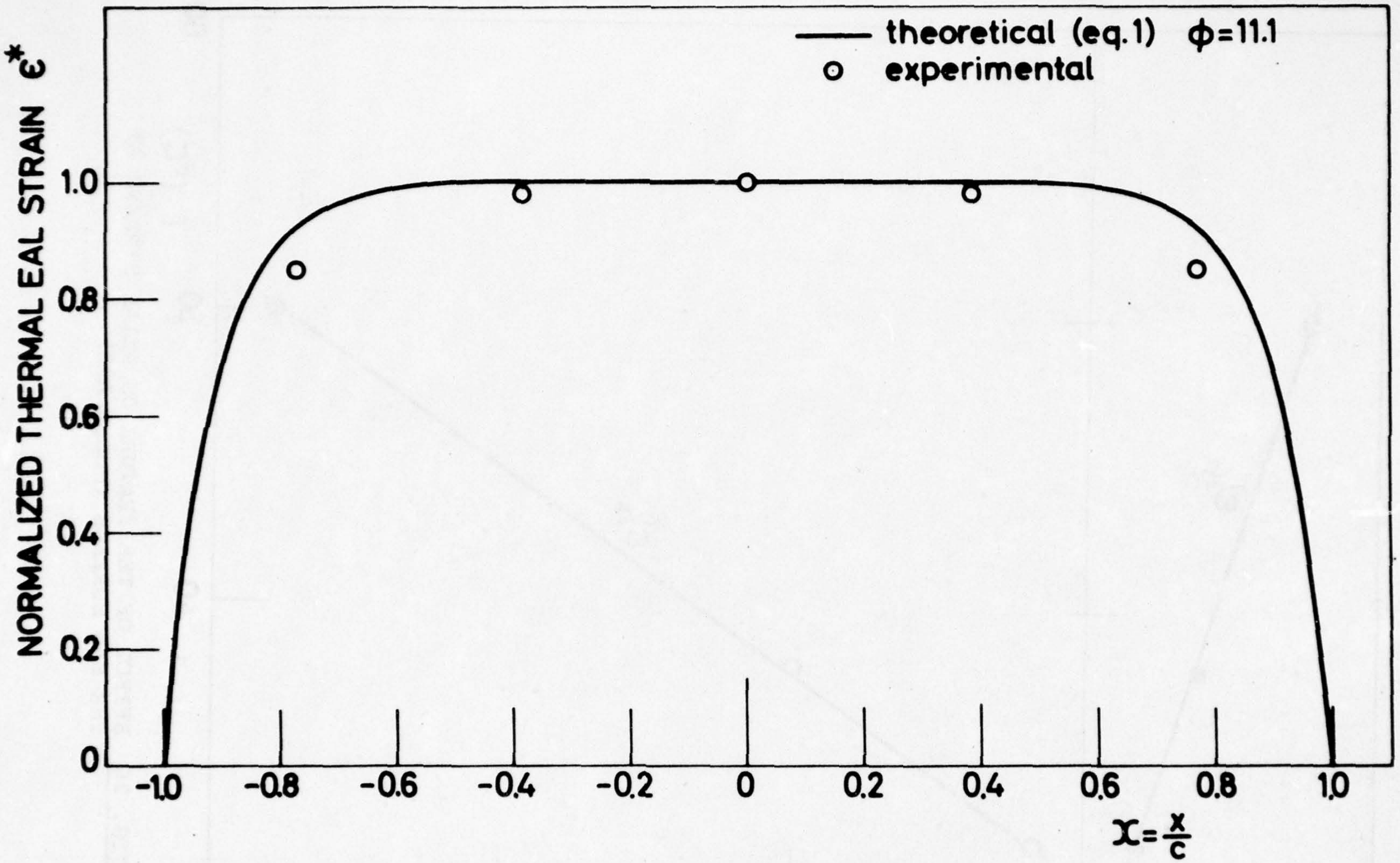

FIG. 27 NORMALIZED STRAIN DISTRIBUTION RESULTING FROM THERMAL CHANGES ALONG THE EAL EXTERNAL SURFACE (MODEL A02).

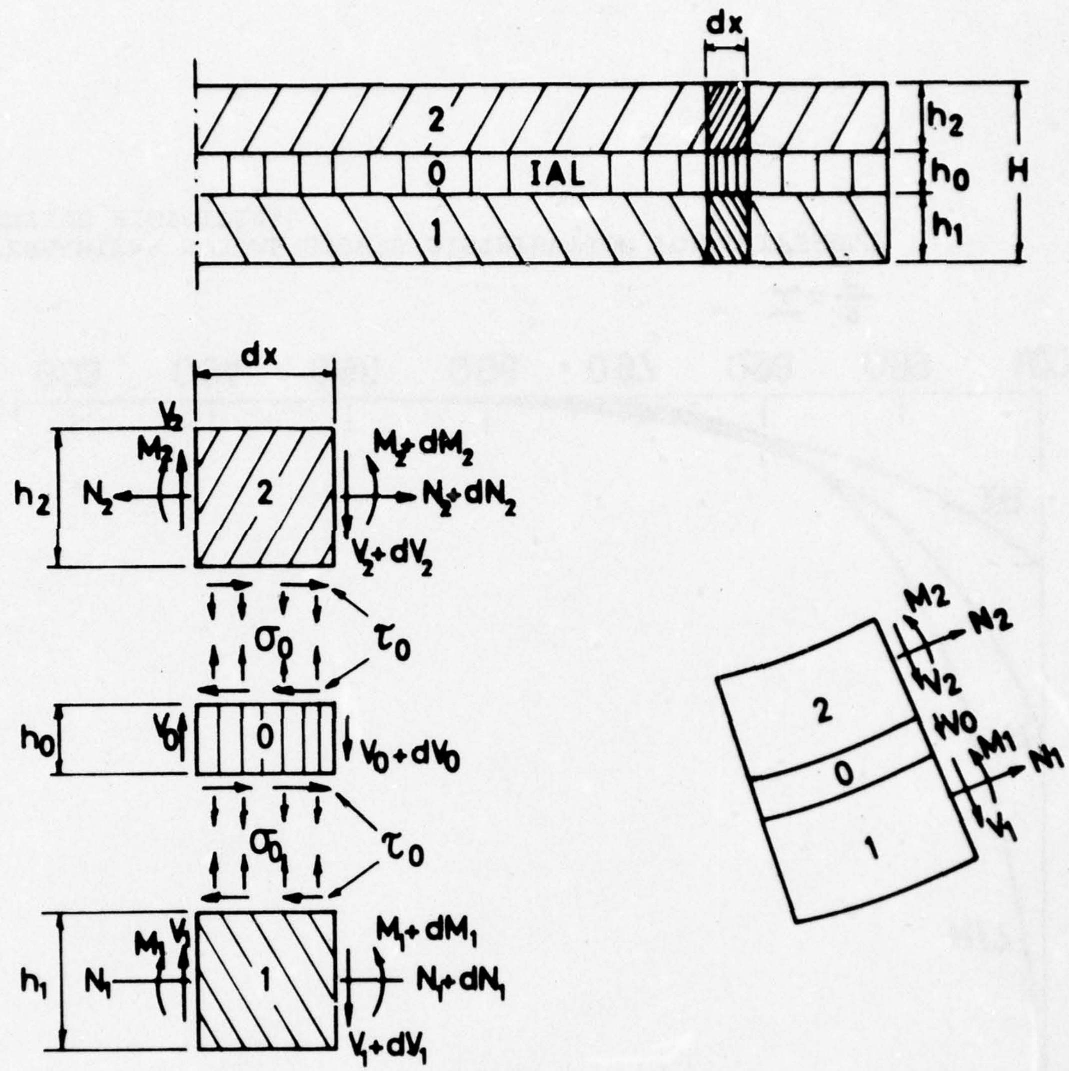

FIG. 28 STRESS ANALYSIS SCHEME OF A NONSYMMETRICAL DOUBLER MODEL (NMD).

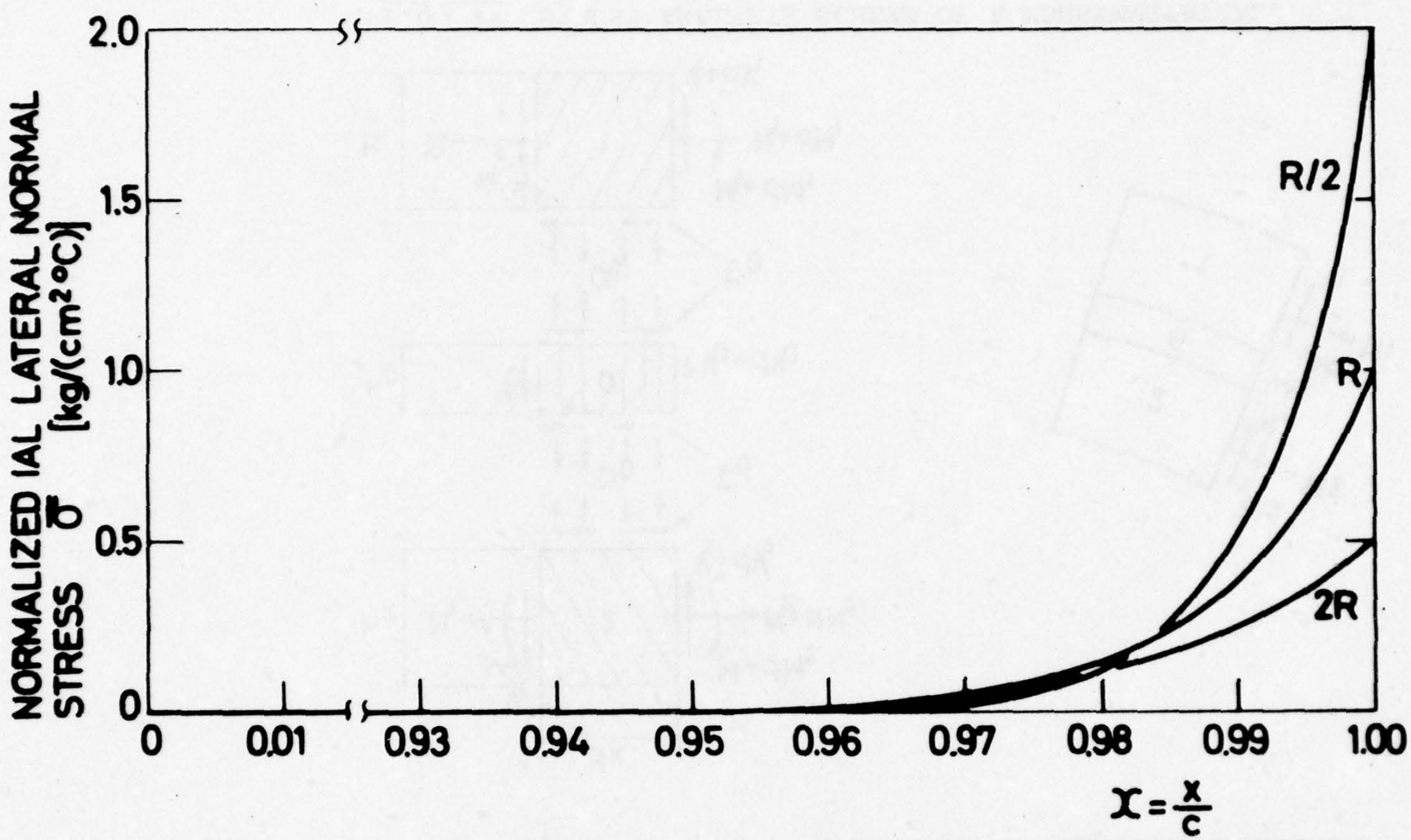

FIG. 29 INTERLAMINAR NORMAL STRESS DISTRIBUTION FOR DIFFERENT ADHESIVE RIGIDITIES.

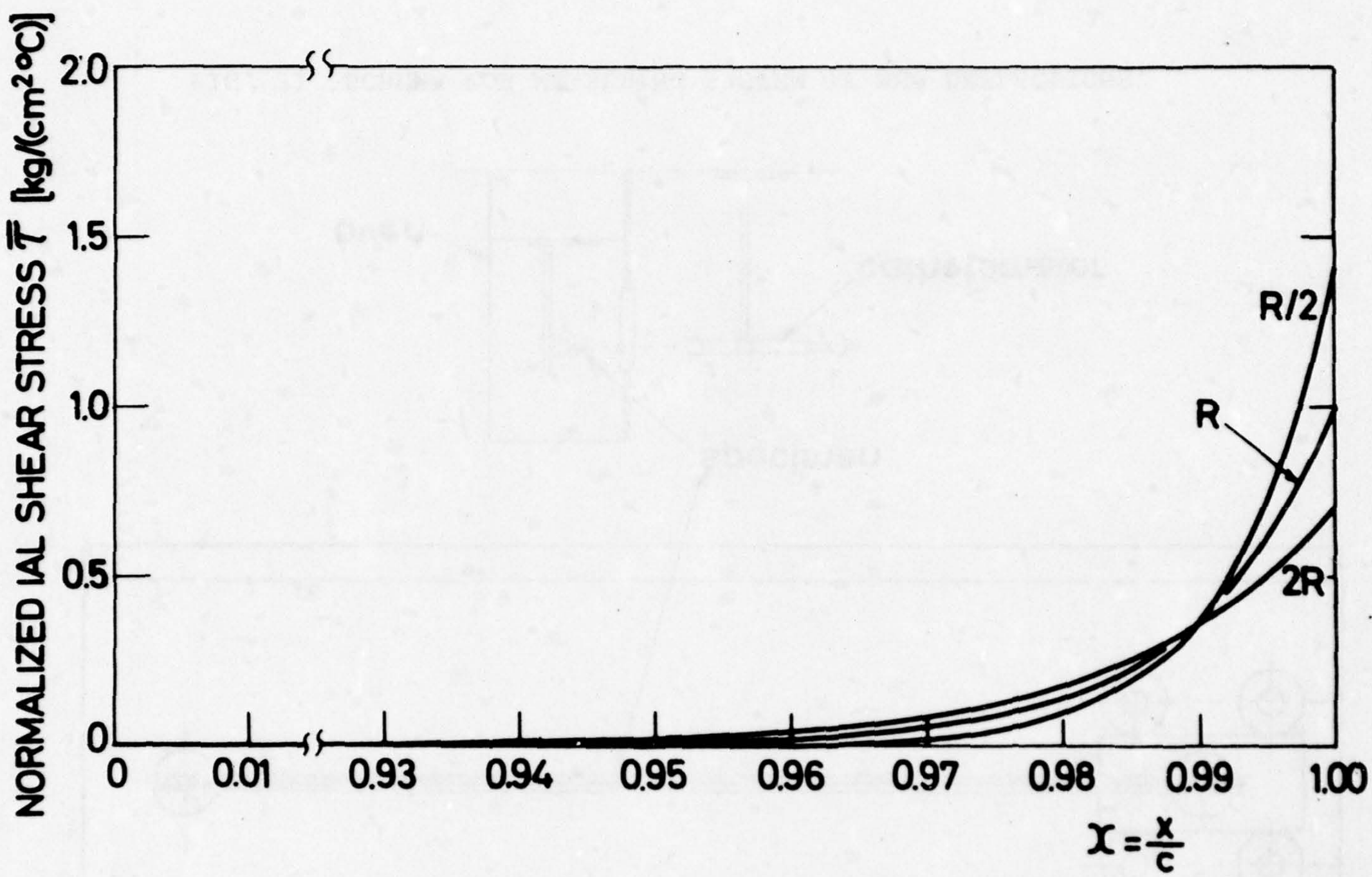

FIG. 30 INTERLAMINAR SHEAR STRESS DISTRIBUTION FOR DIFFERENT ADHESIVE RIGIDITIES.

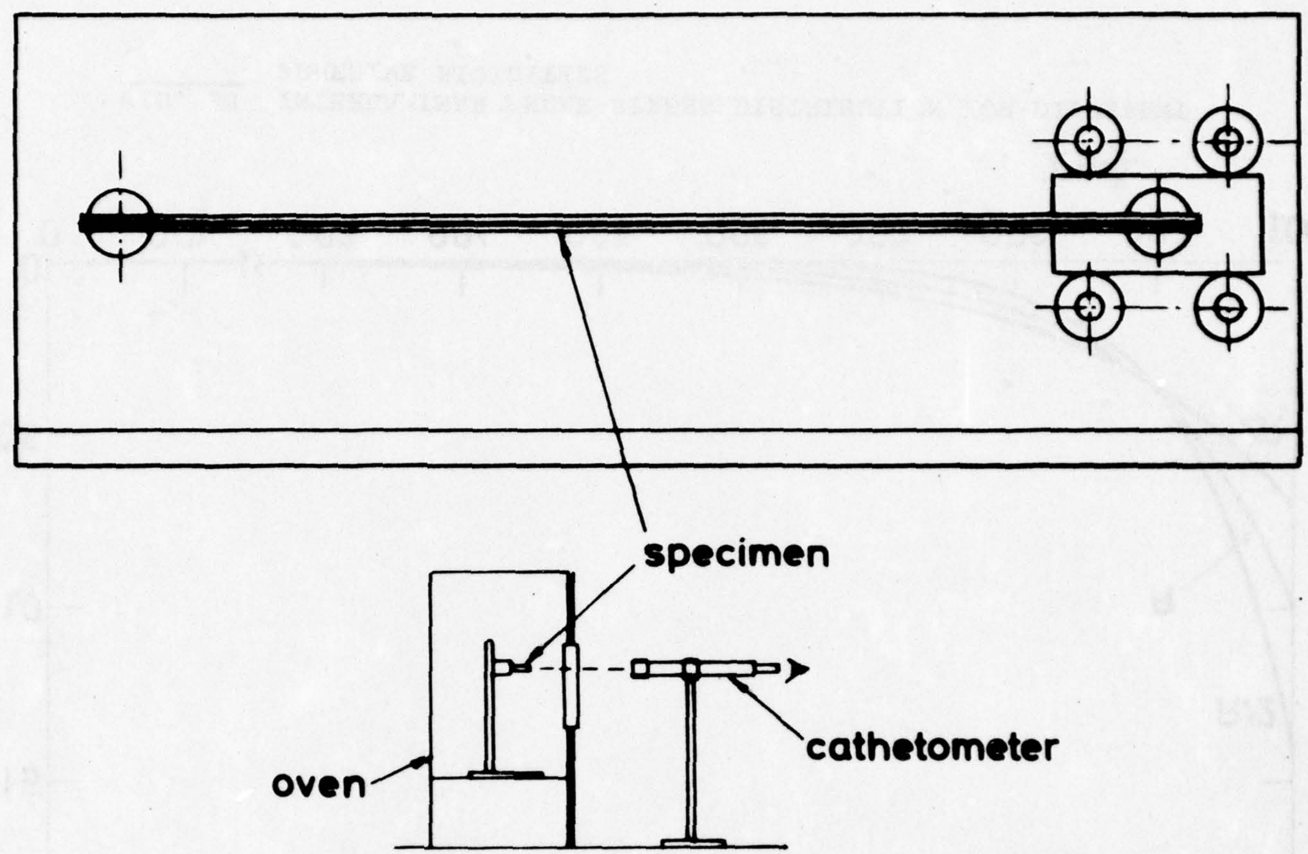

FIG. 31 SCHEMA FOR MEASURING SYSTEM OF NMD DEFLECTIONS.

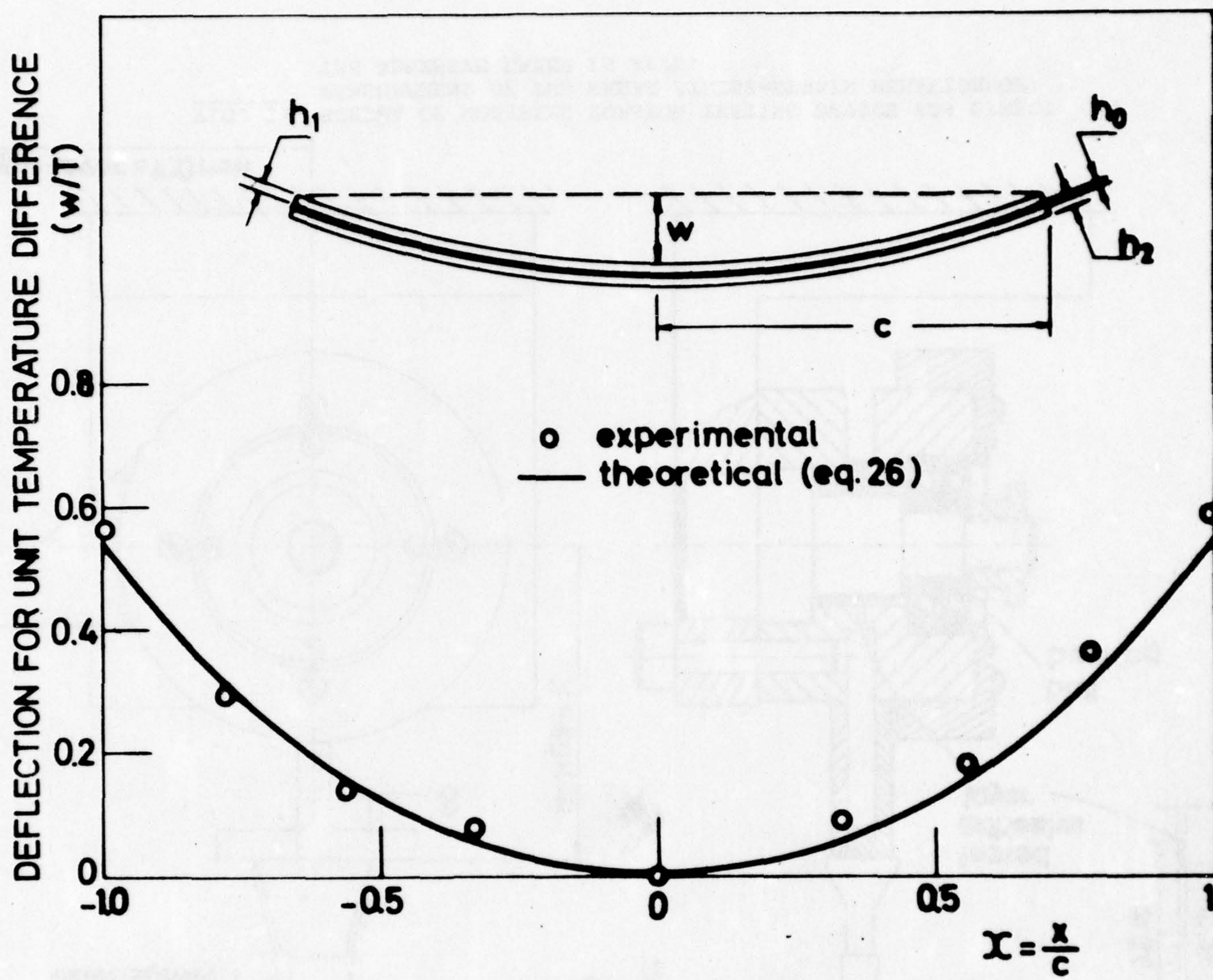

FIG. 32 THERMOELASTIC DEFLECTION CURVE OF NMD.

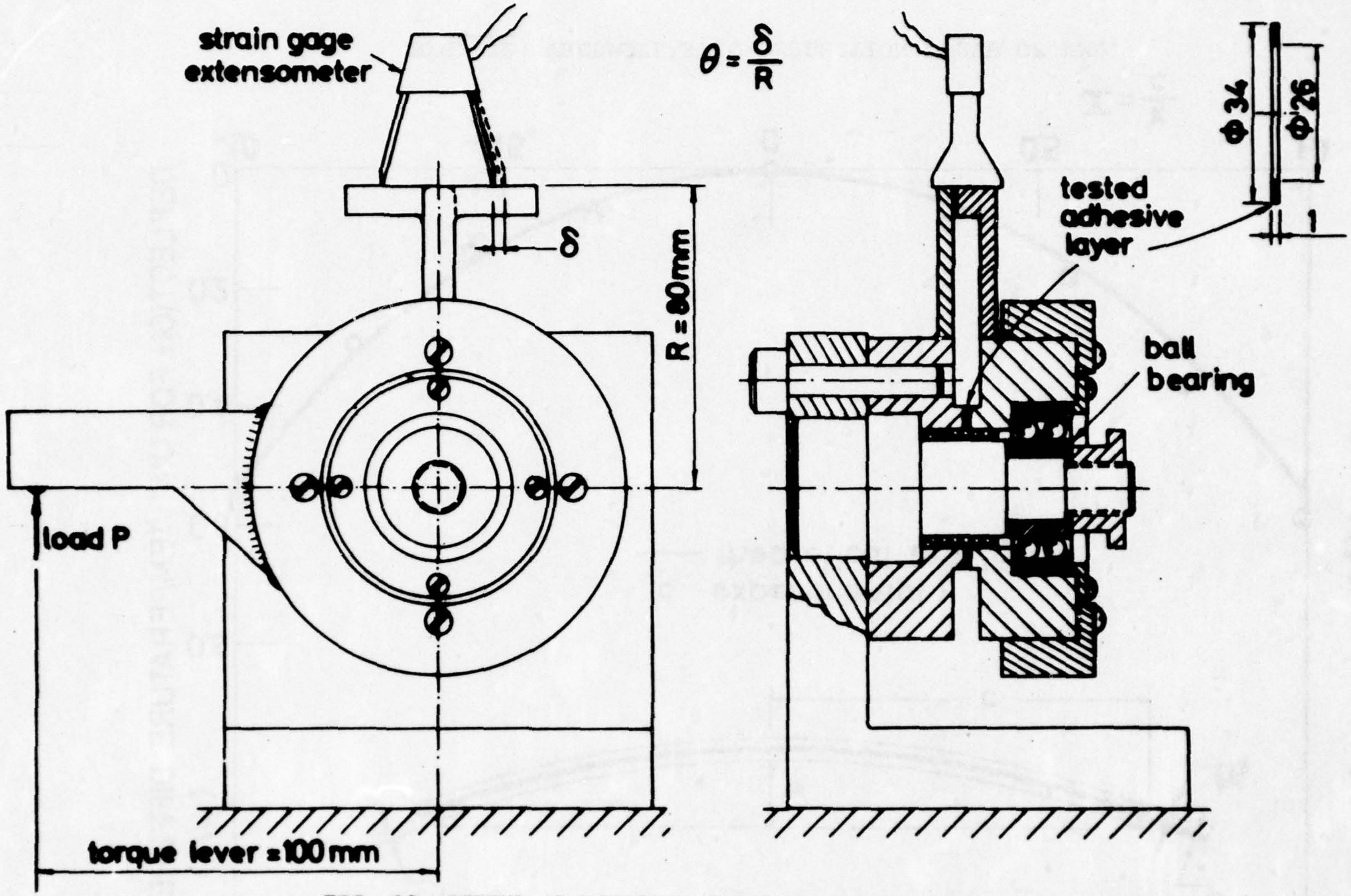

FIG. 33 SCHEMA OF MODIFIED TORSION TESTING DEVICE FOR DIRECT MEASUREMENT OF THE SHEAR STRESS-STRAIN BEHAVIOR OF THE ADHESIVE LAYER *IN SITU*.

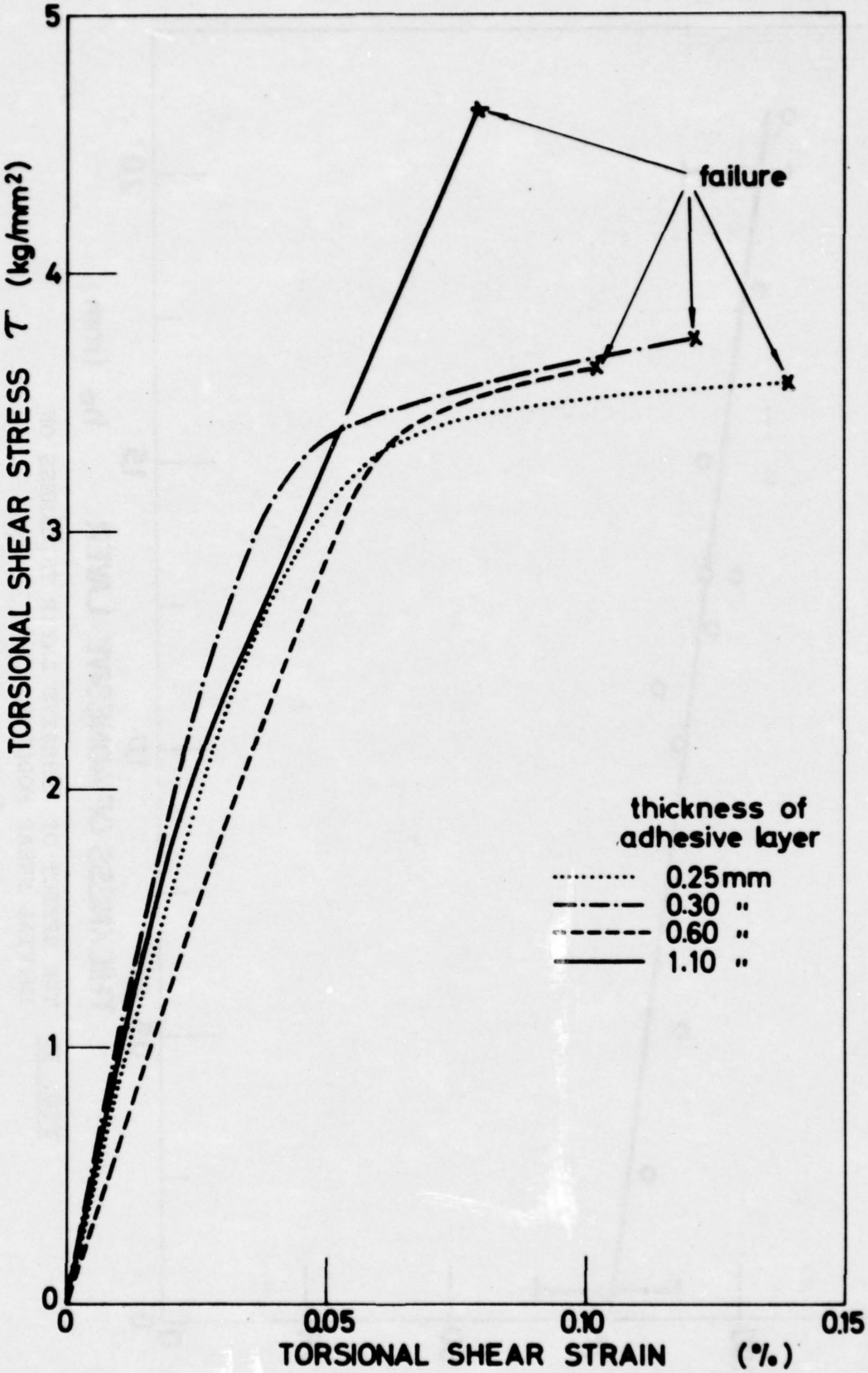

FIG. 34 TYPICAL SHEAR STRESS-STRAIN CURVES FOR THE ADHESIVE LAYER *IN SITU*.

34

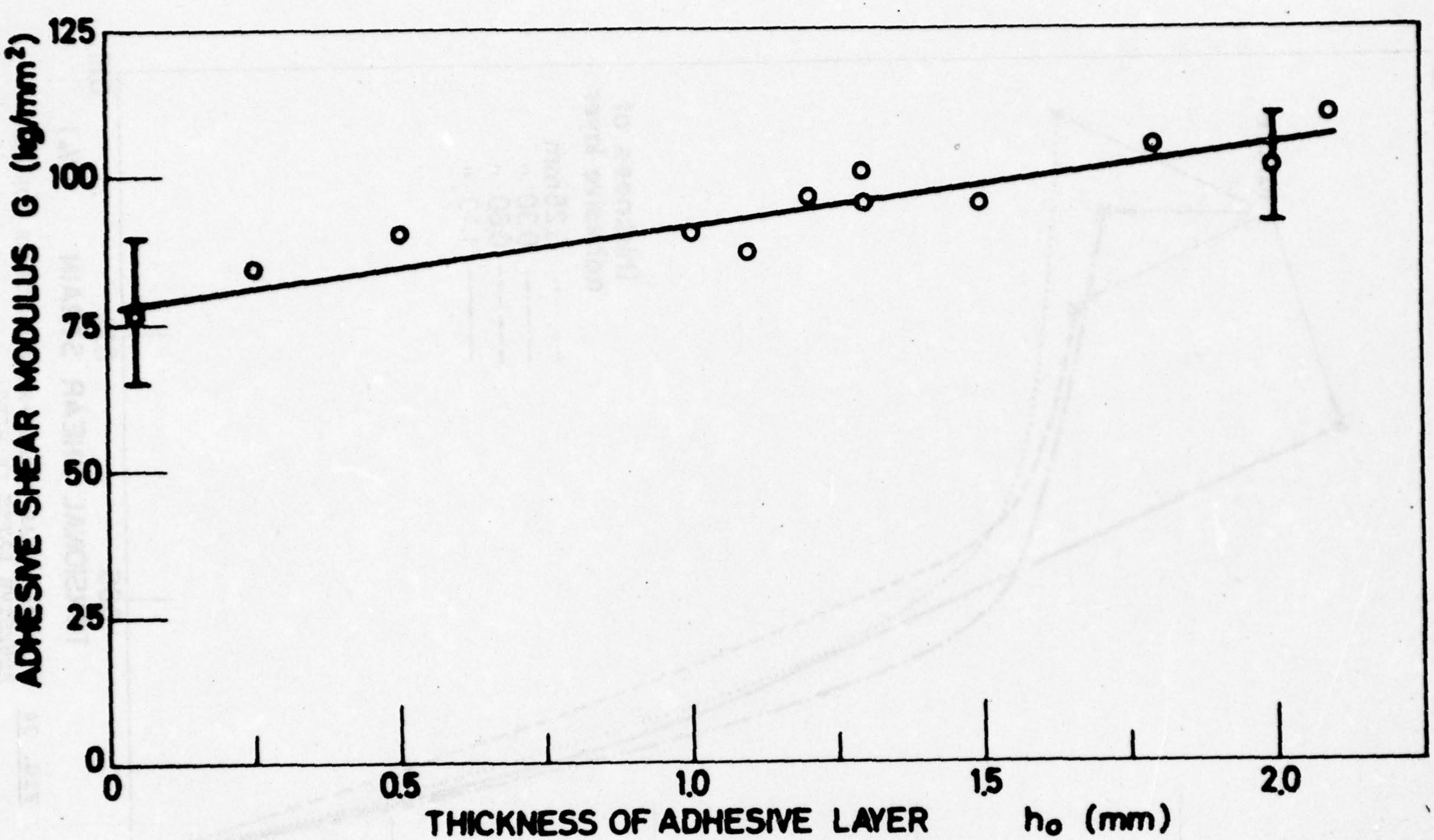

FIG. 35 THE EFFECT OF ADHESIVE LAYER THICKNESS ON INITIAL SHEAR MODULUS.

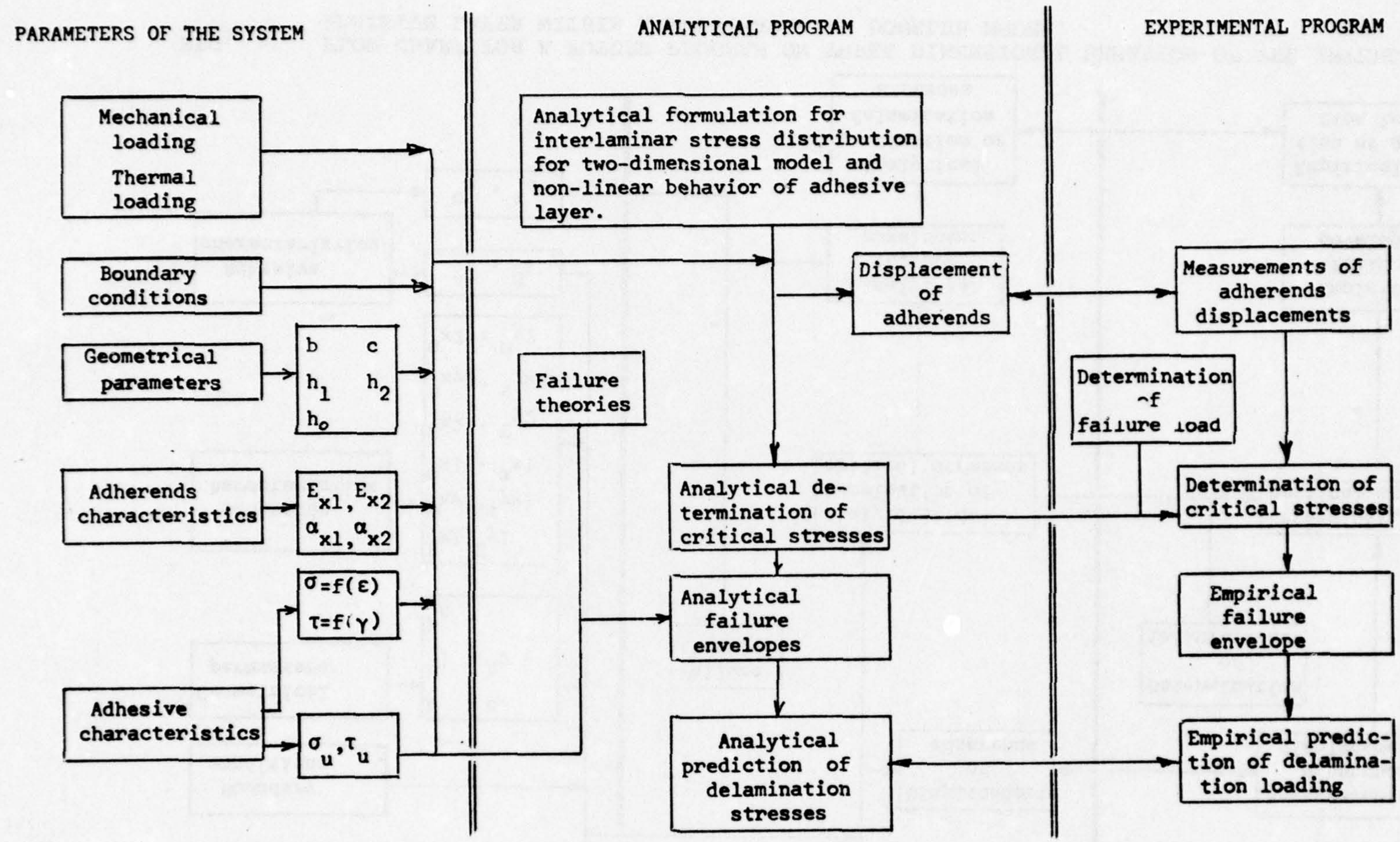

FIG. 36 FLOW CHART FOR A FUTURE PROGRAM ON NON-LINEAR BEHAVIOR OF THE INTERLAMINAR ADHESIVE LAYER WITHIN A MULTIMATERIAL DOUBLER MODEL.

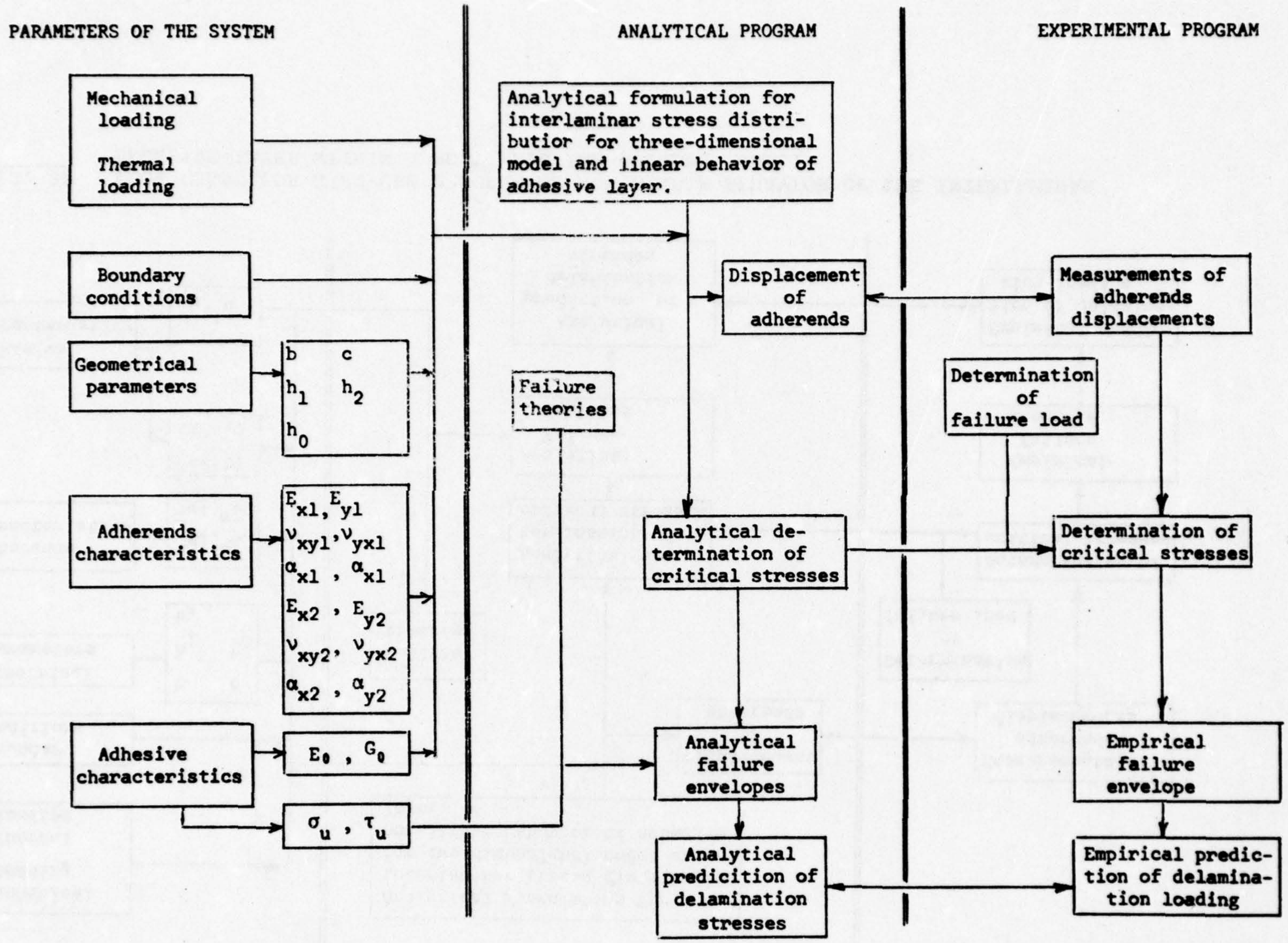

<u>FIG. 37</u> FLOW CHART FOR A FUTURE PROGRAM ON THREE DIMENSIONAL BEHAVIOR OF THE INTERLAMINAR ADHESIVE LAYER WITHIN A MULTIMATERIAL DOUBLER MODEL.

TABLE 1: DIMENSIONS AND ELASTIC PARAMETERS OF TEST MODELS.

Model No.	Elastic Moduli $[kg/mm^2]$				Dimensions [mm]			
	G_0	E_0	E_1	E_2	h_0	h_1	h_2	c
A21	90	250	7500	7500	1.0	1.5	1.0	65
A02	90	250	3500	7500	1.0	1.5	1.0	65

TABLE 2: ELASTIC AND THERMOELASTIC PARAMETERS OF TEST MODEL A02.

Direction	kg/mm^2 Elastic Moduli			Poisson's Ratio		$10^{-6} [c^{-1}]$ Coeff. of Thermal	
	E_1	E_2	G_0	ν_{xy1}	ν_{xy2}	α_1	α_2
x	3500	7500	90	0.28	0.33	∿ 8.5	22
y	1000	7500	90	0.02	0.33	∿22.0	22.0

COMPOSITION OF SMD (TABLES 1,2)

Model	Adherend 1	Adherend 2	Adhesive
A21	Aluminum 2024 T/3, nonclad	Aluminum 2024 T3, nonclad	2:1 mix of epon 828 and versamid 140
A02	E-glass fiber reinforced epoxy unidirectional laminate	"	"

TABLE 3: DIMENSIONS AND ELASTIC PARAMETERS OF NMD TEST MODEL.

Elastic Moduli kg/mm^2				Dimensions (mm)			
G_0	E_0	E_1	E_2	h_0	h_1	h_2	c
90	250	7500	3500	0.1	1	1	90

Composition:

Adherend 1: Aluminum 2024/T3 non-clad.

Adherend 2: E glass fiber reinforced unidirectional laminate.

Adhesive: 2:1 mix of Epon 828 resin and Versamid 140 hardener.

APPENDIX 1

ANALYSIS OF INFORMATION ON: "MECHANICAL BEHAVIOR OF ADHESIVE BONDED JOINTS".

No.	Model Geometry	Materials: Adhesive/ Adherend	Loading and Environment	Mechanical Behavior State of Stress	Analytical Methods	Experimental Techniques	Effect of Structural Parameters	Failure and Strength
2	SLJ	dissimilar adherends	axial tension neglecting bending	only shear adhesive strains; max. shear stress at edge	simplified differential eqs.		stress concentration increase with overlap length	
4	SLJ rectangular sheet adherends of equal thickness	very thin flexible adhesive compared with adherends	tensile axial force with eccentricity	beam theory or cylindrical bent-plate theory; plane strain at adhesive; shear and normal stress distribution	classical differential eqs. preassumption uniform stress distribution through thickness		relatively flexible and rigid adhesive cases	
7	SLJ adherend plates infinite springs adhesive		axial tension related to fatigue loading	beam theory and spring analogy applied to lab fatigue specimen shear and normal stress distribution	differential equation; spring beam analogy	photoelastic and brittle lacquer (stress coat) method	curved adhesive edges effect of thick adhesive	
9	SLJ sheets Butt joints	Araldite adhesive reinforced bakalite adherends metal adherends	uniaxial stress creep of adhesive	mainly plane strain		photoelastic measurements	effect of: overlap length;edge curvature; edge inclination length to thickness ratio in butt joint	
21	DLJ	Epoxy (Araldite)	fatigue tension temperature	shear stress behavior as function of overlap length	simplified solution of dif. eqs.	calculation of joint ultimate load as function of max. optimal lap length	effect of overlap length on strength	shear strength and failure strength

No.	Model Geometry	Materials: Adhesive/ Adherend	Loading and Environment	Mechanical Behavior State of Stress	Analytical Methods	Experimental Techniques	Effect of Structural Parameters	Failure and Strength
23	SLJ Scarfed joint DLJ	boron-epoxy adherend AF31, HT424 adhesives separate and mix	tension	stress concentration factor along joint axis		structural joint tests	effect of adhesive module(mixed rigidity) on joint efficiency	
24	torsion tube	Epon 828/ V40 Aluminum & stainless steel adherends metlbond 329	tension torsion temperature -100÷300°F	pure shear	calculation of shear modulus	measurement of adhesive, shear and tensile moduli in situ	effect of adhesive thickness on moduli	
25	SLJ DLJ different adherends supported & unsupported models scarf joint	adhesives: FM-1000 Metlbond 400 FM-47 (epoxy) adherends: GRP, Scotch-ply, Titanium GA1-4V Steel AISI 1025	static axial loading; fatigue loading	shear & normal stress distribution; elastic behavior plane stress or generalized plane strain	comparison of ref.4, numerical & finite element methods, shear lag analysis	static & fatigue data of DLJ; test of effect of edge tapering	effect of adhesive shear modulus, thickness overlap length, adherend width, thickness, modulus joint efficiency effect of adherend edge tapering	shear strength strength of adhesives fatigue strength
27	SLJ and DLJ	polyester sheet for photoelastic joint model steel adherend	static & fatigue loading	shear stress distribution along adhesive normal stresses along adherend tapered edges	simplified integration of shear stresses along IAL	photoelastic measurements of stress distribution in adhesive brittle lacquer technique	effect of angles of metal edges to reduce adhesive stress concentration; effect of lap length and adherend thickness	adhesive joint designed for metal failure
28	stringer bonded to elastic sheet of infinite size	flexible vs stiff adhesives metal adherends	line uniaxial loading	stringer in simple extension; pure shear in elastic adhesive bending neglected	integral equations method		uniform shear in flexible adhesive; high stress concentration in stiff adhesive	

No.	Model Geometry	Materials: Adhesive/ Adherend	Loading and Environment	Mechanical Behavior State of Stress	Analytical Methods	Experimental Techniques	Effect of Structural Parameters	Failure and Strength
29	SLJ Doubler	Flexible adhesive epoxy	tensile shear	nonlinear stress-strain adhesive shear stress distribution only	nonlinear differential eq. numerical solution finite element		effect of doubler stiffness and bond-line thickness	average shear stress at joint failure
30	Symmetric double lap joints	metal and FRC composite adherends (anisotropic) boron-epoxy-glass epoxy adhesive	axial tension	plane stress in adherends shear and normal stress distribution	differential equations		effect of adhesive thickness	
31	DLJ	plain metal adherends	static and fatigue loading	shear stress distribution only; elastic behavior of adhesive to failure approx. expression for normal stresses	semi-empirical approach and computer programming for optimum lap-length polynomials curve fitting		effect of overlap length on strength adhesive properties in thin film differs from bulk	joint strength optimization applying Hill failure criterion adherend & adhesive failure modes
32	DLJ	FM-123-2 modified nitrile e epoxy adhesive 2024-T3 clad adherends	static and fatigue loading		statistical analysis of fatigue data computer programming	Sontag fatigue machine with static load maintainer	effect of overlap length for optimization of fatigue endurance	S-N fatigue curves with 95% confidence limits

No.	Model Geometry	Materials: Adhesive/ Adherend	Loading and Environment	Mechanical Behavior State of Stress	Analytical Methods	Experimental Techniques	Effect of Structural Parameters	Failure and Strength
35	peel test model	adhesive tapes bakelite plates adherends	tensile peel test	viscoelastic behavior; relaxation weak boundary layer mechanism	rheological models and theories; rate-temperature super-position method	peeling test of adhesive tapes	effect of temperature on strength effect of strain-rate adhesive thickness effect	cohesion vs interfacial failure; failure criteria and envelopes peel strength
36	SLJ DLJ stepped joint	titanium aluminum and boron-epoxy adherends; epoxy adhesive Epon 9601	static and fatigue loadings thermal loading	linear and nonlinear adhesive stress-strain; transverse shear included; zero stresses at IAL edges plastic zone approach	finite element solution compared with closed form solutions computer program for numerical solution (Bonjo)	photostress and strain-gage strain measurements on adherend surfaces	effect of transverse shear in case of composite adherends	
37	SLJ step-J	Boron-Titanium	torsion tension temperature	elastic-linear nonlinear mainly shear stresses	finite element	torsion tube butt tension		shear and tensile adhesive strength
38	SLJ DLJ	$E=20{,}000 kg/mm^2$ $G_0=100\ kg/mm^2$ linear visco-elastic adhesive	constant static tensile stress creep	time-dependent shear stress distribution pure shear assumption in adhesive	classical linear viso-elastic approach collocation method			
40	SLJ — shear springs model	aluminum to steel adherends; high model epoxy adhesive	axial tension	adhesive, transverse & longitudinal shear distribution	approx. analytical closed form vs finite difference solutions	rubber model for measuring transverse adhesive strains	profiled adhesive layer to give uniform stress	

No.	Model Geometry	Materials: Adhesive/ Adherend	Loading and Environment	Mechanical Behavior State of Stress	Analytical Methods	Experimental Techniques	Effect of Structural Parameters	Failure and Strength
41	asymmetrical lap joints	anisotropic adherends: 1002-S GRP 45°/0° - 45°/0° U.S. film adhesive EA951	static and fatigue loading non-uniform fatigue loading	effect of transverse shear & normal stress strain distribution through adherend thickness linear plate theory; normal and shear stress distribution plane strain	comparison with close form solution (4) solution of 8 order linear differential eqs. + 6 boundary conditions	ultrasonic vs destructive tests for modulus shear & normal strength properties of adhesive in situ electro scanning microcopy for fracture	effect of ply orientation adhesive thickness overlap length adhesive shear proportional limit effect on fatigue	maximizing joint strength fatigue life adhesive & interlaminar failure modes
43	DLJ	ductile vs brittle adhesives	static axial load thermal effects	elasto-plastic solution shear and normal stress distribution	bound for nonlinear behavior simplified analytical approach	stress-strain curves for shear (torsion)	mix module adhesive effect of overlap adherend thickness	peel failure mode strength independent on large overlap length
44	SLJ	adherends: aluminum 7075-T6 CFRP, quasi-isotropic & U.D. adhesives: brittle & ductile epoxy	Axial tension	plane stress in adherend; adhesive linear elastic & elastic-plastic	differential eqs; closed form solution		load eccentricity lap/thickness ratio tapering adherend edges	interlaminar adherend failure; adhesive shear & trans verse tension failure
45	Stepped & scarfed joints	ductile vs brittle adhesives: Hysol 951 vs Metlbond, 329 titanium & CFRP adherends	static and thermal loading	elastic-plastic shear stress distribution; shear and normal elastic stress distribution	explicit algebraic formulas for bounds of strength prediction	failure tests of adhesive (torsion) & joints	effect of adhesive plasticity on strength effect of overlap length	shear strength affected by ductility composite interlaminar failure mode

No.	Model Geometry	Materials: Adhesive/ Adherend	Loading and Environment	Mechanical Behavior State of Stress	Analytical Methods	Experimental Techniques	Effect of Structural Parameters	Failure and Strength
47	stepped & tapered lap joints	aluminum, steel adherend; orthotropic composite adherends epoxy adhesive	static in-plane loads	2-dimensional plane-stress plane-strain in plates shear stress distributions	finite element method		effect of adhesive thickness	
48	SLJ	$E=200 kg/mm^2$ $G_0=0.2$ "	static axial tension	only shear stress distribution	classical differential equation approach		effect of varying shear moduli of adhesive (2 steps)	shear fracture strength (max.shear strain energy criterion)
49	SLJ, Doubler cleavage specimen	aluminum/ aluminum	uniaxial tension hostile environment	stress-corrosion analysis of shear stresses only	simplified analysis for max.shear stress	Extensometer for measuring shear displacment		crack propagation in hostile environment
50	double SLJ	adherend: Alum 2024 T3 adhesive: modified epoxy with anticorrosive primer (250°curing)	tensile loading in hot humid environment 120°F 100% R.H.	static stressing at constant level, creep rupture life measurements		constant load maintained by springs	effect of aging history load cycling effect on bond recovery	adhesive failure due to water penetration to interfaces in other cases, cohesive failure, fracture toughness

No.	Model Geometry	Materials: Adhesive/ Adherend	Loading and Environment	Mechanical Behavior State of Stress	Analytical Methods	Experimental Techniques	Effect of Structural Parameters	Failure and Strength
51	SLJ,DLJ Spew vs square edge	epoxy rigid AF-130 adhesives ($G=172kg/mm^2$) Aluminum adherends	tension shear	plane strain 2-d shear stress normal stress and principal adhesive stresses	finite element (triangle elements)		effects of adherend length, overlap length, spew size, adhesive thickness, adherend thickness	effect of adhesive thickness & edge geometry adherend improves strength
52	SLJ	flexible adhesive	uniaxial tension	plane stress plane strain stress distribution through adhesive adherend thickness	finite difference			
54	Doubler SLJ double notch tensile specimen	epoxy film adhesive AF 127; thick bond line	fatigue and environment 120°F 100% R.H.	flexural behavior of bonded structure design allowable data	design analysis; finite element method (NASTRAN)	flexural wing fatigue test. nondestructive inspection	effect of bond-line thickness	endurance test
55	SLJ	GRP adherends (1002 S-glass) Hysol EA951 nylon epoxy adhesive	fatigue and static loading	behavior at the linear elastic range up to proportional limit	use of analysis based on differential equations assumption of uniform adhesive stresses	fatigue life measurements micro observation of failure surfaces	effect of: overlap length, adhesive thickness, laminae orientation, adhesive proportional limit	adhesion-cohesion mode of failure composite interlaminar failure at 45° ply
56	SLJ	ductile adhesive: nylon-epoxy, anisotropic, GRP & Kevlar adherends	fatigue loading spectrum static loading	tensile & shear adhesive stress distribution zero shear at edges	fatigue life theory for two block loading spectrum	fatigue run-out tests	effects of: overlap length laminae orientation adhesive proportional limit	fatigue vs fracture toughness of ductile adhesives

No.	Model Geometry	Materials: Adhesive/ Adherend	Loading and Environment	Mechanical Behavior State of Stress	Analytical Methods	Experimental Techniques	Effect of Structural Parameters	Failure and Strength
59	stepped & tapered lap joints	metal & FRC composite adherends (anisotropic) boron-epoxy glass-epoxy epoxy adhesive	axial tension	plane stress in adherends shear & normal stress distribution	differential equations		effect of adhesive thickness	
60	double cantelever	elastomer-epoxy (CTBN) adhesive	tension, shear, off-axis loading	fracture toughness test interfacial behavior	fracture mechanics	mix failure mode test by inclined adhesive line cleavage test	bond thickness effect	crack propagation high toughness in matrix not reflected in joint
61	SLJ,SLJ step-joint plates	variation in adhesive moduli	uniaxial tension	strain displacement stress strain stress distribution along axial coordinate	polynomials differential equations		effect of edge tapering	
62	DLJ bonded layers		tensile shear	stress intensity factors, shear and normal stresses	singular integral eq. numerical solutions		effect of adherend thickness	
63	SLJ double notch specimen	adherend: S-glass adhesive: epoxy-nylon	fatigue & static tension loading	beyond the linear range interlaminar shear in composite shear and normal stress in adhesive	numerical analysis	double notch shear test	effect of fiber orientation and layer sequence in laminate	fatigue joint strength mainly affected by proportional limit in shear angly ply failed between layers

No.	Model Geometry	Materials: Adhesive/ Adherend	Loading and Environment	Mechanical Behavior State of Stress	Analytical Methods	Experimental Techniques	Effect of Structural Parameters	Failure and Strength
64	Double canti- lever beam	adherends: 2024 T3 bare 7975 clad adhesives: modified epoxy and nitrile phenolic	sustained load- ing at high tem- perature and humidity, weathering ex- posure	time-temperature ef- fects on strength & crack propagation		precracked cleavage model exposed to moist ambient	effect of surface preparation acid anodizing	residual shear strength; fracture toughness; delamination
71	multi- layer laminate panel	orthotropic adherends, isotropic adhesive boron epoxy laminate	static & cycl- ing loading; axial loading	elastic & plastic behavior of adhe- sive; plane stress in adherends interlaminar shear stress distribu- tion	initial strain for inelastic behavior finite ele- ment solu- tion; dis- placement method	stress-strain curves for Ramberg-Osgood parameters	effect of thickness to length ratio and layer number	

APPENDIX 2

FINITE ELEMENT COMPUTER PROGRAM FOR ELASTIC STRESS ANALYSIS IN ORTHOTROPIC BONDED STRUCTURAL SYSTEMS.

```
LEVEL 21.7 ( JAN 73 )                    OS/360  FORTRAN H                                    DATE

          COMPILER OPTIONS - NAME=  MAIN,OPT=02,LINECNT=60,SIZE=0000K,
                             SOURCE,EBCDIC,NOLIST,NODECK,LOAD,NOMAP,NOEDIT,ID,NOXREF
               C
               C  TWO DIMENSION PLAN STRAIN/STRESS FINITE ELEMENT PROGRAM
               C  FOR GENERAL MATERIAL
               C
ISN 0002             REAL*8 TITLE(9)
ISN 0003             COMMON NNP,NEL,NMAT,NSLC,NOPT,NBODY,MTYP,IE(200,5),RO(10),TH(10),
                    1ET(10),LT(10),GGT(10),E1T(10),E2T(10),U12T(10),U21T(10),G12T(10),
                    2CQ(3,3),QM(3,3,10),E,U,GG,E1,E2,U12,U21,G12,QQT(3,3,10),
                    3X(200),Y(200),ULX(200),VLY(200),KODE(200),ISC(20),JSC(20),
                    4SURTRX(20,2),SURTRY(20,2),EP(10)
ISN 0004             COMMON/ONE/CK(10,10),Q(10),B(3,10),C(3,3),BT(3,6),XQ(5),YQ(5)
ISN 0005             COMMON /TWO/ IBAND,NEQ, R(400), AK(400,50)
ISN 0006             DATA MAXEL, MAXNP, MAXMAT, MAXBW, MAXSLC
                    1    /  200,   200,    10,    50,     20/
ISN 0007        9999 READ 100,NPROB, (TITLE(I),I=1,9)
ISN 0008                IF(NPROB.LE.0) GO TO 999
ISN 0010        1020 PRINT 200,NPROB,(TITLE(I),I=1,9)
ISN 0011                CALL DATAIN (MAXEL,MAXNP,MAXMAT,MAXSLC,ISTOP)
ISN 0012                    MAXDOF = 2*MAXNP
ISN 0013                    MAXDIF = 0
ISN 0014                DO 1 I=1,NEL
ISN 0015                DO 1 J=1,4
ISN 0016                DO 1 K=1,4
ISN 0017                    LL= IABS(IE(I,J)- IE(I,K))
ISN 0018                IF(LL.GT.MAXDIF) MAXDIF = LL
ISN 0020           1    CONTINUE
ISN 0021                    IBAND = 2*(MAXDIF + 1)
ISN 0022                    NEQ = 2*NNP
ISN 0023                IF(IBAND.GT.MAXBW) GO TO 900
ISN 0025                IF(ISTOP.GT.0) GO TO 999
ISN 0027                CALL ASEMBL(ISTOP)
ISN 0028                IF(ISTOP.GT.0) GO TO 999
ISN 0030                CALL BANSOL(1,AK,R,NEQ,IBAND,MAXDOF,MAXBW)
ISN 0031                CALL BANSOL(2,AK,R,NEQ,IBAND,MAXDOF,MAXBW)
ISN 0032             PRINT 300, (I,R(2*I-1),R(2*I),I=1,NNP)
ISN 0033                CALL STRESS
ISN 0034                GO TO 9999
ISN 0035         900 PRINT 901, IBAND, MAXBW
ISN 0036             GO TO 9999
ISN 0037         100 FORMAT( I5,3X,9A8 )
ISN 0038         200 FORMAT( /8H1PROBLEM,I5,3H.. ,9A8 )
ISN 0039         300 FORMAT(37H1OUTPUT TABLE 1.. NODAL DISPLACEMENTS //
                   1         13X,4HNODE, 9X, 11HU = X-DISP.,9X, 11HV = Y-DISP./
                   2        (5X,I12,2E20.8))
ISN 0040         901 FORMAT(///12H BANDWIDTH =,I4,25H EXCEEDS MAX. ALLOWABLE =,I4//
                   1 30H GO ON TO NEXT PROBLEM        )
ISN 0041         999 STOP
ISN 0042             END
```

```
LEVEL 21.7 ( JAN 73 )                                   OS/360  FORTRAN H                                   DATE

          COMPILER OPTIONS - NAME=  MAIN,OPT=02,LINECNT=60,SIZE=0000K,
                             SOURCE,EBCDIC,NOLIST,NODECK,LOAD,NOMAP,NOEDIT,ID,NOXREF
ISN 0002          SUBROUTINE DATAIN(      MAXEL,MAXNP,MAXMAT,MAXSLC,ISTOP)                              00001000
ISN 0003          COMMON NNP,NEL,NMAT,NSLC,NOPT,NECDY,MTYP,IE(200,5),RO(10),TH(10),                     00002000
                 1ET(10),UT(10),GGT(10),E1T(10),E2T(10),U12T(10),U21T(10),G12T(10),                     00003000
                 2QQ(3,3),GM(3,3,10),E,U,GG,E1,E2,U12,U21,G12,GQT(3,3,10),                              00003500
                 3X(200),Y(200),ULX(200),VLY(200),KODE(200),ISC(20),JSC(20),                            00004000
                 4SURTRX(20,2),SURTRY(20,2),EP(10)                                                      00005000
      C                                                                                                 00006000
ISN 0004          ISTOP = 0                                                                             00007000
ISN 0005          READ 1,NNP,NEL,NMAT,NSLC,NOPT,NECDY                                                   00008000
      C                                                                                                 00009000
ISN 0006          PRINT 100,NNP,NEL,NMAT,NSLC,NOPT,NECDY                                                00010000
ISN 0007              IF(NNP.LE.MAXNP) GO TO 201                                                        00013000
ISN 0009                      ISTOP = ISTOP + 1                                                         00014000
ISN 0010          PRINT 251, MAXNP                                                                      00015000
ISN 0011      201     IF(NEL.LE.MAXEL) GO TO 202                                                        00016000
ISN 0013                      ISTOP = ISTOP + 1                                                         00017000
ISN 0014          PRINT 252, MAXEL                                                                      00018000
ISN 0015      202     IF(NMAT.LE.MAXMAT) GO TO 203                                                      00019000
ISN 0017                      ISTOP = ISTOP + 1                                                         00020000
ISN 0018          PRINT 253, MAXMAT                                                                     00021000
ISN 0019      203     IF(NSLC.LE.MAXSLC) GO TO 204                                                      00022000
ISN 0021                      ISTOP = ISTOP + 1                                                         00023000
ISN 0022          PRINT 254, MAXSLC                                                                     00024000
ISN 0023      204     IF(ISTOP.EQ.0) GO TO 205                                                          00025000
ISN 0025          PRINT 255, ISTOP                                                                      00026000
ISN 0026          STOP                                                                                  00027000
      C                                                                                                 00028000
ISN 0027      205 READ 2, (RO(I),TH(I),I=1,NMAT)                                                        00029000
ISN 0028          PRINT 101                                                                             00030000
ISN 0029          PRINT 51, (I,RO(I),TH(I),I=1,NMAT)                                                    00031000
ISN 0030          READ 10,(ET(I),UT(I),GGT(I),E1T(I),E2T(I),U12T(I),U21T(I),                            00031010
                 1G12T(I),I=1,NMAT)                                                                     00031020
ISN 0031          PRINT 80, (I,ET(I),UT(I),GGT(I),E1T(I),E2T(I),U12T(I),U21T(I),                        00031040
                 1G12T(I),I=1,NMAT)                                                                     00031050
ISN 0032          DO 150 IMAT=1,NMAT                                                                    00031110
ISN 0033          DO 150 I=1,3                                                                          00031120
ISN 0034          READ 11, (QQT(I,J,IMAT),J=1,3)                                                        00031130
ISN 0035          PRINT 81, (QQT(I,J,IMAT),J=1,3)                                                       00031140
ISN 0036      150 CONTINUE                                                                              00031150
ISN 0037          CALL MATERP                                                                           00031500
ISN 0038           DO 550 IMAT=1,NMAT                                                                   00031510
ISN 0039          DO 550 I=1,3                                                                          00031520
ISN 0040          PRINT 82, (GM(I,J,IMAT),J=1,3)                                                        00031530
ISN 0041      550 CONTINUE                                                                              00031540
ISN 0042          PRINT 103                                                                             00034000
ISN 0043                  N=1                                                                           00035000
ISN 0044        5 READ 3, M,KODE(M),X(M),Y(M),ULX(M),VLY(M)                                             00036000
ISN 0045              IF(M-N)4,6,7                                                                      00037000
ISN 0046        4 PRINT 105, M                                                                          00038000
ISN 0047          PRINT 52,M,KODE(M), X(M),Y(M),ULX(M),VLY(M)                                           00039000
ISN 0048                      ISTOP= ISTOP +1                                                           00040000
ISN 0049            GO TO 5                                                                             00041000
ISN 0050        7             DF = M + 1 - N                                                            00042000
ISN 0051                      RX=(X(M)-X(N-1))/DF                                                       00043000
ISN 0052                      RY=(Y(M)-Y(N-1))/DF                                                       00044000
ISN 0053        8             KODE(N)=0                                                                 00045000
```

```
ISN 0054                    X(N)=X(N-1)+RX                                        00046000
ISN 0055                    Y(N)=Y(N-1)+RY                                        00047000
ISN 0056                    ULX(N)=0.0                                            00048000
ISN 0057                    VLY(N)=0.0                                            00049000
ISN 0058          6 PRINT 52,N,KODE(N),X(N),Y(N),ULX(N),VLY(N)                    00050000
ISN 0059                    N=N+1                                                 00051000
ISN 0060                IF(M-N)9,6,8                                              00052000
ISN 0061          9     IF(N.LE.NNP) GO TO 5                                      00053000
ISN 0063            PRINT 106                                                     00056000
ISN 0064         13         L=0                                                   00057000
ISN 0065         14 READ 15, M,(IE(M,I),I=1,5)                                    00058000
ISN 0066         16         L=L+1                                                 00059000
ISN 0067                IF(M-L)117,17,18                                          00060000
ISN 0068        117 PRINT 118,M                                                   00061000
ISN 0069            PRINT 53,M, (IE(M,I), I=1,5)                                  00062000
ISN 0070                    ISTOP=ISTOP+1                                         00063000
ISN 0071                GO TO 14                                                  00064000
ISN 0072         18         IE(L,1)= IE(L-1,1)+1                                  00065000
ISN 0073                    IE(L,2)= IE(L-1,2)+1                                  00066000
ISN 0074                    IE(L,3)=IE(L-1,3)+1                                   00067000
ISN 0075                    IE(L,4)=IE(L-1,4)+1                                   00068000
ISN 0076                    IE(L,5)=IE(L-1,5)                                     00069000
ISN 0077         17 PRINT 53, L,(IE(L,I),I=1,5)                                   00070000
ISN 0078                IF(M-L)20,20,16                                           00071000
ISN 0079         20     IF(NEL-L)21,21,14                                         00072000
ISN 0080         21     CONTINUE                                                  00073000
ISN 0081                IF(NSLC.EQ.0) GO TO 31                                    00076000
ISN 0083         30 PRINT 108                                                     00077000
ISN 0084                DO 40 L=1,NSLC                                            00078000
ISN 0085            READ 41,ISC(L),JSC(L),SURTRX(L,1),SURTRX(L,2),SURTRY(L,1),    00079000
                  1 SURTRY(L,2)                                                   00080000
ISN 0086         40 PRINT 42,ISC(L),JSC(L),SURTRX(L,1),SURTRX(L,2),SURTRY(L,1),   00081000
                  1 SURTRY(L,2)                                                   00082000
ISN 0087         31     IF(ISTOP.EQ.0) GO TO 999                                  00083000
ISN 0089            PRINT 900, ISTOP                                              00084000
          C                                                                       00085000
ISN 0090          1 FORMAT(6I5)                                                   00086000
ISN 0091        100 FORMAT(35H0INPUT TABLE 1.. BASIC PARAMETERS   //              00087000
                  1        5X, 40H NUMBER OF NODAL POINTS. . . . . . . . ..I5/    00088000
                  2        5X, 40H NUMBER OF ELEMENTS. . . . . . . . . ..I5/      00089000
                  3        5X, 40H NUMBER OF DIFFERENT MATERIALS . . . . ..I5/    00090000
                  4        5X, 40H NUMBER OF SURFACE LOAD CARDS. . . . . ..I5/    00091000
                  5        5X, 40H 1 = PLANE STRAIN, 2 = PLANE STRESS. . ..I5/    00092000
                  6        5X, 40H BODY FORCES(1 = IN -Y DIREC., 0 = NONE),I5)    00093000
ISN 0092        251 FORMAT(////33H TOO MANY NODAL POINTS, MAXIMUM =, I5)          00094000
ISN 0093        252 FORMAT(////30H TOO MANY ELEMENTS, MAXIMUM = ,I5)              00095000
ISN 0094        253 FORMAT(////30H TOO MANY MATERIALS, MAXIMUM =,I5)              00096000
ISN 0095        254 FORMAT(////40H TOO MANY SURFACE LOAD CARDS, MAXIMUM = ,I5)    00097000
ISN 0096        255 FORMAT(////28H EXECUTION HALTED BECAUSE OF,I5,13H FATAL ERRORS/)  00098000
ISN 0097          2 FORMAT(2F10.3)                                                00099000
ISN 0098        101 FORMAT(36H0INPUT TABLE 2.. MATERIAL PROPERTIES //             00100000
                  1        10H  MATERIAL,5X,10HMODULUS OF,6X,9HPOISSON'S,7X,      00101000
                    28HMATERIAL,7X,   8HMATERIAL /                                00102000
                    34X,6HNUMBER,5X,10HELASTICITY,8X,7H   RATIO,8X,7HDENSITY,6X,  00103000
                    49HTHICKNESS )                                                00104000
ISN 0099         51 FORMAT(I10,2E15.4)                                            00105000
ISN 0100         10 FORMAT(8F10.3)                                                00105010
ISN 0101         80 FORMAT(I10,5F15.4)                                            00105020
```

```
ISN 0102        11 FORMAT(3E10.3)                                                      C0105030
ISN 0103        81 FORMAT(3E10.3)                                                      C0105040
ISN 0104        82 FORMAT(3E10.3)                                                      C0105050
ISN 0105       103 FORMAT(34H1INPUT TABLE 3.. NODAL POINT DATA //                      C0106000
                  1        5X,5HNODAL,48X,7HX-DISP.,8X,7HY-DISP./                      C0107000
                  25X,5HPOINT,6X,4HTYPE,14X,1HX,14X,1HY,8X,7HOR LOAD,8X,7HOR LOAD)     C0108000
ISN 0106         3 FORMAT(2I5,4E10.3)                                                  C0109000
ISN 0107       105 FORMAT(5X,17HERROR IN CARD NO.,I5/)                                 C0110000
ISN 0108        52 FORMAT(2I10,4E15.4)                                                 C0111000
ISN 0109       106 FORMAT(34H1INPUT TABLE 4.. ELEMENT DATA        //                   C0112000
                  1        11X,31HGLOBAL INDICES OF ELEMENT NODES/3X,7HELEMENT,        C0113000
                  27X,1H1,7X,1H2,7X,1H3,7X,1H4,2X,8HMATERIAL)                          C0114000
ISN 0110       118 FORMAT( 5X, 25HERROR IN ELEMENT CARD NO., I5 )                      C0115000
ISN 0111        15 FORMAT(6I5)                                                         C0116000
ISN 0112        53 FORMAT(I10,4I8,I10)                                                 C0117000
ISN 0113       108 FORMAT(37H1INPUT TABLE 5.. SURFACE LOADING DATA  //                 C0118000
                  117X, 33HSURFACE LOAD INTENSITIES AT NODES/                          C0119000
                  24X,6HNODE I,4X,6HNODE J,10X,2HXI,10X,2HXJ,10X,2HYI,10X,2HYJ)        C0120000
ISN 0114        41 FORMAT(2I5,4E10.3)                                                  C0121000
ISN 0115        42 FORMAT(2I10,4E12.4)                                                 C0122000
ISN 0116       900 FORMAT(///45H ASSEMBLY AND SOLUTION WILL NOT BE PERFORMED,,I5,      C0123000
                  121H  FATAL CARD ERRORS          )                                   C0124000
ISN 0117       999 RETURN                                                              C0125000
ISN 0118           END                                                                 C0126000
```

```
LEVEL 21.7 ( JAN 73 )                              OS/360  FORTRAN H                                DATE

          COMPILER OPTIONS - NAME=  MAIN,OPT=02,LINECNT=60,SIZE=0000K,
                             SOURCE,EBCDIC,NOLIST,NODECK,LOAD,NOMAP,NOEDIT,ID,NOXREF
ISN 0002            SUBROUTINE  MATERP
ISN 0003            COMMON NNP,NEL,NMAT,NSLC,NOPT,NBODY,MTYP,IE(200,5),RO(10),TH(10),
                   1ET(10),UT(10),GGT(10),E1T(10),E2T(10),U12T(10),U21T(10),G12T(10),
                   2QQ(3,3),OM(3,3,10),E,U,GG,E1,E2,U12,U21,G12,QQT(3,3,10),
                   3X(200),Y(200),ULX(200),VLY(200),KODE(200),ISC(20),JSC(20),
                   4SURTRX(20,2),SURTRY(20,2),FP(10)
ISN 0004            DO 250 IMAT=1,NMAT
ISN 0005            E=ET(IMAT)
ISN 0006            U=UT(IMAT)
ISN 0007            GG=GGT(IMAT)
ISN 0008            E1=E1T(IMAT)
ISN 0009            E2=E2T(IMAT)
ISN 0010            U12=U12T(IMAT)
ISN 0011            U21=U21T(IMAT)
ISN 0012            G12=G12T(IMAT)
ISN 0013            DO 350 I=1,3
ISN 0014            DO 350 J=1,3
ISN 0015        350 QQ(I,J)=QQT(I,J,IMAT)
ISN 0016            IF ( E .EQ. 0. .AND.GG .EQ. 0. ) GO TO 500
ISN 0018            IF ( E .EQ. 0. ) GO TO 300
ISN 0020            IF ( U .EQ. 0. ) GO TO 200
ISN 0022            IF (GG .EQ. 0. )GG = E*0.5/(1.+U)
ISN 0024            GO TO 400
ISN 0025        200 IF (GG .NE. 0. ) U = 1. - E*0.5/GG
ISN 0027            GO TO 400
ISN 0028        300 IF ( U .EQ. 0. ) GO TO 400
ISN 0030            E = 2.*(1.+U)*GG
ISN 0031        400 IF(NOPT.EQ.1)GO TO 450
ISN 0033            QQ(1,1) = E/(1.-U*U)
ISN 0034            QQ(2,1) = U*QQ(1,1)
ISN 0035            QQ(2,2) = QQ(1,1)
ISN 0036            QQ(3,3) = GG
ISN 0037            GO  TO 1000
ISN 0038        450 QQ(1,1)=E*(1-U)/((1+U)*(1-2*U))
ISN 0039            QQ(2,1)=E*U/((1+U)*(1-2*U))
ISN 0040            QQ(2,2)=QQ(1,1)
ISN 0041            QQ(3,3)=GG
ISN 0042            GO TO 1000
ISN 0043        500 IF ( E1 .EQ. 0. .AND.  E2 .EQ. 0. ) GO TO 1000
ISN 0045            IF ( U12 .EQ. 0. ) GO TO 700
ISN 0047            IF ( U21 .EQ. 0. ) U21 = U12*E2/E1
ISN 0049            GO TO 800
ISN 0050        700 U12 = U21*E1/E2
ISN 0051        800 QQ(1,1) = E1/(1.-U12*U21)
ISN 0052            QQ(2,1) = U21*QQ(1,1)
ISN 0053            QQ(2,2) = E2/(1.-U12*U21)
ISN 0054            QQ(3,3) = G12
ISN 0055       1000 DO  1200 I=1,3
ISN 0056            DO  1200 J=1,I
ISN 0057            OM(I,J,IMAT)=QQ(I,J)
ISN 0058            OM(J,I,IMAT)=QQ(I,J)
ISN 0059       1200 CONTINUE
ISN 0060            DO  1300 I=1,3
ISN 0061       1300 OM(I,3,IMAT)=2.*OM(I,3,IMAT)
ISN 0062        250 CONTINUE
ISN 0063            RETURN
ISN 0064            END
```

AD-A032 011 TECHNION RESEARCH AND DEVELOPMENT FOUNDATION LTD HAI--ETC F/G 11/1
MECHANICAL BEHAVIOR OF MULTIMATERIAL COMPOSITE SYSTEMS. INTERLA--ETC(U)
APR 76 O ISHAI, D PERETZ, S GALI DAJA37-75-C-1890

UNCLASSIFIED NL

2 OF 2
AD
A032011

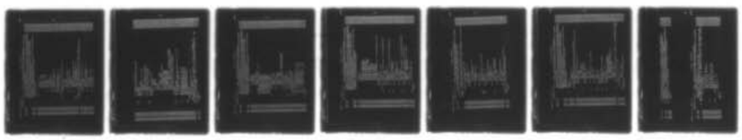

END
DATE
FILMED
1-77

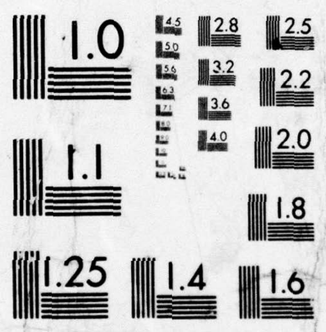

MICROCOPY RESOLUTION TEST CHART
NATIONAL BUREAU OF STANDARDS-1963-A

```
          COMPILER OPTIONS - NAME=  MAIN,OPT=02,LINECNT=60,SIZE=0000K,
                             SOURCE,EBCDIC,NOLIST,NODECK,LOAD,NOMAP,NOEDIT,ID,NOXREF
ISN 0002          SUBROUTINE  ASEMBL(ISTOP)                                              00001000
ISN 0003          COMMON NNP,NEL,NMAT,NSLC,NOPT,NBODY,MTYP,IE(200,5),RO(10),TH(10),      00002000
                 1ET(10),LT(10),GGT(10),E1T(10),E2T(10),U12T(10),U21T(10),G12T(10),     00003000
                 2QQ(3,3),QM(3,3,10),F,U,GG,E1,E2,U12,U21,G12,QOT(3,3,10),              00003500
                 3X(200),Y(200),ULX(200),VLY(200),KODE(200),ISC(20),JSC(20),            00004000
                 4SURTRX(20,2),SURTRY(20,2),EP(10)                                      00005000
ISN 0004          COMMON/ONE/ QK(10,10),Q(10),B(3,10),C(3,3),BT(3,6),XQ(5),YQ(5)         00006000
ISN 0005          COMMON/TWO/ IBAND,NEQ,R(400), AK(400,50)                               00007000
ISN 0006          DIMENSION LP(8)                                                        00008000
          C                                                                              00009000
ISN 0007          REWIND 1                                                               00010000
ISN 0008                    ISTOP = 0                                                    00012000
ISN 0009                    BT(1,4)  =  0.0                                              00014000
ISN 0010                    BT(1,5)  =  0.0                                              00015000
ISN 0011                    BT(1,6)  =  0.0                                              00016000
ISN 0012                    BT(2,1)  =  0.0                                              00017000
ISN 0013                    BT(2,2)  =  0.0                                              00018000
ISN 0014                    BT(2,3)  =  0.0                                              00019000
ISN 0015               DO   2 I=1,NEQ                                                    00026000
ISN 0016                  R(I)=0.0                                                       00027000
ISN 0017               DO   2 J =1,IBAND                                                 00028000
ISN 0018          2       AK(I,J) = 0.0                                                  00029000
ISN 0019               DO 10 M=1,NEL                                                     00033000
ISN 0020               IF(IE(M,5).GT.0) GO TO 11                                         00034000
ISN 0022                    ISTOP = ISTOP + 1                                            00035000
ISN 0023               GO TO 10                                                          00036000
ISN 0024         11    CALL QUAD(M,AREA)                                                 00037000
ISN 0025               IF(AREA.GT.0.0) GO TO 16                                          00038000
ISN 0027                    ISTOP = ISTOP + 1                                            00039000
ISN 0028          PRINT 20,M                                                             00040000
ISN 0029         16    IF(IE(M,3).EQ.IE(M,4)) GO TO 26                                   00044000
ISN 0031               DO 31 J = 1,2                                                     00045000
ISN 0032                  IJ= 10-J                                                       00046000
ISN 0033                  IK= IJ+1                                                       00047000
ISN 0034                  PIVOT = QK(IK,IK)                                              00048000
ISN 0035               DO 32 K= 1,IJ                                                     00049000
ISN 0036                  F = QK(IK,K)/PIVOT                                             00050000
ISN 0037                  QK(IK,K)=F                                                     00051000
ISN 0038               DO 33 I=K,IJ                                                      00052000
ISN 0039                  QK(I,K)=QK(I,K)- F*QK(I,IK)                                    00053000
ISN 0040         33       QK(K,I) = QK(I,K)                                              00054000
ISN 0041         32       Q(K) =Q(K)-QK(IK,K)*Q(IK)                                      00055000
ISN 0042         31       Q(IK) =Q(IK)/PIVOT                                             00056000
ISN 0043         26 WRITE (1) ((QK(I,J),J=1,10),I=9,10), Q(9), Q(10),                    00061000
                 1((B(I,J),J=1,10),I=1,3),((C(I,J),J=1,3),I=1,3),XQ(5),YQ(5)            00062000
ISN 0044                  LIM=8                                                          00066000
ISN 0045               IF(IE(M,3).EQ.IE(M,4)) LIM = 6                                    00067000
ISN 0047               DO 40 I=2,LIM,2                                                   00068000
ISN 0048                  IJ = I/2                                                       00069000
ISN 0049                  LP(I-1) = 2*IE(M,IJ) - 1                                       00070000
ISN 0050         40       LP(I) = 2*IE(M,IJ)                                             00071000
ISN 0051               DO 50 LL=1,LIM                                                    00072000
ISN 0052                  I = LP(LL)                                                     00073000
ISN 0053                  R(I) = R(I) + Q(LL)                                            00074000
ISN 0054               DO 50 MM=1,LIM                                                    00075000
ISN 0055                  J = LP(MM) - I + 1                                             00076000
```

```
ISN 0056              IF (J.LE. 0 ) GO TO 50                                    00077000
ISN 0058                    AK(I,J)= AK(I,J)+ GK(LL,MM)                         00078000
ISN 0059      50      CONTINUE                                                  00079000
ISN 0060      10      CONTINUE                                                  00080000
ISN 0061              DO 55 N=1,NNF                                             00083000
ISN 0062              IF(KODE(N).EQ.3) GO TO 55                                 00084000
ISN 0064                    K=2*N                                               00085000
ISN 0065              IF( KODE(N).EQ.1) GO TO 57                                00086000
ISN 0067                    R(K-1) = R(K-1) + ULX(N)                            00087000
ISN 0068              IF(KODE(N).NE.0) GO TO 55                                 00088000
ISN 0070      57            R(K) = R(K) + VLY(N)                                00089000
ISN 0071      55      CONTINUE                                                  00090000
ISN 0072              IF(NSLC.EQ.0) GO TO 60                                    00094000
ISN 0074              DO 61 L = 1,NSLC                                          00095000
ISN 0075                    I = ISC(L)                                          00096000
ISN 0076                    J = JSC(L)                                          00097000
ISN 0077                    II=2*I                                              00098000
ISN 0078                    JJ=2*J                                              00099000
ISN 0079                    DX = X(J) - X(I)                                    00100000
ISN 0080                    DY = Y(J) - Y(I)                                    00101000
ISN 0081                    EL = SQRT(DX*DX + DY*DY)                            00102000
ISN 0082                    PXI=SURTRX(L,1)*EL                                  00103000
ISN 0083                    PXJ=SURTRX(L,2)*EL                                  00104000
ISN 0084                    PYI=SURTRY(L,1)*EL                                  00105000
ISN 0085                    PYJ=SURTRY(L,2)*EL                                  00106000
ISN 0086                    R(II-1) = R(II-1) + PXI/3.0 + PXJ/6.0               00107000
ISN 0087                    R(JJ-1) = R(JJ-1) + PXI/6.0 + PXJ/6.0               00108000
ISN 0088                    R(II)=R(II)+ PYI/3.0 + PYJ/6.0                      00109000
ISN 0089                    R(JJ)= R(JJ) + PYI/6.0 + PYJ/3.0                    00110000
ISN 0090      61      CONTINUE                                                  00111000
ISN 0091      60      DO 70 M=1,NNF                                             00116000
ISN 0092              IF(KODE(M).GE.0.AND.KODE(M).LE.3) GO TO 72                00117000
ISN 0094                    ISTOP = ISTOP + 1                                   00118000
ISN 0095              GO TO 70                                                  00119000
ISN 0096      72      IF(KODE(M).EQ.0) GO TO 70                                 00120000
ISN 0098              IF(KODE(M).EQ.2) GO TO 71                                 00121000
ISN 0100              CALL GEOMBC(ULX(M),2*M-1)                                 00122000
ISN 0101              IF(KODE(M).EQ.1) GO TO 70                                 00123000
ISN 0103      71      CALL GEOMBC(VLY(M),2*M)                                   00124000
ISN 0104      70      CONTINUE                                                  00125000
ISN 0105           ENDFILE 1                                                    00126000
ISN 0106              IF(ISTOP.EQ.0) GO TO 81                                   00127000
ISN 0108           PRINT 100, ISTOP                                             00128000
ISN 0109      20   FORMAT(/5X,17H AREA OF ELEMENT ,I5,14H  IS NEGATIVE  /)      00129000
ISN 0110     100   FORMAT(////42H SOLUTION WILL NOT BE PERFORMED BECAUSE OF  ,I5,   00130000
                  1 15H   DATA ERRORS         /)                                00131000
ISN 0111      81   RETURN                                                       00132000
ISN 0112           END                                                          00133000
```

```
LEVEL 21.7 ( JAN 73 )                         OS/360  FORTRAN H                                DATE

         COMPILER OPTIONS - NAME=  MAIN,OPT=02,LINECNT=60,SIZE=0000K,
                            SOURCE,EBCDIC,NOLIST,NODECK,LOAD,NOMAP,NOEDIT,ID,NOXREF
ISN 0002          SUBROUTINE QUAD(M,TOTALA)                                                  C0001000
ISN 0003          COMMON NNP,NEL,NMAT,NSLC,NCPT,NBCDY,MTYP,IE(200,5),RO(10),TH(10),         00002000
                 1ET(10),LT(10),GGT(10),E1T(10),E2T(10),U12T(10),U21T(10),G12T(10),         C0003000
                 2CO(3,3),CM(3,3,10),E,U,GG,E1,E2,U12,U21,G12,CGT(3,3,10),                  C0003500
                 3X(200),Y(200),ULX(200),VLY(200),KODE(200),ISC(20),JSC(20),                C0004000
                 4SURTRX(20,2),SURTRY(20,2),EP(10)                                          C0005000
ISN 0004          COMMON/ONE/ QK(10,10),Q(10),B(3,10),C(3,3),ET(3,6),XQ(5),YQ(5)            C0006000
ISN 0005          COMMON/TWO/ IBAND,NEQ,R(400), AK(400,50)                                  C0007000
            C                                                                               C0008000
ISN 0006                I= IE(M,1)                                                          C0009000
ISN 0007                J= IE(M,2)                                                          C0010000
ISN 0008                K= IE(M,3)                                                          C0011000
ISN 0009                L= IE(M,4)                                                          C0012000
ISN 0010                MTYP = IE(M,5)                                                      C0013000
ISN 0011                TOTALA = 0.0                                                        C0014000
ISN 0012          IF(NMAT.EQ.1.AND.M.GT.1) GO TO 5                                          C0019000
ISN 0014          C(1,1)=CM(1,1,MTYP)                                                       C0020000
ISN 0015          C(1,2)=CM(1,2,MTYP)                                                       C0021000
ISN 0016          C(1,3)=CM(1,3,MTYP)                                                       C0022000
ISN 0017          C(2,1)=CM(2,1,MTYP)                                                       C0023000
ISN 0018          C(2,2)=CM(2,2,MTYP)                                                       C0024000
ISN 0019          C(2,3)=CM(2,3,MTYP)                                                       C0025000
ISN 0020          C(3,1)=CM(3,1,MTYP)                                                       C0026000
ISN 0021          C(3,2)=CM(3,2,MTYP)                                                       C0027000
ISN 0022          C(3,3)=CM(3,3,MTYP)                                                       C0028000
ISN 0023        5       LIM = 4                                                             C0033000
ISN 0024            IF(K.EQ.L) LIM = 3                                                      C0034000
ISN 0026                XQ(5) = 0.0                                                         C0035000
ISN 0027                YQ(5) = 0.0                                                         C0036000
ISN 0028            DO 10 N=1,LIM                                                           C0037000
ISN 0029                NN = IE(M,N)                                                        C0038000
ISN 0030                XQ(N) = X(NN)                                                       C0039000
ISN 0031                YQ(N) = Y(NN)                                                       C0040000
ISN 0032                XQ(5) = XQ(5) + X(NN)/FLOAT(LIM)                                    C0041000
ISN 0033       10       YQ(5) = YQ(5) + Y(NN)/FLOAT(LIM)                                    C0042000
ISN 0034            DO 13 II =1,10                                                          C0045000
ISN 0035                Q(II)=0.0                                                           C0046000
ISN 0036            DO 12 JJ = 1,10                                                         C0047000
ISN 0037       12       QK(II,JJ)=0.0                                                       C0048000
ISN 0038            DO 13 JJ=1,3                                                            C0049000
ISN 0039       13       B(JJ,II) = 0.0                                                      C0050000
ISN 0040            IF(K.NE.L) GO TO 15                                                     C0051000
ISN 0042          CALL CST(1,2,3,TOTALA)                                                    C0052000
ISN 0043            GO TO 999                                                               C0053000
ISN 0044       15 CALL CST(1,2,5,AREA)                                                      C0054000
ISN 0045                TOTALA = TOTALA + AREA                                              C0055000
ISN 0046          CALL CST(2,3,5,AREA)                                                      C0056000
ISN 0047                TOTALA = TOTALA + AREA                                              C0057000
ISN 0048          CALL CST(3,4,5,AREA)                                                      C0058000
ISN 0049                TOTALA = TOTALA + AREA                                              C0059000
ISN 0050          CALL CST(4,1,5,AREA)                                                      C0060000
ISN 0051                TOTALA = TOTALA + AREA                                              C0061000
ISN 0052      999 RETURN                                                                    C0062000
ISN 0053          END                                                                       C0063000
```

```
LEVEL 21.7 ( JAN 73 )                          OS/360  FORTRAN H                                        DATE

          COMPILER OPTIONS - NAME=  MAIN,OPT=02,LINECNT=60,SIZE=0000K,
                             SOURCE,EBCDIC,NOLIST,NODECK,LOAD,NOMAP,NOEDIT,ID,NOXREF
ISN 0002          SUBROUTINE  CST(I,J,K,AREA)                                                   00001000
ISN 0003          COMMON NNF,NEL,NMAT,NSLC,NCPT,NBODY,MTYP,IE(200,5),RO(10),TH(10),             00002000
                 1ET(10),LT(10),GGT(10),E1T(10),E2T(10),U12T(10),U21T(10),G12T(10),             00003000
                 2QQ(3,3),CM(3,3,10),F,U,GG,E1,E2,U12,U21,G12,GGT(3,3,10),                      00003500
                 3X(200),Y(200),LLX(200),VLY(200),KODE(200),ISC(20),JSC(20),                    00004000
                 4SURTRX(20,2),SURTRY(20,2),EP(10)                                              00005000
ISN 0004          COMMON/ONE/ GK(10,10),G(10),B(3,10),C(3,3),ET(3,6),XQ(5),YQ(5)                00006000
ISN 0005          COMMON/TWO/ IBAND,NEC,R(400), AK(400,50)                                      00007000
ISN 0006          DIMENSION CB(3,6),LC(6),LT(3),TK(6,6)                                         00008000
          C                                                                                     00009000
ISN 0007                    LT(1)= I                                                            00010000
ISN 0008                    LT(2)= J                                                            00011000
ISN 0009                    LT(3)= K                                                            00012000
ISN 0010                    BT(1,1)= YQ(J)-YQ(K)                                                00015000
ISN 0011                    BT(1,2)= YQ(K)-YQ(I)                                                00016000
ISN 0012                    BT(1,3) = YQ(I)-YQ(J)                                               00017000
ISN 0013                    BT(2,4)=XQ(K)-XQ(J)                                                 00018000
ISN 0014                    BT(2,5) = XQ (I)-XQ(K)                                              00019000
ISN 0015                    BT(2,6) = XQ(J) -XQ(I)                                              00020000
ISN 0016                    BT(3,1)=BT(2,4)                                                     00021000
ISN 0017                    BT(3,2) = BT(2,5)                                                   00022000
ISN 0018                    BT(3,3) = BT(2,6)                                                   00023000
ISN 0019                    BT(3,4) = BT(1,1)                                                   00024000
ISN 0020                    BT(3,5)= BT(1,2)                                                    00025000
ISN 0021                    BT(3,6)= BT(1,3)                                                    00026000
ISN 0022                    AREA =(BT(2,4)*BT(1,3) - BT(2,6)*BT(1,1))/2.0                       00027000
ISN 0023              DO 10 II=1,3                                                              00030000
ISN 0024              DO 10JJ = 1,6                                                             00031000
ISN 0025                    CB(II,JJ) = 0.0                                                     00032000
ISN 0026          DO 10 KK = 1,3                                                                00033000
ISN 0027    10              CB(II,JJ) = CB(II,JJ) + C (II,KK)*BT(KK,JJ)                         00034000
ISN 0028              DO 12 II = 1,6                                                            00037000
ISN 0029              DO 12 JJ = 1,6                                                            00038000
ISN 0030                    TK(II,JJ)=0.0                                                       00039000
ISN 0031              DO 12 KK=1,3                                                              00040000
ISN 0032    12              TK(II,JJ)=    TK(II,JJ)+BT(KK,II)*CB(KK,JJ)                         00041000
ISN 0033              DO 15 II=1,3                                                              00046000
ISN 0034                    LC(II) = 2*LT(II) - 1                                               00047000
ISN 0035    15              LC(II+3) = 2*LT(II)                                                 00048000
ISN 0036              DO 30 II=1,6                                                              00049000
ISN 0037                    LL = LC(II)                                                         00050000
ISN 0038                    FK = 1.0/(4.0*AREA)                                                 00051000
ISN 0039                    FB = 2.0*FK                                                         00052000
ISN 0040              DO 20 JJ=1,6                                                              00053000
ISN 0041                    MM = LC(JJ)                                                         00054000
ISN 0042    20              GK(LL,MM) = GK(LL,MM) + TK(II,JJ)*TH(MTYP)*FK                       00055000
ISN 0043              DO 30 JJ = 1,3                                                            00056000
ISN 0044    30              B(JJ,LL) = B(JJ,LL) + BT(JJ,II)*FB                                  00057000
ISN 0045              IF(NBODY.EQ.0) GO TO 999                                                  00060000
ISN 0047                    TBODYF =   AREA* RO(MTYP)*   TH(MTYP)                               00061000
ISN 0048                    BODYF   = -TBODYF/3.0                                               00062000
ISN 0049              DO 35 II=1,3                                                              00063000
ISN 0050                    JJ= 2* LT(II)                                                       00064000
ISN 0051    35              Q(JJ)= G(JJ)+ BODYF                                                 00065000
ISN 0052   999    RETURN                                                                        00066000
ISN 0053          END                                                                           00067000
```

```
LEVEL 21.7 ( JAN 73 )                    OS/360   FORTRAN H                                     DATE

          COMPILER OPTIONS - NAME=  MAIN,OPT=02,LINECNT=60,SIZE=0000K,
                             SOURCE,EBCDIC,NOLIST,NODECK,LOAD,NOMAP,NOEDIT,ID,NOXREF
ISN 0002              SUBROUTINE BANSOL(KKK,AK,R,NEQ,IBAND,NDIM,MDIM)                    00001000
            C SYMMETRIC BAND MATRIX EQUATION SOLVER.  (REF. 2)                             00002000
            C                                                                              00003000
            C KKK = 1 TRIANGULARIZES THE BAND MATRIX AK, EQ. (2-2)                         00004000
            C KKK = 2 SOLVES FOR RIGHT HAND SIDE R. SOLUTION RETURNS IN R. EQ.(2-3)        00005000
            C                                                                              00006000
ISN 0003              DIMENSION AK(NDIM,MDIM), R(1)                                        00007000
ISN 0004                      NRS = NEQ - 1                                                00008000
ISN 0005                      NR = NEQ                                                     00009000
ISN 0006                IF(KKK.EQ.2) GO TO 200                                             00010000
ISN 0008                DO 120 N= 1,NRS                                                    00011000
ISN 0009                      M= N-1                                                       00012000
ISN 0010                      MR = MINO(IBAND,NR-M)                                        00013000
ISN 0011                      PIVOT = AK(N,1)                                              00014000
ISN 0012                DO 120 L=2,MR                                                      00015000
ISN 0013                      CP= AK(N,L)/PIVOT                                            00016000
ISN 0014                      I = M+L                                                      00017000
ISN 0015                      J = 0                                                        00018000
ISN 0016                DO 110 K=L,MR                                                      00019000
ISN 0017                      J = J + 1                                                    00020000
ISN 0018       110            AK(I,J)= AK(I,J) -CP*AK(N,K)                                 00021000
ISN 0019       120            AK(N,L) = CP                                                 00022000
ISN 0020                GO TO 400                                                          00023000
ISN 0021       200      DO 220 N=1,NRS                                                     00024000
ISN 0022                      M= N-1                                                       00025000
ISN 0023                      MR = MINO(IBAND,NR-M)                                        00026000
ISN 0024                      CP= R(N)                                                     00027000
ISN 0025                      R(N) =CP/AK(N,1)                                             00028000
ISN 0026                DO 220  L=2,MR                                                     00029000
ISN 0027                      I = M + L                                                    00030000
ISN 0028       220            R(I)= R(I) - AK(N,L)*CP                                      00031000
ISN 0029                      R(NR) = R(NR)/AK(NR,1)                                       00032000
ISN 0030                DO 320 I = 1,NRS                                                   00033000
ISN 0031                      N= NR- I                                                     00034000
ISN 0032                      M= N-1                                                       00035000
ISN 0033                      MR = MINO(IBAND,NR-M)                                        00036000
ISN 0034                DO 320 K = 2,MR                                                    00037000
ISN 0035                      L = M+K                                                      00038000
            C    STORE COMPUTED DISPLACEMENTS IN LOAD VECTOR R                             00039000
ISN 0036       320            R(N)= R(N)- AK(N,K)*R(L)                                     00040000
ISN 0037       400    RETURN                                                               00041000
ISN 0038              END                                                                  00042000
```

```
LEVEL 21.7 ( JAN 73 )                              OS/360  FORTRAN H                                      DATE

         COMPILER OPTIONS - NAME=  MAIN,OPT=02,LINECNT=60,SIZE=0000K,
                            SOURCE,EBCDIC,NOLIST,NODECK,LOAD,NOMAP,NOEDIT,ID,NOXREF
ISN 0002            SUBROUTINE STRESS                                                          00001000
ISN 0003            COMMON NNF,NEL,NMAT,NSLC,NCPT,NBCDY,MTYP,IE(200,5),RO(10),TH(10),          00002000
                   1ET(10),UT(10),GGT(10),E1T(10),E2T(10),U12T(10),U21T(10),G12T(10),          00003000
                   2QQ(3,3),QM(3,3,10),E,U,GG,E1,E2,U12,U21,G12,GGT(3,3,10),                  00003500
                   3X(200),Y(200),ULX(200),VLY(200),KODE(200),ISC(20),JSC(20),                 00004000
                   4SURTRX(20,2),SURTRY(20,2),EP(10)                                           00005000
ISN 0004            COMMON/ONE/ QK(10,10),G(10),B(3,10),C(3,3),BT(3,6),XQ(5),YQ(5)            00006000
ISN 0005            COMMON/TWO/ IBAND,NEQ,R(400), AK(400,50)                                   00007000
ISN 0006            DIMENSION SIG(6)                                                           00008000
      C                                                                                        00009000
ISN 0007            REWIND 1                                                                   00010000
ISN 0008            PRINT 300                                                                  00011000
ISN 0009                  NOLINE = 47                                                          00012000
ISN 0010               DO 5 M=1,NEL                                                            00016000
ISN 0011            READ(1) ((GK(I,J),J=1,10),I=1,2),  G(9), Q(10),                            00017000
                  1    ((E(I,J),J=1,10),I=1,3), (((C(I,J),J=1,3),I=1,3), XC,YC                 00018000
ISN 0012                  LIM = 4                                                              00021000
ISN 0013              IF(IE(M,3).EQ.IE(M,4)) LIM = 3                                           00022000
ISN 0015              DO 10 I=1,LIM                                                            00023000
ISN 0016                  II = 2*I                                                             00024000
ISN 0017                  JJ = 2*IE(M,I)                                                       00025000
ISN 0018                  Q(II-1) = R(JJ-1)                                                    00026000
ISN 0019      10          Q(II) = R(JJ)                                                        00027000
ISN 0020              IF(LIM.EQ.3) GO TO 16                                                    00030000
ISN 0022              DO 15 K=1,2                                                              00031000
ISN 0023                  JK = K + 8                                                           00032000
ISN 0024                  IK = JK - 1                                                          00033000
ISN 0025              DO 15 L=1,IK                                                             00034000
ISN 0026      15          Q(JK) = Q(JK) - QK(K,L)*Q(L)                                         00035000
ISN 0027                  LIM = 10                                                             00036000
ISN 0028                  FAC = 0.25                                                           00039000
ISN 0029              GO TO 17                                                                 00040000
ISN 0030      16          LIM = 6                                                              00041000
ISN 0031                  FAC = 1.0                                                            00042000
ISN 0032      17      DO 20 I=1,3                                                              00043000
ISN 0033              EP(I)=0.0                                                                00044000
ISN 0034              DO 20 J=1, LIM                                                           00045000
ISN 0035      20       EP(I)=EP(I)+B(I,J)*Q(J)*FAC                                             00046000
ISN 0036              DO 30 I=1,3                                                              00049000
ISN 0037                  SIG(I) = 0.0                                                         00050000
ISN 0038              DO 30 J=1,3                                                              00051000
ISN 0039      30       SIG(I)=SIG(I)+C(I,J)*EP(J)                                              00052000
ISN 0040                  SP = (SIG(1)+SIG(2))/2.0                                             00054000
ISN 0041                  SM = (SIG(1)-SIG(2))/2.0                                             00055000
ISN 0042                  DS = SQRT(SM*SM+SIG(3)*SIG(3))                                       00056000
ISN 0043                  SIG(4) = SP + DS                                                     00057000
ISN 0044                  SIG(5) = SP - DS                                                     00058000
ISN 0045                  SIG(6) = 0.0                                                         00059000
ISN 0046              IF(SIG(3).NE.0.0.AND.SM.NE.0.0) SIG(6) = 28.648*ATAN2(SIG(3),            00060000
                  1                                                             SM)            00061000
ISN 0048              IF(NOLINE.GT.0) GO TO 54                                                 00063000
ISN 0050            PRINT 1000                                                                 00064000
ISN 0051                  NOLINE = 49                                                          00065000
ISN 0052      54          NOLINE = NOLINE - 1                                                  00066000
ISN 0053       5    PRINT 1010, M,XC,YC,(SIG(I),I=1,6)                                         00067000
ISN 0054              ENDFILE 1                                                                00068000
```

```
ISN 0055      300 FORMAT(47H1OUTPUT TABLE 2.. STRESSES AT ELEMENT CENTROIDS //      00069000
                 11X,7HELEMENT,9X,1HX,9X,1HY,4X,8HSIGMA(X),4X,8HSIGMA(Y),4X,        00070000
                 28HTAU(X,Y),4X,8HSIGMA(1),4X,8HSIGMA(2), 7X,5HANGLE )              00071000
ISN 0056     1000 FORMAT(1H1,    7HELEMENT,9X,1HX,9X,1HY,4X8HSIGMA(X),4X,8HSIGMA(Y), 00072000
                 14X,3HTAU(X,Y),4X,8HSIGMA(1),4X,8HSIGMA(2), 7X,5HANGLE )           00073000
ISN 0057     1010 FORMAT(I8, 2F10.2,1P6E12.4)                                       00074000
ISN 0058          RETURN                                                            00075000
ISN 0059          END                                                               00076000

LEVEL 21.7 ( JAN 73 )                  OS/360  FORTRAN H                                    DATE

     COMPILER OPTIONS - NAME=  MAIN,OPT=02,LINECNT=60,SIZE=0000K,
                        SOURCE,EBCDIC,NOLIST,NODECK,LOAD,NOMAP,NOEDIT,ID,NOXREF
ISN 0002          SUBROUTINE GEOMBC(U,N)                                            00001000
ISN 0003          COMMON/TWO/ IBAND,NEQ,R(400), AK(400,50)                          00002000
            C  THIS SUBROUTINE MODIFIES THE ASSEMBLAGE STIFFNESS AND LOADS FOR THE  00003000
            C  PRESCRIBED DISPLACEMENT U AT DEGREE OF FREEDOM N, EQ.(6-18B). (REF.1)00004000
ISN 0004             DO 100 M=2,IBAND                                               00005000
ISN 0005                K = N - M + 1                                               00006000
ISN 0006                IF(K.LE.0) GO TO 50                                         00007000
ISN 0008                R(K) = R(K) - AK(K,M)*U                                     00008000
ISN 0009                AK(K,M) = 0.0                                               00009000
ISN 0010       50       K = N + M - 1                                               00010000
ISN 0011                IF(K.GT.NEQ) GO TO 100                                      00011000
ISN 0013                R(K) = R(K) - AK(N,M)*U                                     00012000
ISN 0014                AK(N,M) = 0.0                                               00013000
ISN 0015      100    CONTINUE                                                       00014000
ISN 0016                AK(N,1) = 1.0                                               00015000
ISN 0017                R(N) = U                                                    00016000
ISN 0018          RETURN                                                            00017000
ISN 0019          END                                                               00018000
```